

Scuola Internazionale Superiore Studi Avanzati

SISSA

PhD Program in Functional and Structural Genomics



# Towards *Emx2* therapy of Glioblastoma multiforme

THESIS SUBMITTED FOR THE DEGREE OF “DOCTOR PHILOSOPHIAE”

Candidate:  
Jessica Zucco

Supervisor:  
Prof. A. Mallamaci

Academic Year 2018-2019

# ABSTRACT

The homeodomain-containing transcription factor *Emx2* encodes for a homeobox protein essential for territorial specification of rostral CNS as well as for proper spatio-temporal tuning of neural cell growth and differentiation (Gangemi et al. 2006).

Previous experiments done in my laboratory demonstrated its role in inhibiting cortico-cerebral astrogenesis, limiting proliferation of astrocytes-committed progenitors upon its overexpression in neural stem cells. This control takes place via a functional cascade, which includes stimulation of Bmp signaling and *Sox2* repression, through the downregulation of *Egfr* and *Fgf9* (Falcone et al., 2015). Meanwhile, studies by other labs also reported an inverse correlation between *Emx2* expression levels and aggressiveness of several human cancers, including lung, endometrial and gastric tumours (Okamoto et al. 2010) (Li et al. 2012).

Inspired by these findings, we activated a research program aimed at exploring the possibility to use *Emx2* in therapy of glioblastoma multiforme. This neoplasm is the most common and aggressive malignant primary tumor of the CNS, responsible of 4% of all tumor death in humans. Conventional therapeutic options for it are unfortunately limited: after surgical resection, GBM-affected patients routinely undergo radiotherapy and adjuvant chemotherapy (temozolomide, TMZ); nevertheless, their median survival is no longer than 14 months.

In 2016, Carmen Falcone demonstrated that *Emx2* overexpression suppresses a number of different glioblastomas in vitro, within 7-10 days, by inducing cell death and inhibiting cell proliferation. Molecular mechanisms underlying this phenomenon resulted to be highly pleiotropic, indeed *Emx2* affects different pathways and genes, including RTK cascades, cell cycle control circuitries and other malignancy-related processes (Falcone et al. 2016).

Then, given limits of conventional therapies, we decided to score the actual benefit of experimental *Emx2* gene therapy, evaluate its possible interaction with standard chemo- and radiotherapy, and explore novel routes for its delivery. These issues were investigated under the framework of this thesis. Results were as follows.

First, *Emx2* displayed a therapeutically appealing, anti-oncogenic activity *in vivo*. Indeed the median survival time of mice transplanted with *Emx2*-GOF tumour cells was twenty days longer compared to the control group (i.e. 35 days), outperforming TMZ.

Next, these results were confirmed by *in vitro* kinetic assays. Here we observed at least an additive effect between TMZ and *Emx2*-GOF treatments; specifically, in case of the U87 line, *Emx2* sensitized GBM cells to chemotherapy.

As for X-rays, we found that their association to *Emx2* overexpression resulted in an enhanced anti-oncogenic effect. By means of *ad hoc* calibrated, *in vitro* kinetic assays, we discovered that *Emx2* sensitized GBM cells to radiation. This was predominantly due to an inhibition of homologous recombination-based DNA-repair, likely leading to GBM cell suicide. A pronounced downregulation of *SOX2* and *FOXG1*, two key drivers of GBM malignancy, was instrumental to that.

Finally, interested in developing new effective and biosafe strategies for *in vivo* delivery of the therapeutic *Emx2* transgene, we collected preliminary proofs of principle, supporting the feasibility of a novel design based on combined use of HSV-1-derived, oncolytic viruses and amplicon vectors.

# INDEX

<b>1.</b>	<b>INTRODUCTION</b>	<b>6</b>
<b>1.1.</b>	<b>GLIOMAS</b>	<b>6</b>
1.1.1.	Epidemiology, classification and grading	6
<b>1.2.</b>	<b>GLIOBLASTOMA MULTIFORME</b>	<b>8</b>
1.2.1.	Epidemiology and classification	8
1.2.2.	Etiology and Pathogenesis	10
1.2.3.	Molecular heterogeneity	11
1.2.4.	Standard therapies	13
<b>1.3.</b>	<b>EMX2 GENE</b>	<b>15</b>
1.3.1.	Emx2 structure	15
1.3.2.	Emx2 expression in brain development	15
1.3.3.	Emx2 in tumours	17
<b>1.4.</b>	<b>HERPETIC VIRAL VECTORS IN ONCOTHERAPY</b>	<b>18</b>
1.4.1.	HSV-1 structure	18
1.4.2.	HSV-1 life cycle	21
1.4.3.	HSV-1 vector generation	23
1.4.4.	Oncolytic HSV viruses	24
1.4.5.	Amplicon HSV vectors	28
<b>2.</b>	<b>AIM</b>	<b>30</b>
<b>3.</b>	<b>MATERIALS AND METHODS</b>	<b>31</b>
3.1.	Lentiviral vectors packaging and titration	31
3.2.	Animal handling and embryo dissection	32
3.3.	GBM mice xenografts	33
3.4.	Glioblastoma cell cultures	33
3.5.	GBM cell growth curves under temozolomide treatment	34
3.6.	GBM cell growth curves upon X-rays treatment	34
3.7.	GBM cell growth curves upon Myb34.5 HSV-1 infection	35
3.8.	U87MG and murine neocortical tissue co-cultures upon Myb34.5 HSV-1 infection	35
3.9.	U87MG cell growth curves upon Myb34.5 HSV-1 and Emx2-LV infection	36
3.11.	“Healthy” human perinatal neocortex tissue hosts Myb34.5-helped amplification of Egfp-encoding herpetoviral amplicon vector (vAM-GFP)	37
3.12.	RNA sequencing	37
3.13.	RNA profiling	38
3.14.	Immunofluorescence analysis of $\gamma$ -H2AX foci	40
3.15.	Traffic light reporter assay: homologous recombination-mediated DNA repair detection by flow cytometry and Real Time PCR	40
3.16.	Statistical analysis	41
<b>4.</b>	<b>RESULTS</b>	<b>42</b>
<b>4.1.</b>	<b>EMX2 OVEREXPRESSION INCREASES THE SURVIVAL OF IMMUNOCOMPROMISED GBM-XENOGRAFTED HOSTS AND ENHANCES GBM SENSITIVITY TO TEMOZOLOMIDE (TMZ) TREATMENT</b>	<b>42</b>

4.1.1.	Emx2 overexpression outperforms TMZ treatment in experimental therapy of GBM-xenografted mouse hosts	42
4.1.2.	The outcome of combined Emx2/TMZ delivery exceeds the antitumorigenic impact of single Emx2 and TMZ treatments on GBM cultures	43
4.1.3.	Screening for molecular mediators of Emx2 enhancement of TMZ impact on GBM	45
<b>4.2.</b>	<b><i>EMX2 OVEREXPRESSION RADIOSENSITIZES GBM CELLS, BY DEPRESSING HR-MEDIATED DNA REPAIR</i></b>	<b>47</b>
4.2.1.	Emx2 overexpression radio-sensitizes GBM cells	47
4.2.2.	Emx2 overexpression increases $\gamma$ -H2AX foci, in basal conditions and upon irradiation	48
4.2.3.	Emx2 overexpression inhibits DNA repair via homologous recombination	49
4.2.4.	Screening for potential mediators of Emx2 HR-repair suppressing activity	52
4.2.5.	Validation of selected presumptive mediators of anti-HR Emx2 activity	55
<b>4.3.</b>	<b><i>HERPETIC VIRAL VECTORS AS SUITABLE TOOLS FOR EMX2 DELIVERY IN VIVO</i></b>	<b>58</b>
4.3.1.	The oncolytic Myb34.5 HSV-1 displays a pronounced anti-GBM activity	58
4.3.2.	Low Myb34.5 titres are able to eradicate U87MG cultures, while not affecting "healthy" murine, perinatal neocortical tissue, in vitro	59
4.3.3.	Myb34.5 and lentiviral Emx2 expressors exert a synergic anti-blastic effect on U87MG GBM cultures	60
4.3.4.	Both U87MG-GBM cells and "healthy" human neocortex precursors are able to host Myb34.5-helped amplification of EGFP-encoding herpes viral amplicon vectors	61
<b>5.</b>	<b><i>DISCUSSION</i></b>	<b>65</b>
<b>6.</b>	<b><i>BIBLIOGRAPHY</i></b>	<b>71</b>

# 1. INTRODUCTION

## 1.1. *Gliomas*

### 1.1.1. *Epidemiology, classification and grading*

Gliomas are the most frequent primary tumours of the central nervous system that display histologic features of glial cells (ie, astrocytes, oligodendrocytes, and ependymal cells); among these tumours, the most frequent and malignant histological type is glioblastoma multiforme (GBM).

In the past, the classification of brain tumours was controversial and very hard, and tumours of the central nervous system were classified by considering their histological features, immunohistochemical patterns, ultrastructural characterisation and genetic profiles. In 2016, the World Health Organisation (WHO) published a new summary on brain tumour classification, introducing for the first-time molecular parameters, in addition to histology, to define many tumour entities and deleting some variants and patterns that no longer have diagnostic or biological relevance. Therefore, brain tumour diagnosis is based on phenotypic and genotypic parameters and nomenclature should consist of a histopathological name followed by genetic features; for some tumour types, lacking any molecular diagnostic test information, a NOS (not otherwise specified) designation is needed; this means that there are insufficient information to assign a more specific code.

According to their degree of malignancy, determined by their histopathological characteristics, such as cytological atypia, anaplasia, mitotic activity, microvascular proliferation, and necrosis, gliomas are also graded on a scale I to IV (Louis et al. 2016): in particular grade I and II belong to low grade gliomas, whereas grade III and IV are considered high grade gliomas. Specifically, grade I tumours are biologically benign, can be surgically resected and finally cured; grade II tumours may follow long clinical courses, but early diffuse infiltration of the surrounding brain renders them incurable by surgery; grade III tumours are characterized by increased anaplasia and proliferation over grade II and are more rapidly fatal; grade IV tumours exhibit more advanced features of malignancy, including neo-angiogenesis and necrosis, are resistance to chemo and radiotherapy and are generally lethal within 12-14 months (Furnari et al. 2007).

Gliomas affecting adult cerebral hemispheres are called “diffuse gliomas”, due to their tendency to infiltrate throughout the brain. Based on the resemblance of the tumour cells with non-neoplastic glial cells (i.e. astrocytes or oligodendroglial cells), most diffuse gliomas can be typed as astrocytomas, oligodendrogliomas or mixed oligo-astrocytomas. More in detail, in this new classification, diffuse gliomas include the WHO grade II and grade III astrocytic tumours, the grade II and grade III oligodendrogliomas, the grade IV glioblastomas, as well as the related diffuse gliomas of childhood.

Astrocytic tumour cells, which include fibrillary astrocytoma, protoplasmic astrocytoma and gemistocytic astrocytoma, display nuclear atypia, mitotic activity and diffuse infiltration; oligodendrogliomas are characterized by cells with a round nucleus surrounded by a perinuclear halo and presence of branching network of capillaries called ‘chickenwire pattern’ and extensive calcification within the tumour. Finally, the key criterion for the diagnosis of mixed oligoastrocytomas is the presence of neoplastic glial cells with morphological characteristics of both astrocytes and oligodendrocytes.

Incidence rates of glioma differ significantly by histologic type, age at diagnosis, gender, race, and country; overall age-adjusted incidence rates for all gliomas range from 4.67 to 5.73 per 100.000 persons. Age-adjusted incidence of glioblastoma, the most common and most deadly glioma subtype in adults, ranges from 0.59 to 3.69 per 100.000 persons (Ostrom et al. 2014). Anaplastic astrocytoma and glioblastoma increase in incidence with age, peaking in the 75 – 84 age group. Oligodendrogliomas and oligoastrocytomas are most common in the 35 – 44 age group. In general, gliomas are more common in men than women, except for pilocytic astrocytoma, which occurs similarly in both genders(Ostrom et al. 2014).

Patients with low-grade gliomas have a better prognosis, with median survival times ranging between 4.6 to 6.5 years and median time to malignant progression of 8.8 to 11.4 years when the extent of resection is greater than 90 % (Hervey-Jumper and Berger 2014). Even so, 50–75 % of patients with low-grade gliomas will finally recover from their disease. Differently, patients affected by glioblastoma multiforme have a median survival time from 12.2 to 18.2 months, whereas anaplastic astrocytomas (WHO grade III) have a 41-month median survival.

## **1.2. Glioblastoma multiforme**

### *1.2.1. Epidemiology and classification*

Glioblastoma multiforme is the most aggressive, invasive and frequent type of primary astrocytomas and accounts for more than 60% of all brain tumours in adults. Despite new therapeutic advances have been developed, it remains a deadly disease with extremely poor prognosis. Patients affected by this tumour usually have a median survival of approximately 14 to 15 months from the diagnosis. It has an incidence of 5 per 100.000 persons, it's more frequent in men than women and it increases with age; it's very rare in children, while the average age of diagnosis is around 64 years old (Hanif et al. 2017).

Grade IV astrocytoma, also called glioblastoma multiforme due to its heterogenous histologic appearance and proliferation of multiple cell types, is defined by the hallmark features of high malignancy, in particular high cellularity and pleomorphism, nuclear atypia, rapid and uncontrolled cellular proliferation, diffuse infiltration, propensity for necrosis, robust neo-angiogenesis, intense resistance to apoptosis, and a huge genomic instability. Furthermore, it is characterised by a significant intertumoral and intra-tumoral heterogeneity on the cytopathological, transcriptional and genomic levels, making this cancer one of the most difficult to understand and to treat.

Morphologically, there are several phenotypical variants of glioblastoma multiforme: the giant cell glioblastoma which is the most frequent and is characterised by multinucleated, giant tumour cells, the small cell glioblastoma with a predominance of small, relatively monomorphous tumour cells with a small cytoplasm and the gliosarcoma variant with an extensive presence of a sarcomatoid phenotype. The identification of these variants is important because of the differential diagnosis with other brain tumours that requires different treatments (Wesseling, Kros, and Jeuken 2011).

The 90% of diagnosed glioblastoma are de novo primary tumours that develop rapidly in elderly patients, without clinical or histologic evidence of a less malignant precursor lesion. They differ from secondary glioblastoma, which develop from low-grade diffuse astrocytoma or anaplastic astrocytoma in younger patients, have a less degree of necrosis, are preferentially located in the frontal lobe, and carry a significantly better prognosis.

Primary and secondary glioblastomas are indistinguishable from the histological point of view, but they differ in their genetic and epigenetic profiles. Primary GBM are characterized by loss of heterozygosity (LOH) 10q (70% of cases), *EGFR* amplification (36%), *p16INK4a*



deletion (31%), and *PTEN* mutations (25%). 19q loss and *TP53* mutations are the most frequent and earliest detectable genetic alterations in secondary glioblastoma and are mutations that are already present in 60% of precursor low-grade astrocytomas. Only 1 out of 49 glioblastomas shares both *TP53* mutation and *EGFR* overexpression, indicating that these alterations are mutually exclusive events, belonging to two different genetic pathways in the evolution of glioblastoma (Watanabe et al. 1996).

In 2008 Parsons and colleagues reported that *IDH1* mutations occur in a large fraction of young patients and in most patients with secondary glioblastoma (Parsons et al. 2008); furthermore, they are still present in the 80% of diffuse astrocytoma (WHO grade II) and anaplastic astrocytoma (WHO grade III), that are the precursor lesions of secondary GBM. Nowadays, it is considered a definitive diagnostic molecular marker of secondary glioblastoma and is associated with an increased overall survival.

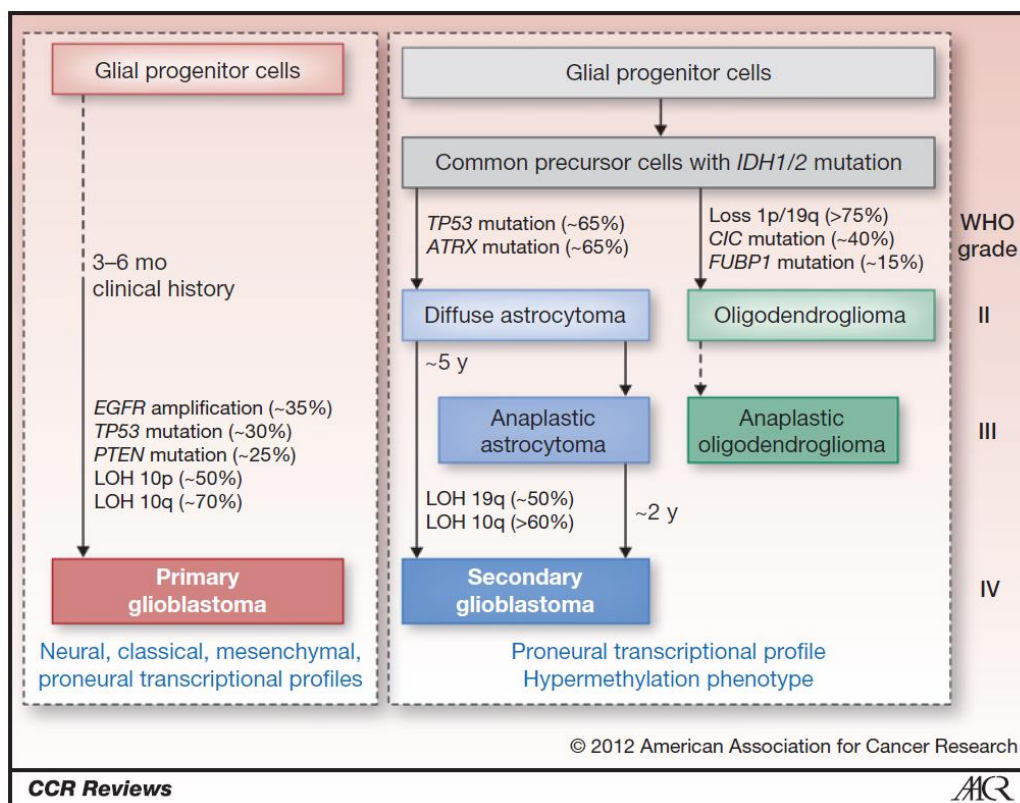


Figure 1. Genetic pathways to primary and secondary glioblastomas (Ohgaki and Kleihues 2013).

On the basis of genomic, epigenomic and transcriptomic expression profiles, GBM were classified in four distinct subtypes named proneural (PN), neural, (NE), mesenchymal (MES), and classical (CL) (Verhaak et al. 2010).

Two major characteristics of the proneural class were alterations of *PDGFRA* and point mutations in *IDH1*. Focal amplifications of the locus at 4q12 harboring *PDGFRA* were seen in all subtypes of GBM, but at a much higher rate in proneural samples; furthermore, there are also present *IDH1* and *TP53* mutations, all of which have previously been associated with secondary GBM; this is why most known secondary GBMs were classified as proneural. It is also associated with younger age. The neural subtype is characterised by the expression of neuron markers such as *NEFL*, *GABRA1*, *SYT1* and *SLC12A5*. The identity of the classical subtype is defined by a huge number of genomic aberrations, with 93% of samples harbouring chromosome 7 amplifications and 10 deletions, 95% showing *EGFR* amplification and 95% showing homozygous deletion spanning the *Ink4a/ARF* locus. This class also shows a distinct lack of additional abnormalities in *TP53*, *NF1*, *PDGFRA* or *IDH1*. Finally, the mesenchymal class is defined by an elevated expression of *CHI3L1* and *MET* (Phillips et al. 2006); there is also a strong association with the high frequency of *NF1* mutation/deletion. Glioblastoma multiforme is localized mainly in the cerebral hemispheres, in particular the 95% of these tumours arise in supratentorial region, while only few percent of tumours occur in cerebellum, brainstem and spinal cord (Nakada et al. 2011).

### 1.2.2. Etiology and Pathogenesis

Little is known about the etiology of brain neoplasms which are usually highly incurable; to date the only confirmed risk factor is associated to high dose ionizing radiation exposure (Ohgaki 2009); other studies reported an estimated overall risk of developing GBM following radiotherapy of 2.5% (Salvati et al. 2003); furthermore, it has been shown that patients treated for acute lymphoid leukemia are more prone to develop GBM, due to tumour complications and the chemotherapeutic agents used (Salvati et al. 2003). Moreover, there is no evidence of a possible correlation between GBM growth and environmental factors such as smoking, dietary risk factors, cell phones or electromagnetic field, severe head injury, occupational risk factors and pesticide exposure (Ohgaki 2009); (Agnihotri et al. 2013). Only 5-10% of GBM tumours are associated to genetic predisposition (Fisher et al. 2007).

Understanding the molecular, cellular and genetic mechanisms of GBM pathogenesis is very intricate and complex; at the cellular level, the tumour is highly heterogeneous, and consists of multiple cellular subpopulations of cancer cells. Glioblastoma stem cells (GSCs) represent

the core of the tumour and, due to their self-renewal ability, they give rise to a wide range of hierarchical distinct cell types. GSCs are known to be the major source of the tumour, due to their ability to replicate and differentiate, as well the major cause of tumour drug resistance and relapse, due to their ability to survive after chemo and radiotherapy. Furthermore, they show a strong and efficient DNA damage response and prevent cytotoxicity through high drug efflux by ABC transporters.

However, this unidirectional model, where GSCs represent a specific and rare subset of cells responsible for tumour growth and relapse, has been challenged by novel studies that highlights the importance of tumour cell plasticity in gliomagenesis, giving rise to a new model based on a clonal evolution. It was demonstrated that Sox2, a well-known transcription factor involved in stemness maintenance, might be central in tumour cell plasticity by regulating dedifferentiation and acquisition of GSCs properties, through a transcriptional regulation of distinct genes set in differentiated tumour cells and GSCs (Berezovsky et al. 2014). In this scenario, all tumour cells might have the potential to become CSCs through a dedifferentiation process.

Because gliomas share common features with glial precursors populations, another possible explanation for glioblastoma development could be represented by a malignant transformation of healthy glial precursors after gliogenic switch. These cells share with GSCs different markers, including *SOX2*, *BRN2*, *Olig2* and *NFIA*; in particular, Lee and colleagues discovered that astrocyte-like neural stem cells in the subventricular zone may be the cells from which GBM originates (Lee et al. 2018).

It is possible that some astrocytes are more prone to malignant transformation or trigger de-differentiation than others, and this could explain the immense cellular diversity of the bulk tumour. This hypothesis could be supported also by the evidence that four out five astrocyte subpopulations found in the adult brain are present in primary human glioma and multiple mouse models of glioma (Lin et al. 2017).

### *1.2.3. Molecular heterogeneity*

Like other tumours, GBM tumour cells are characterised by genetic and epigenetic alterations that accumulate during tumour progression and lead to activation of proto-oncogenes or inactivation of tumour suppressor genes. In particular, the majority of GBM tumours share loss, amplification, or mutation of EGFR (including expression of the

constitutively active form EGFRvIII), PDGFR $\alpha$ , NF1, PTEN, RB1, and p53, resulting in the deregulation of many signalling pathways. Furthermore, epigenetic modifications include the methylation of the O6-methylguanine methyltransferase (MGMT) promoter, a DNA repair enzyme involved in the fixation of damages induced by alkylating agents such as temozolomide (TMZ). It is considered an important predictive biomarker for temozolomide treatment success.

The most frequent molecular alterations in GBM involved receptor tyrosine kinases (RTKs) pathways: RTKs are cell-surface receptors that upon growth factors binding, undergo dimerization and conformational shift, activating the downstream signalling cascades.

The epidermal growth factor receptor gene (EGFR) is the most frequent amplified and overexpressed in GBM, affecting approximately 40% of these tumours, in particular the EGFR variant III (EGFRvIII) results in a constitutively activated truncated receptor protein lacking the ligand binding domain, leading to an uncontrolled increase in phosphorylation activity, resulting in tumour proliferation and invasion (Wesseling et al. 2011).

The Akt (PI3K/PTEN/Akt) pathway is also frequently mutated and hyper-activated; in particular, Akt is a downstream effector of PIP3 that induce cell proliferation and inhibition of apoptosis; in this pathway, the main inhibitor of PI3K is PTEN, a tumour suppressor gene that is frequently inactivated, either by loss of heterozygosity (LOH) or mutation, resulting in increased PI3K availability.

Other two tumour suppressor genes are frequently inactivated in GBM: RB and TP53. The retinoblastoma (RB) pathway plays a key role in the cell cycle: normally it is hypo-phosphorylated and actively binds to the transcription factor E2F, to prevent the transcription of genes active during mitosis; many GBM tumours display a methylation of the RB promoter, leading to gene silencing and negative regulation of this pathway.

The TP53 pathway is very crucial due to its involvement in different cellular processes, including cell cycle control, DNA damage response, cell death and differentiation. When DNA damage occurs, the cell becomes stressed and activates the TP53 pathway; in turn, it activates the transcription of p21 gene leading to cell cycle blockade and DNA repair; if DNA damage could not be repaired, TP53 will induce cell death to prevent cell divisions containing mutated or damaged DNA.

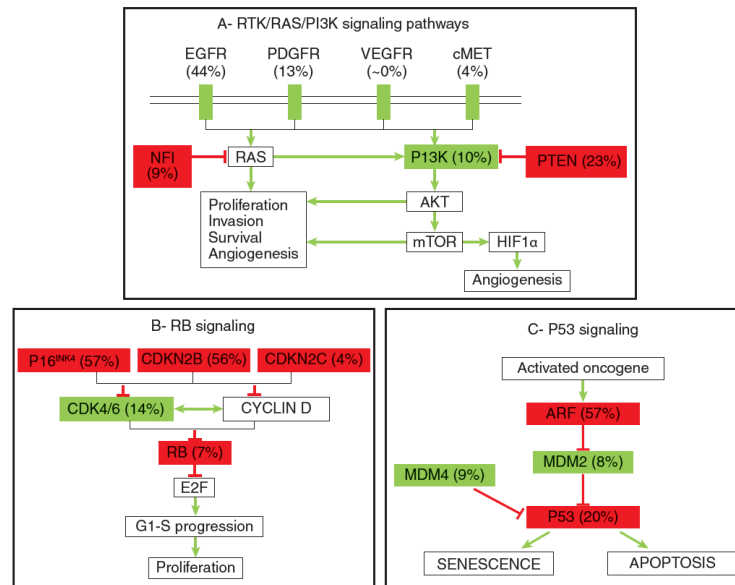


Figure 2: Principal impaired pathways in glioblastoma multiforme (TCGA 2008)

Another important predictive marker during GBM treatment is the methylation of *MGMT* gene promoter. *MGMT* encodes a DNA repair methyltransferase that removes alkyl groups from the O6 position of guanine, where they are introduced by alkylating chemotherapeutic agents (like temozolomide). If left in place, these alkyls would cause incorrect pairing with thymine and trigger MMR system, leading to double strand break of the genome and subsequent arrest of the cell cycle. That is what often happens in high grade gliomas. Conversely, in diffuse gliomas, *MGMT* is frequently hypermethylated, leading to gene silencing and resulting into a more favourable prognosis.

#### 1.2.4. Standard therapies

As mentioned above, glioblastoma multiforme is the most deadly among the four different grade of gliomas due to its frequent relapse and resistance to all current therapies: these include surgical resection associated to radiotherapy and chemotherapy; nevertheless, patients affected by this tumour have a median survival time of 15 month (Stupp et al. 2005). There are several reasons why it is so difficult to find an effective treatment against glioblastoma: first, this tumour is characterised by many genes and pathways that are mis-regulated, meaning that one single therapy should at the same time block or repair all the genes involved (Aliferis and Trafalis 2015), which is hard to achieve; second, it is very tricky to remove all tumour cells during surgery, due to its infiltrating nature; moreover, it's

difficult to carry out an early diagnosis, which is fundamental to improve treatment efficacy; finally, tumour cells could not be efficiently reached by drugs due to the presence of the blood brain barrier, that physically blocks drug diffusion.

At the moment, the current standard of care is based on a combined approach, made up of surgery associated to radiotherapy alone, or with chemotherapy, both before and after surgery. However, such therapies are often proved to be ineffective, given the high rate of relapse and general tumour resistance appearance over time, coupled with a serious neurological deterioration of the patient.

Surgical resection represents the first step of the therapeutic plan, in order to minimize the tumour mass; however, this treatment is limited by the tumour aggressiveness which is characterized by infiltration into surrounding tissue and extensive vascularization. It is followed by a strong hypo-fractionated radiotherapy of 1.8–2 Gy fractions to a total dose of 54–60 Gy.

Radiotherapy is often associated to chemotherapy; at the moment, temozolomide (TMZ) is the preferred FDA-approved chemotherapeutic agent for treating glioblastoma (Alifieris and Trafalis 2015). In particular, GBM-affected patients are treated with a dosage of 75mg/m<sup>2</sup>/daily followed by six cycles of maintenance (150–200 mg/m<sup>2</sup>, 5/28 days) (Perry et al. 2017).

Temozolomide-based chemotherapy is very promising for patients characterized by the methylation of MGMT promoter: as reported above, this protein reduces temozolomide efficacy and treatment success; therefore, methylation of this gene prevents TMZ resistance and increases the median survival times of TMZ-treated patients.

In the last few years, novel approaches have been developed, in particular anti-angiogenic drugs that interfere with the development of blood vessels essential to tumour growth and invasiveness (Friedman et al. 2009).

In 2010, a multigene diagnostic test called DecisionDx-GBM, was developed in order to determine the molecular pattern of GBM tumors and help identify the most effective existing therapy and/or suggest new treatments for tumors that do not respond to the standard therapies (Colman et al. 2010).

Although much efforts have been made to develop new strategies in order to cure and treat this tumour, its heterogeneity, associated to its highly infiltrative nature and aggressiveness render the glioblastoma multiforme incurable.

### 1.3. *Emx2* gene

#### 1.3.1. *Emx2* structure

The empty spiracles homeobox 2 (*Emx2*) gene encodes for a homeobox-containing transcription factor that is one of the two mammalian homologs of the *Drosophila m. 'empty spiracles'* gene. In the mouse genome, the *Emx2* gene is located on chromosome 19; its full mRNA transcript is 2916 bps long and includes three coding exons encoding for a transcription factor of 253 amino acids; there is also a shorter splice variant, of 69 aa. Differently, in the human genome, the gene is located on chromosome 10 and has 4 different mRNA splice variants.

Interestingly, a lncRNA called *EMX2OS* was found both in human and in mouse (Noonan et al. 2003) that overlaps with the *Emx2* mRNA gene head to head. In 2010, Spigoni and colleagues demonstrated that *Emx2* antisense transcript stimulates and refines *Emx2* expression at transcriptional and post-transcriptional levels (Spigoni et al., 2010). In fact, the two transcripts, *Emx2* and its antisense, are both expressed by periventricular neural precursors of the cortical primordium but display a mutually exclusive pattern in post-mitotic progenies of such precursors. While newborn neurons belonging to the cortical plate strongly express *Emx2OS*-ncRNA but not *Emx2*-mRNA, pioneer Cajal-Retzius neurons lying in the marginal zone conversely express huge amounts of *Emx2* mRNA and protein, but no antisense transcript at all.

#### 1.3.2. *Emx2* expression in brain development

*Emx2* is expressed in the developing urogenital and central nervous systems and is involved in the proper morphogenesis of its structures, in particular along the rostro-caudal and dorso-ventral axis (Pellegrini et al. 1996).

During the mouse embryonic development, *Emx2* displays different patterns of expression: it is expressed early during cerebral cortex development, being activated in the mouse embryonic central nervous system at E 8.0-E8.5 (Gulisano et al. 1996): the two major sites of mRNA expression are the anterior CNS and the olfactory epithelium; from this stage, it becomes more expressed in the anterior dorsal neuroectodermal regions of the embryo. At E10, the *Emx2* cerebral domain encompasses the dorsal telencephalon and the floor of the presumptive diencephalon (Simeone et al. 1992) (Simeone et al. 2000) to become more confined to the proliferating neuroepithelium; at this stage it is absent in most postmitotic

cells of the so-called transitional field and the cortical plate; this may suggest that *Emx2* controls the proliferation of pallial neuroblasts and leads the radial migration of neuronal precursors from the ventricular zone onto the forming cortical plate (Simeone et al. 1992) (Gulisano et al. 1996).

At E12.5, *Emx2*-mRNA becomes restricted to the ventricular zone, following a posterior/medial<sup>high</sup>-anterior/lateral<sup>low</sup> gradient. This pattern of expression becomes more pronounced from E14.5 onwards (Simeone et al. 1992) (Gulisano et al. 1996). Furthermore, the distribution of the *Emx2* protein displays the same anterior-posterior and medio-lateral gradient. Until E17.0, *Emx2* domain of expression remains confined to the proliferative layers of the cortex plus the pioneer neurons of Cajal-Retzius (Mallamaci et al. 1998).

As for dorso-ventral specification of the rostral neural tube, it confers cortico-cerebral identity to precursors in the dorsal telencephalic vesicle and represses the activation of striatal morphogenetic programs (Muzio, DiBenedetto, et al. 2002). Furthermore, as for rostro-caudal specification of the CNS, it promotes hippocampus and occipital cortex specification and antagonizes rostral-lateral areal programs (Muzio, DiBenedetto, et al. 2002).

It is also very important in the stimulation of neural precursors' self-renewal, while inhibiting neuronal differentiation; finally, *Emx2* is crucial to proper inside-out layering of the neocortical primordium. In its absence, pioneer Cajal-Retzius cells orchestrating such process are severely reduced and the neocortical lamination profile is deeply distorted, in a *reeler*-like way (Mallamaci et al. 2000)(Shinozaki et al. 2002).

The brain of homozygous *Emx2*-knock-out embryos displays several abnormalities: the dentate gyrus is absent, the hippocampus proper and the medial limbic cortex are greatly reduced in size. The development of neocortical plate is impaired and olfactory bulbs are disorganized and, in addition, the olfactory epithelium fails to project to the olfactory bulb (Yoshida et al. 1997).

Mutations in the human *EMX2* gene have been described to specifically occur in patients affected by schizencephaly, a very rare human congenital malformation characterized by full-thickness clefts within the cerebral hemispheres. This developmental disorder has been hypothesized to be a consequence of defects in neuroblast proliferation and/or neuronal migration (Granata et al. 1997). However this *Emx2* link to schizencephaly has been subsequently questioned (Kim et al. 2007).



Taken together, these findings indicate that *Emx2* may control proliferation and differentiation of neural precursor cells in the VZ and their radial migration into the cortical plate. Furthermore, the observed persistence of *Emx2* protein in postnatal mice (up to P15) in proliferating cells of the subgranular zone of the dentate gyrus (Mallamaci et al. 1998) suggests that this role could be maintained also in adult life.

Gangemi and colleagues found also high *Emx2* levels in adult neural stem cells (NSCs), which decrease upon differentiation into neurons and glia. *Emx2* overexpression in late NSCs has an anti-proliferative effect, suggesting that *Emx2* may act promoting an asymmetric mode of cell division thereby increasing the size of a transit amplifying population. (Gangemi et al. 2001).

Furthermore, its overexpression in the neural stem cell compartment also inhibits astrogenesis, via a cell autonomous way; it leads to a strong decrease of astrocyte-committed progenitors proliferation, resulting in a severe reduction of their ultimate astroglial output, through the downregulation of *Egfr* and *Fgf9* pathways, by promoting *Bmp* signaling and suppressing *Sox2* respectively (Falcone et al. 2015).

### 1.3.3. *Emx2* in tumours

The first evidence of a possible involvement of *Emx2* in human cancers date back to 2001, when Noonan and colleagues discovered a decreased *Emx2* expression in a subset of primary endometrial tumours, and four of six endometrial cancer cell lines tested failed to express this gene (Noonan et al. 2001). Only 9 years later, it was demonstrated for the first time the importance of *Emx2* as a tumour suppressor in lung carcinogenesis. When compared to normal tissue, *Emx2* mRNA and protein levels were found to be less expressed, and this was consistently associated with an hypermethylation of its promoter (Okamoto et al. 2010) (Li et al. 2012). Furthermore, it was proposed also as a prognostic bio-marker for adenocarcinoma, the most prevalent histologic subtype of lung cancer. On a cohort of 144 patients with stage I–IV lung adenocarcinoma, the *EMX2*-high mRNA expressing group had statistically significant better overall survival (OS) and better recurrence-free survival (RFS) than the *EMX2*-low mRNA expressing group (Okamoto et al. 2011).

Dongsheng and colleagues studied the involvement of *Emx2* in another lung tumour, called squamous cell carcinomas (SCC) that accounts for approximately 30% of non-small cell lung cancer (NSCLC). As known, *EMX2* expression was down-regulated in lung SCC tissue samples

compared to their matched adjacent normal tissues; what it's interesting is that positive EMX2 expression was significantly correlated with improved overall survival in stage I lung SCC patients, and in stage II/IIIA lung SCC patients receiving adjuvant chemotherapy. EMX2 expression was also associated with epithelial-mesenchymal transition markers in both lung SCC cell lines and tissue samples. Furthermore, Emx2 knock-down in lung SCC cells promotes chemo-resistance and cell migration (Yue et al. 2015).

The role of Emx2 was also studied in gastric tumorigenesis; Li and colleagues demonstrated for the first time an improved overall survival of mice treated with Emx2-overexpressing adenovirus Ad-EMX2, offering a new tool for gastric tumour gene therapy (Li et al. 2012).

Furthermore, our and Mosser's groups studied *Emx2* involvement in glioblastoma multiforme, a highly invasive primary brain tumour (Monnier et al. 2018; Falcone et al. 2016). In particular, Falcone and colleagues demonstrated that lentiviral *Emx2* overexpression induced the collapse of seven out of seven *in vitro* tested glioblastoma cell lines and it suppressed four out of four of these lines *in vivo*. Moreover, in two out of two tested lines, the tumor culture collapses also when Emx2 was driven by a restricted neural stem cell-specific promoter, likely active within tumor-initiating cells.

The antioncogenic activity of Emx2 may regulate tumorigenesis by affecting different genes and pathways involved mainly in cell cycle control and receptor tyrosine kinase (RTK) cascade (Falcone et al. 2016); furthermore, the canonical Wnt signaling pathway, that regulates cell fate determination, tissue development and tumorigenesis is recurrently impaired (Okamoto et al. 2010) (Li et al. 2012)(Aykut et al. 2017).

## **1.4. Herpetic viral vectors in oncotherapy**

### **1.4.1. HSV-1 structure**

Herpes simplex virus 1 (HSV-1) belongs to the Herpesviridae family and is a large neurotropic enveloped, dsDNA virus. This virus is highly infectious and replicates rapidly, producing progeny particles in approximately 10h.

Its genome consists of 152 kb of linear sequence, which encodes for a minimum of 75 different proteins; it is organised as two unique regions, a long and a short one (UL and US) flanked by inverted repeated sequences (TR<sub>L</sub>, TR<sub>S</sub>, IR<sub>L</sub> and IR<sub>S</sub>), that contain two immediate-early (IE) genes (ICP4 and ICP0), a late (L) gene ( $\gamma$ 34.5) and the latency associated transcripts that are each present in two copies; additionally, the HSV-1 genome harbours three lytic

origins of replication, two located within the unique short (oriS) segment and one in the unique long segment (oriL) (Vlazny and Frenkel 1981). HSV genes can be classified as essential or nonessential based on their requirement for virus replication in a permissive tissue culture environment; the first are required for virus growth, indeed viral mutants lacking these genes can only establish a lytic infection; the second are often required for virus–host cell interactions, such as evasion of the host immune response and are, therefore, required for growth during *in vivo* infection, but are not needed for growth in tissue culture. These nonessential viral functions are manipulated to create oncolytic vectors (Frampton et al. 2005). Approximately half of the genes are not essential for viral replication in cultured cells, and thus can be replaced by exogenous DNA sequences, allowing the development of HSV-1-based vectors for gene therapy (Krisky et al. 1998).

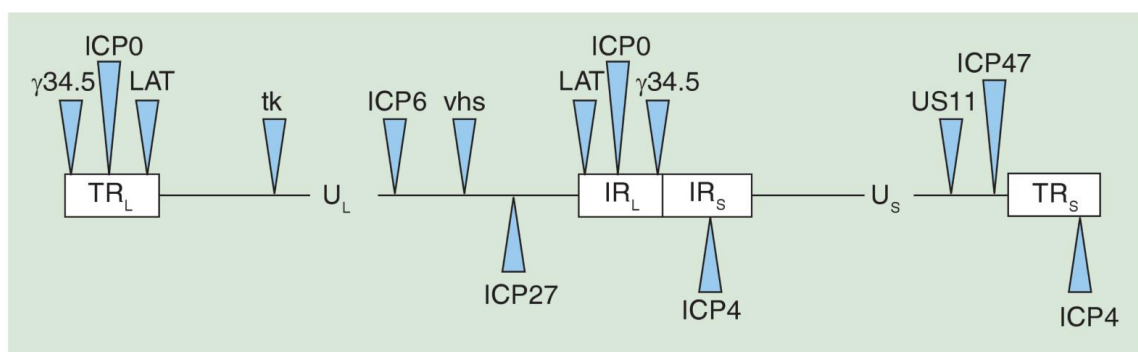


Figure 3: HSV-1 genome (Glorioso 2009)

The genome is encapsulated within an icosahedral capsid, which consists of 162 capsomers made up of four capsid proteins: VP5, VP26, VP23, and VP19C. Furthermore, encapsidation and release of viral DNA occurs through a portal situated within the capsid, which is formed by a dodecamer of the pUL6 protein. The capsid is surrounded by a proteinaceous layer called tegument; it contains primarily virus-encoded proteins involved in transcriptional regulation of immediate-early viral genes (e.g. VP16), and regulation of host-cell transcription (virion-host-shutoff protein); there is also the VP22 protein, which has been implicated in the stabilization of certain viral proteins such as gE, gD and ICP0, and involved in viral spread during lytic infection (Duffy, et al., 2009). Finally, a trilaminar lipid membrane called envelope surrounds the tegument protein layer. It is composed by 10 viral glycoproteins that facilitate receptor-mediated cellular entry during viral infection. Among

these, glycoprotein B (gB), gC, gD, gH, and gL are important for cellular attachment, fusion, and internalization of the virus (Laquerre et al. 1998)(Pertel et al. 2001).

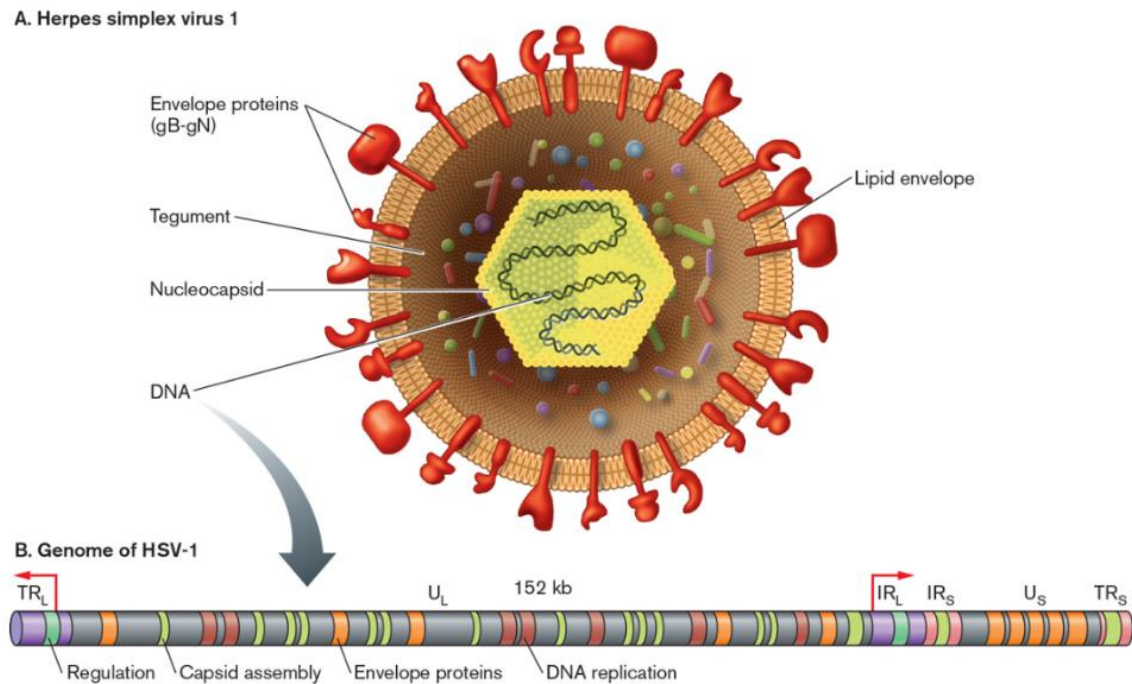


Figure 4: Genome and structure of HSV-1

There are two main phases of transcription: the early phase takes place prior to genome replication, whereas the late phase takes place upon replicated genomes formed in the infected cell nucleus. Three different classes of mRNAs are generated: alpha, beta and gamma, which are regulated in a coordinated, cascade manner. The alpha transcript contains the five immediate-early genes, encoding for regulatory proteins, whose production is required for the transcription of the Beta and Gamma gene classes; among these proteins, ICP4 is the major regulatory one, essential for viral replication and transactivation of the other two transcripts. Immediate early transcription takes place at five promoters immediately upon the viral genomes entering the nucleus. Here, virion-associated Alpha-TIF binds to cellular Oct1, which has bound to TAATGARAT sequences in enhancers upstream of the immediate early promoters, allowing the assembly of the pre-initiation complex (Sp1, TBC, CTF and CTB) at the TATA box site and the subsequent transcription mediated by RNA Pol-II (Li et al. 2017). Immediate early transcripts are then transported to the cytoplasm, translated, and the IE proteins return to the nucleus. All

further transcription requires the action of these proteins, particularly the Alpha4 protein, which is a generalized transcription activator that works by binding multiple sites on the genome and then interacts with nearby TATA boxes in order to facilitate the assembly of pre-initiation complexes and activate Beta or early gene expression. The Beta proteins include enzymes that are essential for viral genome replication: a DNA polymerase, a single-strand DNA-binding protein, a primosome or helicase-primase, an origin-binding protein, and a set of enzymes implicated in DNA repair and in deoxynucleotide metabolism.

Beta proteins appearance initiates the viral DNA synthesis, which ends with the presence of Gamma or late proteins, that represent the structural proteins of the virus. This late transcription is controlled by several promoters that have different functional architectures but share many sequence elements downstream of the TATA box, essential in stabilizing the formation of pre-initiation complexes.

#### *1.4.2. HSV-1 life cycle*

Once a viral particle entered host cell, the lytic phase begins, leading to a productive infection or establishing latency in the nuclei of sensory neurons upon retrograde transport of the virus. Not well understood are the molecular and viral factors that control which phase the virus will enter. Natural HSV-1 lytic cycle begins with the virus attachment to the plasma membrane of host cells; this process is mediated by the activity of three essential glycoproteins present in the virus lipid envelope: gB, gD and gH. Among these, gD engages the virus receptor and subsequently signals the other essential components to mediate fusion/entry of the envelope with the cellular plasma membrane. The target cell interacts with different receptors, including HVEM (HveA), nectin-1 (HveC), 3-O-sulfated heparin sulfate and nectin-2 (HveB) (Frampton et al. 2005). The viral capsids are transported from the entry site to the nucleus of the host cell by the microtubules-mediated retrograde axonal transport, where the viral genes are expressed in a tightly regulated, interdependent temporal sequence and consist of IE, early (E) and L gene functions. The IE gene products (infected cell proteins ICP0, ICP4, ICP22, ICP27 and ICP47) induce expression of E genes that encode enzymes necessary for viral DNA replication and L genes that encode structural proteins involved in virion assembly. The envelope is acquired by budding through the nuclear membrane with further envelope processing in the cytoplasmic Golgi complex.

Finally, the newly formed infectious viral particles could be transported anterogradely to the termini of the axon where they fuse with the cell membrane and are released into the extracellular space. The viral replication cycle could also lead to a rapid cell death, inducing a release of new viral particles during cell lysis. An exception is virus infection of sensory neurons, where latency is established with long-term viral genome persistence as a circular episome. During this quiescent state, the viral lytic genes are silenced whereas the viral latency-associated transcripts (LATs) are transcribed. Recent studies have demonstrated that these non-protein coding LATs play a role in regulating the assembly of facultative heterochromatin on lytic gene promoters, thereby inducing transcriptional repression (Cliffe, Garber, and Knipe 2009)(Kwiatkowski, Thompson, and Bloom 2009). Alterations in virus-host interactions can lead to the “reactivation” of the latent HSV-1 genome, resulting in a productive infection. The virus lytic cycle occurring in tumour cells defines the oncolytic virus OV phenotype (Glorioso 2009).

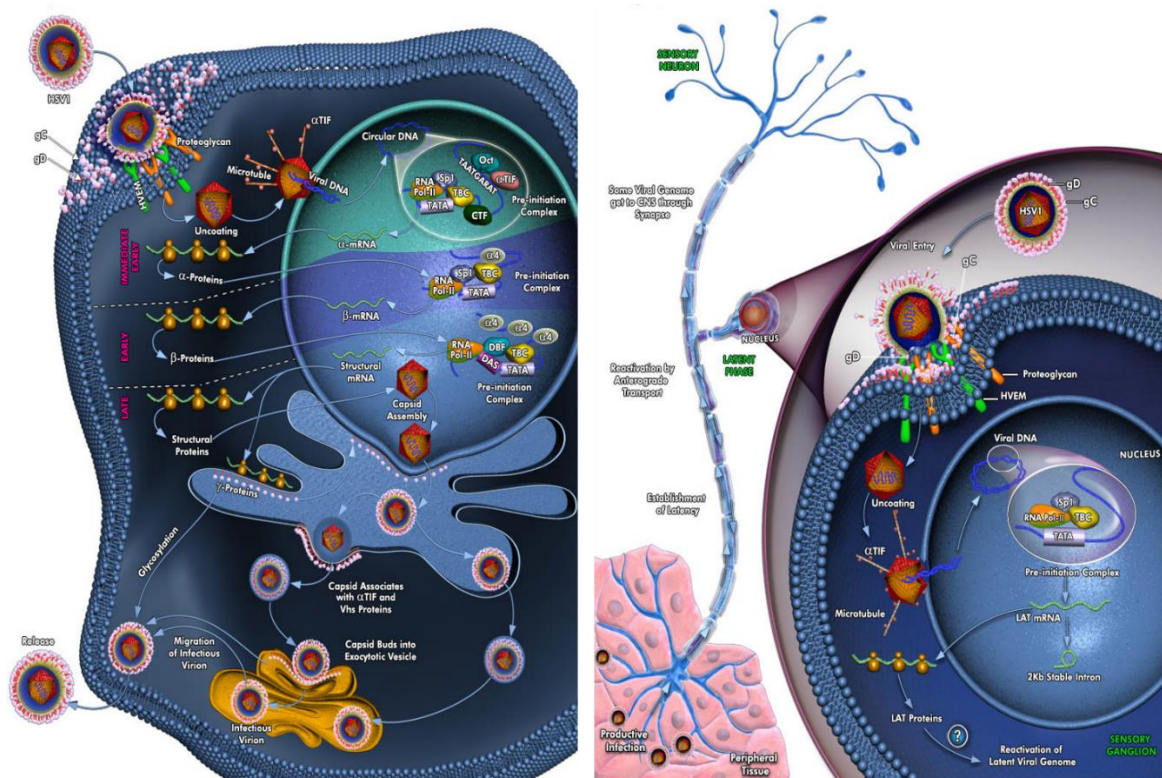


Figure 5: Lytic and latent HSV-1 cycle (Qiagen)

### 1.4.3. HSV-1 vector generation

As mentioned before, HSV-1 genome contains a significant portion of coding sequences that are considered “non-essential” and can be removed without affecting viral replication in cultured cells. These findings have paved the way to the development of several HSV-1-derived vectors: conditionally replicating vectors, replication-defective vectors, and amplicon-based vectors.

Conditionally replicating HSV-1 vectors can replicate only in specific cell types and tissue types *in vivo*, due to the deletion of non-essential viral genes, such as thymidine kinase and ICP34. These vectors, referred to as oncolytic HSV-1 vectors, were employed as therapeutic strategies for malignant brain tumours, including glioblastoma multiforme. Since replication is restricted to rapidly proliferating tumour cells, it has been possible to employ suicide gene therapy for the targeted destruction of these malignant cells. However, replication-defective HSV-1 vectors, even if deprived of genes necessary for lytic replication and reactivation, like the immediate early genes ICP0, ICP4, ICP27, and ICP47, are still able to establish cellular latency (de Silva and Bowers 2009).

Consequently, replication-defective recombinant HSV-1 virions require the use of complementing cell lines to produce the deleted viral gene product, which is essential for replication and virion production. The ability for these vectors to maintain latency within the transduced cell has enabled the design of gene transfer modalities using replication defective HSV-1 vectors; this approach was adopted for the treatment of some neurodegenerative diseases and chronic pain (Glorioso 2009).

Furthermore, Assudani and colleagues developed a new model of antitumor viral vector, called disabled infectious single cycle herpes simplex virus (DISC-HIV) that efficiently transduces various tumour cell lines, suggesting a new useful tool for the further development of cell-based vaccines. More in detail, HSV genome was deleted for glycoprotein H (gH), limiting its capacity of single round of infection. This strategy allows the virus to propagate after infecting the susceptible cells, but the progeny is non-infectious, thus preventing the subsequent infection of other cells (Assudani et al. 2006).

Finally, Spaete and Frenkel generated another type of replication-defective HSV-1 vector, through the incorporation of a single origin of replication (*oriS*) and a single packaging/cleavage signal (*pac*) from the wild-type HSV-1 genome into a standard bacterial plasmid, which they termed “amplicon” (Spaete and Frenkel 1982). A transgene expression

cassette can be cloned into the amplicon plasmid, and subsequently replicated and packaged into defective viral particles using several strategies.

#### *1.4.4. Oncolytic HSV viruses*

Oncolytic virus immunotherapy is a newly and highly versatile platform for the treatment of cancer that employs native or genetically modified viruses that selectively replicate within tumour cells in situ, leading to cell lysis and death.

Oncolytic viruses have been generated from both DNA and RNA viruses: DNA viruses are advantageous due to their large genome, that could be edited without impairing viral replication; they also express high fidelity DNA polymerases, ensuring viral genome integrity and efficient replication (Kaufman, Kohlhapp, and Zloza 2015); on the other hand, RNA viruses are smaller, leading them to cross the blood brain barrier, making them a powerful tool for targeting tumours of the central nervous system, although their small genome limits their ability to encode large transgenes; they are also more suitable for systemic delivery.

Oncolytic viruses are thought to mediate anti-tumour activity through two distinct mechanisms: they replicate selectively in cancer cells, leading to a direct lytic effect and activate a systemic antitumor immunity. Different factors may contribute to the implementation of these mechanisms, depending on the nature and type of cancer cell, the characteristics of the viral vector, and the interaction between the virus, tumour microenvironment and host immune system; for example, certain viruses have the ability to enter cancer cells and selectively replicate within these cells. Although oncolytic viruses can enter both normal and cancer cells, they can find an advantageous environment for their replications in tumour cells, due to their inherent abnormalities in cell response to stress, cell signalling and homeostasis (Hanahan and Weinberg 2011); furthermore, the antiviral machinery, which is responsible for the detection and clearance of viruses, may be abnormal in tumour cells. For example, the protein kinase R (PKR), an essential protein involved in the clearance of intracellular viral infections, may be absent in some tumour cells, allowing increased viral replication, whereas it may be active in others, such as low-grade tumours, and these differences can influence the therapeutic activity of an oncolytic virus.

The anti-oncogenic activity of oncolytic viruses affects several key steps in the cancer cycle: most of them act through the direct killing of host tumour cells and this activity depends on the efficiency of cell receptor targeting, viral replication and host cell antiviral response



elements. Moreover, cell lysis could also be influenced by the type of virus, its dosage, natural and induced viral tropism, and the susceptibility of the cancer cell to the different forms of cell death (such as apoptosis, necrosis, pyroptosis and autophagy).

Furthermore, they induce immunogenic cell death and release of soluble factors and danger signals, recruiting immature dendritic cells and innate lymphoid cells and starting the innate immune responses.

In non-neoplastic cells, pathogenic viral particles are detected and cleaned by different signalling pathways (fig. 5), that can be activated by the presence of local interferon (IFN) or through extracellular and intracellular Toll-like receptors (TLRs), which are activated by specific antigens called pathogen-associated molecular patterns (PAMPs): these latter include viral elements such as DNA and RNA, viral protein products or capsid elements. The TLRs stimulation leads to the activation of antiviral responses and systemic innate immunity. Several downstream host cell factors involved in oncolytic virus clearance have been identified, including TNF-associated factor 3 (TRAF3), IFN-related factor 3 (IRF3), IRF7 and retinoic acid-inducible gene 1 (RIG-1). These factors activate the JAK–STAT pathway, which coordinates the antiviral machinery in infected cells. The antiviral machinery supports local IFN release, which in turn activates an intracellular protein kinase, called PKR, that recognizes double-stranded RNA and other viral components, leading to protein synthesis blockage and cell death promotion. In tumour cells, the IFN pathway is impaired and PKR activity may be abnormal, avoiding viral clearance (Kaufman et al. 2015).

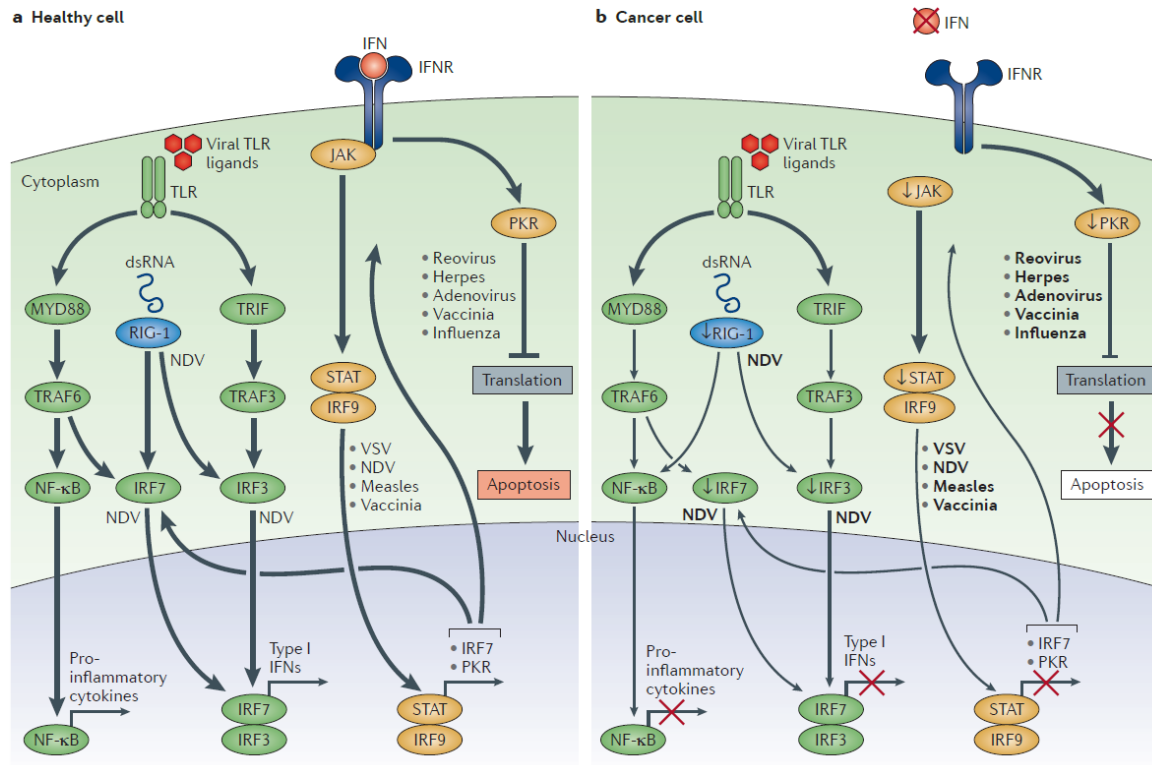


Figure 6: Oncolytic viruses can exploit cancer immune evasion pathways (Kaufman et al. 2015).

To date, different classes of viruses were employed into early phase clinical trials, including adenoviruses, poxviruses, HSV-1, coxsackieviruses, poliovirus, measles virus, Newcastle disease virus (NDV), reovirus, and others (Martuza et al. 1991); DNA or RNA virus choice depends on different aspects, that take into account their potential pathogenicity, immunogenicity, tumour tropism, their ability to encode therapeutic transgenes and the viral stability (Bommareddy, Shettigar, and Kaufman 2018).

The first oncolytic virus immunotherapy approved by the US Food and Drug Administration (FDA) for the treatment of cancer is called talimogene laherparepvec (T-VEC; Amgen) and it is a modified herpes simplex virus type 1 (HSV-1), encoding for granulocyte–macrophage colony-stimulating factor (GM-CSF): in a recent randomized Phase III clinical trial, it was demonstrated an improved durable response rate for patients with advanced melanoma treated with it (Andtbacka et al. 2015).

Several oncolytic viruses have been tested in clinical trial against glioblastoma multiforme: in particular, G207, a doubly mutated HSV-1 (deletion of both  $\gamma$ 134.5 loci and insertional inactivation of UL39) was stereo-tactically inoculated in patients with recurrent malignant gliomas, showing radiographic and neuropathologic evidence of antitumor activity; furthermore, no patient developed HSV encephalitis or required treatment with acyclovir;

finally, it was reported the safety for multiple dose delivery, including direct inoculation into the brain surrounding tumor resection cavity (Markert et al. 2009).

One of the strategies in cancer gene therapy is the employment of genetically engineered, replication-conditional oncolytic viruses to deliver cytotoxic genes to neoplastic cells as well as destroy them directly via lytic infection. The use of replication-conditional HSV-1 mutants seems to be promising for both purposes, as its intra-neoplastic replication should allow enhanced anatomic spread of anticancer effects throughout an inoculated tumor mass and augmentation of this effect by delivery of anticancer genes. This might circumvent the limited anatomic spread observed with the inoculation of replication-defective vectors and/or producer cells into human tumours (Chung, Saeki, and Chiocca 1999).

For example, myb34.5 is a HSV-1 mutant virus deleted in the gene for ribonucleotide reductase ICP6. It also carries a version of  $\gamma_134.5$ , a viral gene product that promotes the dephosphorylation of eIF-2 $\alpha$ , that is under control of the E2F-responsive cellular B-myb promoter, rather than of its endogenous promoter. Infection and replication of Myb34.5 in tumour cells results in their destruction, a process called oncolysis.  $\gamma_134.5$  expression by HSV-1 subverts an important cell defence mechanism against viral replication by preventing shutoff of protein synthesis after viral infection (figure 7). Nakamura and colleagues demonstrated that colon carcinoma cells infected with Myb34.5 display a greater eIF-2 $\alpha$  dephosphorylation and viral replication compared with HSV-1 mutants infection, completely lacking the  $\gamma_134.5$  expression. Furthermore, when injected intravascularly into mice with diffuse liver metastases, Myb34.5 displays a huge anti-oncogenic activity, a more controlled biodistribution, and a reduced virulence and toxicity compared with HSV-1 mutants, lacking  $\gamma_134.5$  expression. (Nakamura et al. 2002).

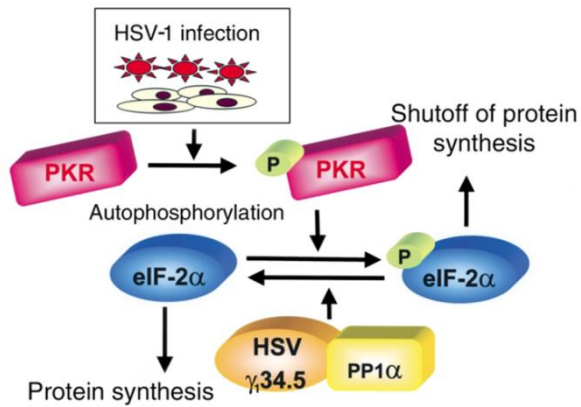


Figure 7: Diagram of the regulation of protein synthesis by  $\gamma_{134.5}$  in HSV-1–infected cells. (Nakamura et al. 2002)

#### 1.4.5. Amplicon HSV vectors

Amplicon vectors can be considered as “modular viruses” as they are HSV-1 cloning-amplifying defective virus particles, identical to wild type HSV-1 from the structural and host-range point of view, but which carry a concatemeric form of a DNA plasmid, named amplicon plasmid, instead of the 152 Kb viral genome.

The conventional HSV-1 amplicon vector consists of a plasmid backbone harbouring a bacterial origin of DNA replication (e.g. ColE1) and an antibiotic resistance gene (e.g., AmpR) for propagation in prokaryotic cells; furthermore, there are two non-coding sequences from the wild-type HSV-1 genome required for replication (ori) and packaging (pac) of the amplicon into infectious particles and finally a transgene expression cassette (figure 8) (de Silva and Bowers 2009). Once packaged into viral particles in the presence of helper viruses, the amplicon vector, which is completely replication-defective, is able to infect different cell types, without integrating into the genome but maintaining an episomal state within the nucleus of the transduced cell; on one hand, it confers a stable expression in post-mitotic, non-dividing cells but on the other, it undergoes to unequal segregation in proliferating cells, allowing a transient gene expression.

As a gene delivery vector, the conventional amplicon can deliver transgene units up to 150 kb in size; furthermore, since it does not integrate into the genome, host cells do not undergo insertional mutagenesis, thus increasing its safety profile as a gene therapy vector. (de Silva and Bowers 2009).

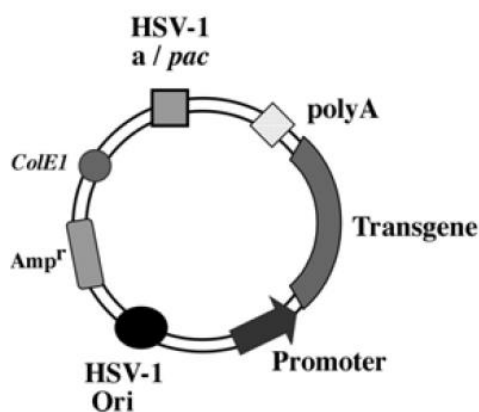


Figure 8: Amplicon vector genome structure. (Modified from De silva et al., 2009).

The ability to deliver exogenous genetic material up to 150 kb, associated with its capacity to efficiently transduce numerous cell types, including those of the central nervous system (CNS), a strong gene expression due to high copy number and high multiplicity of infection makes HSV-1 amplicon a versatile gene transfer vector for the treatment of several disorders and conditions affecting the CNS.

Furthermore, these “modular viruses” confer a stable gene expression without modification of the cell genome, an homogeneous gene expression as different genes can be transferred at once from the same amplicon vector as well as physiological gene expression can be achieved as a complete genomic locus can be introduced in one single vector; finally, they are completely safe (Epstein 2005).

Nevertheless, limitations are still present in the production of amplicon vectors, indeed they require a co-propagated HSV-1 helper virus, resulting in viral stocks that are a mixture of helper and amplicon viruses. Furthermore, in the past, nonspecific cytotoxic effects of defective amplicon vectors limited the amount of vector that could be used to infect cells.

A variety of anti-cancer therapies utilizing HSV-1 amplicon vectors are currently being investigated in preclinical animal models. In particular, referring to glioblastoma multiforme, HSV-1 amplicons have also been utilized to deliver genes involved in pro-drug activation (e.g., thymidine kinase) (Wang et al. 2002) and apoptosis (e.g., TRAIL) (Shah et al. 2003), or they have been used to express double stranded-hairpin RNA for targeted knockdown of EGFR in human Gli36 glioma cells (Saydam et al. 2005).

## 2. AIM

*Emx2* is a homeobox gene whose family encodes for transcription factors that play a prominent role in the regulation of morphogenesis and cell differentiation during embryogenesis. In particular, during astrogenesis, a prolonged overexpression of this gene in early pallial neural stem cells induces a marked decrease of the glial output, by decreasing the proliferation of astrocyte-committed precursors. This control takes place via a functional cascade, which includes Bmp signalling and *Sox2*, through the downregulation of *Egfr* and *Fgf9* (Falcone et al. 2015).

Moreover, recent studies suggest a possible involvement of *Emx2* in several human cancers, including lung, colorectal and gastric tumours (Okamoto et al., 2010, Li et al. 2012, Aykut et al. 2017). Inspired by these findings, we wondered if *Emx2* overexpression might be employed as a therapeutic tool against glioblastoma multiforme.

Our group has previously demonstrated that *Emx2* overexpression induces the collapse of GBM cultures in around one week, by promoting cell death and inhibiting cell proliferation. The impact on GBM metabolism was very complex and a huge number of genes and pathways sensitive to its overexpression are misregulated (Falcone et al. 2016).

Starting from these data, aims of my projects are:

- ✚ validate the efficacy of *Emx2* gene therapy in long term *in vivo* experiments, with special emphasis on its impact on survival of GBM-transplanted animals;
- ✚ evaluate the efficacy of *Emx2* gene therapy, especially its possible interaction with current standard therapies;
- ✚ identify possible mediators and pathways involved in *Emx2*-mediated chemo-and radio-sensitivity, in order to overcome tumour resistance;
- ✚ develop novel, effective and biosafe strategies for *in vivo* delivery of *Emx2*, overcoming intrinsic limits of lentiviral transduction we have employed until now.

## 3. MATERIALS and METHODS

### 3.1. *Lentiviral vectors packaging and titration*

Third generation self-inactivating (SIN) lentiviral vectors (LVs) were generated as previously described (Follenzi and Naldini, 2002) with some adjustments. In brief, HEK293T cells were co-transfected with the transfer vector plasmid plus three auxiliary plasmids in the presence of LipoD293™ (SigmaGen). Auxiliary plasmids are different depending on integrating or not integrating LVs. pMD2 VSV.G, pMDLg/pRRE and pRSV-REV are employed for integrating competent LVs packaging, whereas pMD2 VSV.G, pRSV-REV and pMD.Lg/pRRE.D64Vin are specific for integrating defective LVs (ID-LVs).



The conditioned medium was collected after 48 and 72 hours, filtered 0,45um and ultra-centrifuged at 50000 RCF on a fixed angle rotor (JA25.50 Beckmann Coulter) for 3 hours at 4°C. Lentiviral pellets were then resuspended in PBS 1X without BSA (Gibco).

LVs were titrated by Real Time quantitative PCR after infection of HEK293T cells, as previously reported (Sastry et al., 2002). One end point fluorescence titrated LV was included in each PCR titration session and PCR-titers were adjusted to fluorescence-equivalent titers throughout the study.

Where necessary, specific lentiviral plasmids were constructed with basic cloning techniques. DNA manipulations (extraction, purification and ligation), bacterial cultures and transformations were performed according to standard methods. Restriction and modification enzymes were obtained from New England Biolabs and Promega; DNA fragments were purified from agarose gel by QIAquick Gel Extraction Kit (Qiagen); plasmid preparations were done by DN PLASMID PURIFICATION KIT (Qiagen). Plasmids were grown in E. Coli, XL1-blue or ElectroMAX™ Stbl4™ Competent Cells (Invitrogen).

LVs used for this study were referred to throughout the thesis according to the standard nomenclature: LV:pX-GOI, where pX is the promoter and GOI is the gene of interest.

They were:

-  LV\_pPgk1-rtTA2S-M2-WPRE (Spigoni et al., 2010),
-  LV\_pPgk1-tTA-WPRE, obtained by transferring the BamHI/XhoI-cut tTA-cds fragment from LV:pTYF-1xSYN-tTA (Addgene #19980) into the BamHI/SalI-cut LV\_pPgk1-EGFP-WPRE, in place of EGFP.

- ✚ LV\_TREt-Emx2-IRES2-EGFP (Brancaccio et al., 2010);
- ✚ LV\_TREt-Emx2-WPRE, aka LV:TREt-Emx2 (Furuta et al., 1997);
- ✚ LV\_TREt-Foxg1 (Raciti et al. 2013);
- ✚ LV\_Pgk1p-mCherry-WPRE, constructed by transferring the mCherry module from LV\_pTa1- mCherry into LV\_pPgk1-EGFP-WPRE, in place of EGFP;
- ✚ LV\_TREt-IRES2-EGFP (derived from LV:TREt-luc- IRES2-EGFP, via deletion of the luc and the IRES2-EGFP cassettes, respectively)
- ✚ LV\_TREt-IRES-PLAP-WPRE, obtained by replacing the XhoI/SalI fragment of LV\_Pgk1p-EGFP-WPRE (see below) by an XhoI-compatible/ SalI-compatible element, including the XbaI-AgeI 0.35kb TREt fragment of P199 and the EcoRI/ SalI 2.2kb IRES-PLAP fragment from pCLE [5];
- ✚ LV\_TREt-Sox2, aka TetO-FUW-sox2 (Brambrink et al., 2008), corresponding to plasmid #20326 of the Addgene collection;
- ✚ LV\_pCCLsin.PPT.hPGK.EGFR.pre (Mazzoleni et al. 2010);
- ✚ pCVL Traffic Light Reporter 1.1 (Sce target) Ef1a Puro, after called TLR (Addgene 31482).
- ✚ pCVL SFFV d14GFP EF1s HA.NLS.Sce(opt), after called SceI + donor (Addgene 31476).
- ✚ pCVL SFFV d14GFP Donor (Addgene 31475)
- ✚ pCVL SFFV-EF1s HA.NLS.Sce(opt) (Addgene 31479)
- ✚ LV\_U6p-ctr-shRNA, obtained by cleaving the NotI-EcoRI fragment from LV\_ctr-shRNA-EGFP, aka pll3.7 (Addgene #11795).
- ✚ LV\_U6p-anti mouse Foxg1-shRNA (Sigma # SHCLND-NM\_008241)

All lentiviruses were generated and titrated as previously described (Brancaccio et al., 2010).

### ***3.2. Animal handling and embryo dissection***

Animal handling and subsequent procedures were in accordance to European and Italian laws [European Parliament and Council Directive of 22 September 2010 (2010/63/EU); Italian Government Decree of 4 March 2014, n°26]. Experimental protocols were approved by SISSA OpBA (Institutional SISSA Committee for Animal Care). Mapt<sup>EGFP/+</sup> (Tucker, Meyer, and Barde 2001) or wt CD1 males were mated to wt CD1 females (purchased from Envigo Laboratories, Italy) and maintained at the SISSA mouse facility.



All embryos were staged by timed breeding and vaginal plug inspection. Pregnant females were sacrificed by cervical dislocation and embryonic cortices were dissected out in cold PBS, under sterile conditions. *Mapt*<sup>EGFP/+</sup> E16.5 embryos were distinguished from their wild type littermates by inspection under fluorescence microscope.

### **3.3. GBM mice xenografts**

For long term *in vivo* experiment, nude (strain: Hsd:AthymicNude-Foxn1nu) mice were used. 6-weeks-old females were anaesthetized with Ketamine-Xylazine solution. 5 $\mu$ l of a solution containing pre-engineered 300,000 U87MG cells in DMEM-Glutamax medium, was injected through the skull into the striatum, by Hamilton syringe (Hamilton #7105KH), following the stereotaxic coordinates: AP +0.5; L -1.8; V -2.8.

More in detail, one week before the *in vivo* transplantation, U87MG cells were infected with LV\_ P<sub>gk1p</sub>-tTA-WPRE and LV\_TREt-IRES-EGFP-WPRE (Ctrl) or LV\_TREt-Emx2-IRES-EGFP-WPRE (Emx2-GOF), each at a moi = 16 in a medium containing 2 $\mu$ g/mL doxycycline. One day before the injection, the medium was discarded and replaced with a new one, containing a 10% TET-free FBS.

Half of mice (27/54) were injected with 300,000 Control-EGFP<sup>+</sup> U87 cells and the other (27/54) with 300,000 *Emx2*-GOF-EGFP<sup>+</sup> cells. Four days later, we administrated temozolomide to 13 out of 27 “Control” or “Emx2-GOF” transplanted mice (5mg/kg body weight\*day by drinking water).

Animals were left to recover in a warm clean cage. Then, they were checked each day and sacrificed when they showed clear symptoms of suffering. Survival curves were drawn.

### **3.4. Glioblastoma cell cultures**

Human U87MG and U251 grade IV GBM cell lines were purchased from SIGMA (#89081402 and #09063001, respectively). Low passage criopreserved samples of them were employed to perform the experiments. They were kept as adherent cultures in DMEM/Glutamax medium (ThermoFisher, #31966), supplemented with 10% FBS and 1X Pencillin/Streptomycin. Cells were cultured at 2\*10<sup>6</sup> cells in T75 flask and trypsinized at confluency.

Glioblastoma primary cells originate from GBM surgical samples, collected at IRCCS A.O.U. San Martino-IST, Dept of Neuroscience and Sense organs, Unit of Neurosurgery and

Neurotraumatology, with patients' informed consent and in compliance with pertinent Italian law.

They were derived in Antonio Daga laboratory. Low passage criopreserved samples were employed to perform the experiments. GbmA, GbmC, GbmF and GbmG cells were cultured as spheres in NeuroCult™ NS-A Proliferation Kit (Human) (StemCell Technologies, Vancouver - Canada, #05751) supplemented with 1X Penicillin/Streptomycin, 2 µg/ml human heparin (StemCell Technologies #07980), 20 ng/ml recombinant human EGF (ThermoFisher #PHG0311), 20 ng/ml recombinant human FGF2 (ThermoFisher #PHG0261). Primary GBM cells were cultured at  $2 \times 10^6$  cells in T75 flask and passaged by Accutase (Sigma, Milan - Italy, #A6964) once confluent.

Both primary and commercial cell lines were cultured under normoxic conditions (5% CO<sub>2</sub>, 21% O<sub>2</sub>, 74% N<sub>2</sub>).

### **3.5. GBM cell growth curves under temozolomide treatment**

$2 \times 10^5$  U87MG, U251, GbmA and GbmF cells were plated in a 12-well plate and infected with LV\_ P<sub>gk1p</sub>-rtTA-M2-WPRE and LV\_TREt-IRES-EGFP-WPRE (Ctrl) or LV\_TREt-Emx2-IRES-EGFP-WPRE (*Emx2*-GOF), each at a multiplicity of infection (moi) = 8. This moi is enough to infect the almost totality of GBM cells. After three days, doxycycline at 2 µg/mL (Sigma #D9891- 10G) and temozolomide at 200 µM (for U87MG, GbmA and GbmF cells) or 1800 µM (for U251) were added to the medium; viable cells (trypan blue-excluding) were counted at fixed days on a hemocytometer. After every cell count, differently engineered cells were plated at the same concentration ( $2 \times 10^5$  GBM cells/well). Growth curves were interrupted when *Emx2*-GOF/TMZ cell cultures had collapsed.

### **3.6. GBM cell growth curves upon X-rays treatment**

$5 \times 10^5$  U87MG and U251 cells/flask were plated in T25 flasks and irradiated after 24 hours with different X-rays dosage (5-10-15Gy). Viable cells (trypan blue-excluding) were trypsinized and counted at fixed days on a hemocytometer.

\* \* \*

Subsequently,  $5 \times 10^5$  U87MG and U251 cells/flask were plated in T25 flasks and acutely infected with LV\_ p<sub>gk1p</sub>-rtTA-M2-WPRE and LV\_TREt-IRES-EGFP-WPRE (Ctrl) or LV\_TREt-Emx2-IRES-EGFP-WPRE (*Emx2*-GOF), each at moi 8. After 5 days, we changed the medium

by adding 1ng/mL or 30ng/mL doxycycline for U87MG and U251 respectively, and the subsequent day cells were trypsinized and replated at  $1.2 \times 10^6$  cells/flask. 24hrs later, cells were irradiated with 15Gy X-rays dosage. Viable cells (trypan blue-excluding) were counted at fixed days on a hemocytometer. After every cell count, differently engineered cells were plated at the concentration of  $2 \times 10^5$ /well. Growth curves were interrupted when *Emx2*-GOF/X-rays cell cultures had collapsed.

### ***3.7. GBM cell growth curves upon Myb34.5 HSV-1 infection***

The experiment was performed on 2 GBM lines (U87MG and U251) and 2 primary GBM cultures (GbmA and GbmG).  $2 \times 10^5$  cells were seeded in 12-multiwell plate and infected with the oncolytic Myb34.5 HSV-1 at different moi of infection. Viable cells (trypan blue-excluding) were counted at fixed days on a hemocytometer, until cell cultures had collapsed.

### ***3.8. U87MG and murine neocortical tissue co-cultures upon Myb34.5 HSV-1 infection***

*Mapt*<sup>EGFP/+</sup> or CD1 wild type cortical tissue from E17.5 mouse embryos was chopped to small pieces for 5 minutes, in a small volume of ice-cold 1X PBS – 0,6% glucose and 0,1% DNaseI. The minced tissue was then resuspended and digested in 0.25mg/ml trypsin and 4mg/ml DNaseI for 5 minutes at 37°C. Digestion was stopped by adding  $\geq 1.5$  volumes of DMEM/F12/10% FBS. Cortices were spun down and transferred to differentiative medium. The suspension was pipetted 5-8 times with a P1000 gilson pipette and undissociated tissue was left to sediment for 1-2 minutes. The supernatant was collected and living cells were counted.

$1 \times 10^5$  cells were seeded on poly-L-Lysine coated 24-multiwell plates, in 600 $\mu$  of culturing medium: Neurobasal-A, 1X Glutamax (Gibco), 1X B27 supplement (Invitrogen), L-glutamate 25  $\mu$ M, 25  $\mu$ M  $\beta$ -Mercaptoethanol, 2% FBS, 1X Pen/Strept (Gibco), 10 pg/ml fungizone (Gibco).

*Mapt*<sup>EGFP/+</sup> mixed neuronal-astroglial primary cultures were infected after three days with the oncolytic Myb34.5 HSV-1 at moi 0.01 or 0.005; the same day, also mCherry-labelled U87MG cells, plated separately, underwent Myb34.5 infection, at moi 0.01 or 0.005; 24hrs later,  $0.5 \times 10^5$  of these m-Cherry-labelled infected U87MG cells were transferred onto infected neocortex precursors. FACS analysis was performed at post-infection in vitro days

PI-IVD 4 and 8, in order to count the total number of EGFP-labelled neurons and mCherry-labelled U87MG cells. Concomitantly, an immunofluorescence against TUBB3 and GFAP was performed on CD1-WT mouse neocortex cells at post-infection in vitro days PI-IVD 4, to evaluate the neuronal and glial morphology. Briefly, cells were incubated with blocking solution for 40min at RT after being permeabilized with PBS1X + TRITON 0,1% for 10min at RT; they were then incubated with anti-GFAP rabbit polyclonal (DAKO #Z0334) at 1:600 and anti-Tubb3 (TUJ1) mouse monoclonal (Biolegend #MMS-435P) at 1:1000 overnight at 4°C. The following secondary antibodies were used: Alexa 488 goat anti rabbit and Alexa 594 goat anti mouse. Cells were counterstained with DAPI 1:200 for 15 min. Immunofluorescence was photographed on a Nikon Eclipse TI microscope equipped with a 20X objective and a Hamamatsu camera.

### ***3.9. U87MG cell growth curves upon Myb34.5 HSV-1 and Emx2-LV infection***

2x10<sup>5</sup> U87 cells were seeded in 12-multiwell plate and infected with with LV\_ pPgk1-rtTA-M2-WPRE and LV\_TREt-IRES-EGFP-WPRE (Ctrl) or LV\_TREt-Emx2-IRES-EGFP-WPRE (*Emx2-GOF*), each at moi 8. 3 days later, cells were trypsinized, replated in a 12-multiwell plate at the same density in a medium containing 1ng/ml doxycycline and infected with the oncolytic Myb34.5 HSV-1 at moi 0.005. Viable cells (trypan blue-excluding) were counted on a hemocytometer at fixed days, until cell cultures had collapsed.

### ***3.10. U87MG cells host Myb34.5-helped amplification of Egfp-encoding herpetoviral amplicon vector (vAM-GFP)***

As a substrate potentially permissive to Myb34.5-helped vAM-GFP amplification, 2x10<sup>5</sup> U87MG R-cells (R-cells, "reactor") were seeded in 12-multiwell plate and coinfecting by Myb34.5 HSV-1, at moi 0.01, and vAM-GFP, at moi 5, in all four possible Myb34.5 and vAM-GFP combinations. To secure herpetoviral infection and remove the excess of primarily infecting viral particles, 8 hours later, cell medium was discarded, cells were washed twice with 1X PBS and cultured with new fresh medium. Next, 3 days later, one half of such new medium (plus an equal volume of fresh medium) was transferred to U251 S-cells (S-cells, "sensor") which, 3 more days later, were scored for the presence of EGFP<sup>+</sup>-expressing elements, as an index of U87MG-hosted vAM-GFP neosynthesis. Native EGFP<sup>+</sup> U251 S-cells

were photographed on a Nikon Eclipse TI microscope equipped with a 20X objective and a Hamamatsu camera.

### ***3.11. "Healthy" human perinatal neocortex tissue hosts Myb34.5-helped amplification of Egfp-encoding herpetoviral amplicon vector (vAM-GFP)***

Human neural precursors were provided by Dr. Stefano Pluchino (Cambridge University, UK). These cells were cultured as floating neurospheres at clonal density (13.000 cells/cm<sup>2</sup>) in NS-A proliferation medium: Neurocult™ NS-A Proliferation Kit (#05751, StemCell Technologies), 0.2% human Heparin (StemCell Technologies), 10ng/ml bFGF (Gibco), 20ng/ml EGF (Gibco). The growth factors were added every two days and cells were passaged by Accutase (Sigma) every two weeks.

In order to obtain astrocytes, hNPs were dissociated at single cells and plated at 60.000 cells/cm<sup>2</sup> on multiwell plates pre-coated with Matrigel (Corning) in NS-A Differentiation medium: Neurocult™ NS-A Differentiation kit (#05752, StemCell Technologies) without any growth factors. The medium was changed by half every four days.

As a substrate potentially permissive to Myb34.5-helped vAM-GFP amplification, 1x10<sup>5</sup> human R-astrocytes named PCW10 + 150DIV (R-cells, "reactor") were seeded on a 24-multiwell plates, in 600µL of differentiative medium and coinfecting by Myb34.5 HSV-1 at moi 0.01 and vAM-GFP, at moi 1, in all four possible Myb34.5 and vAM-GFP combinations. To secure herpetoviral infection and remove the excess of primarily infecting viral particles, 8 hours later, cell medium was discarded, cells were washed twice with 1X PBS and cultured with new fresh medium. After three days, one half of such new medium (plus an equal volume of fresh medium) was transferred to U251 S-cells (S-cells, "sensor"), which, 3 and 6 more days later, were scored for the presence of EGFP-expressing elements, as an index of U87MG-hosted vAM-GFP neosynthesis.

### ***3.12. RNA sequencing***

RNA sequencing experiment was performed on 4 GBM lines, in particular U87MG cells, U251 cells and 2 primary GBM cultures (GbmA and GbmC). More in detail, 4x10<sup>5</sup> cells were infected with LV\_ pPgk1-rtTA-M2-WPRE and LV\_TREt-IRES-EGFP-WPRE (Ctrl) or LV\_TREt-Emx2-IRES-EGFP-WPRE (*Emx2*-GOF), each at moi 8. After 3 days, we changed the medium by adding 2µg/mL doxycycline and cells were collected after 72h. A paired-end sequencing

strategy was chosen, in which short reads are extracted from both ends of long DNA fragments through high-throughput sequencing. Prior to further analysis, a quality check was performed on the raw sequencing data, removing low quality portions while preserving the longest high-quality part of a NGS read. The minimum length was 35 bp and the quality score 20. The high-quality reads were aligned against the Homo sapiens reference genome sequence (Ensembl GRCh38.p10) with STAR aligner (version 2.5.0c). FeatureCounts (version 1.6) was used to calculate gene expression values as raw read counts (file Raw\_data.xlsx in the folder 2-Expression) and normalized FPKM values were also calculated (file FPKM.xlsx in the folder 2-Expression) across all the samples. All the statistical analyses were performed with R with the package edgeR. The first step has been the removal of not expressed genes and the ones showing too much variability. For this scope, filter was applied to retain the genes with count-per-million (CPM) > 1 in at least 3 samples. As a following step a differential expression analysis was performed comparing the Emx2 overexpressed group against the Control (as reference) taking into account the paired experimental design. We can therefore compare the Emx2 group to the control for each sample separately, so that baseline differences between the samples are subtracted out.

### ***3.13. RNA profiling***

Total RNA was extracted from cells with Trizol™ (ThermoFisher #15596-026), according to Manufacturer's instructions and resuspended in sterile deionized water. Agarose gel electrophoresis and spectrophotometric measurements (NanoDrop ND-1000) were employed to estimate quantity, quality and purity of the resulting RNA. Prior to analysis, samples were processed by the TurboDNFree kit (Ambion™), for 1 hour at 37°C. At least 1.0 µg RNA from each sample was retrotranscribed by SuperScriptIII™ (ThermoFisher #18080044) in the presence of random hexamers, according to manufacturer's instructions. RT-minus samples were scored as controls, in the case of intronless transcripts. cDNAs were finally diluted five times.

Real time PCR reactions were performed using the SsoAdvanced SybrGreen™ Supermix platform (Biorad), according to manufacturer's instructions. Each biological replicate was scored at least in technical triplicate and data were normalized against hGAPDH. Results were averaged and further normalized on their controls. Statistical significance of results was evaluated by the t-test (one-tail; unpaired). "n" is the number of samples.

Protocols were personalized for each primer pair, in accordance to the appropriate annealing temperature. Primers were purchased from Eurofins genomics. The absolute expression was calculated by sample interpolation with a standard curve.

Primer sequences used in the qPCR were:

- ✚ *GAPDH*, h*GAPDH*/Fw, 5' CAT CAC CAT CTT CCA GGA GCG AGA TCC 3', and h*GAPDH*/Rv, 5' CAA ATG AGC CCC AGC CTT CTC CAT GG 3';
- ✚ *EMX2*, *E2S/N2F*, 5' GGA AAG GAA GCA GCT GGC TCACAG TCT CAG TCT TAC 3', and *E2S/N2R*, 5' GTG GTG TGT CCC TTT TTT CTT CTG TTG AGA ATC TGA GCCTTC 3';
- ✚ *EGFR*, h*EGFR*/Fw, 5' GAG ACC CCC AGC GCT ACC TTG TCA TTC A 3', and h*EGFR*/Rv, 5' CCA CCA CGT CGT CCA TGT CTT CTT CAT CCA 3';
- ✚ *SOX2*, h*SOX2*/Fw, 5' CGG CAC GGC CAT TAA CGG CAC ACT G 3', and h*SOX2*/Rv, 5' GTT TTC TCC ATG CTG TTT CTT ACT CTC CTC TTT TG 3';
- ✚ *TRP53*, h*TRP53*/Fw, 5' CCT CCT CAG CAT CTT ATC CGA GTG GAA G 3', and h*TRP53*/Rv, 5' CAT AGG GCAC CAC CAC ACT ATG TCG AAA AG 3';
- ✚ *GADD45A*, h*GADD45A*/Fw 5' GAT GCC CTG GAG GAA GTG CTC AG 3', and h*GADD45A*/Rv 5' CCA TTG ATC CAT GTA GCG ACT TTC CC 3'
- ✚ *GADD45B*, h*GADD45B* /Fw, 5' GAT CGC CTC ACA GTG GGG GTG T 3', and h*GADD45B*/Rv 5' GCAGAAGGACTGGATGAGCGTGA 3';
- ✚ *FOXG1-cds*, h*FOXG1-cds*/Fw, 5' CGA CCC TGC CCT GTG AGT CTT TAA G 3', and h*FOXG1-cds*/Rv 5' GGG TTG GAA GAA GAC CCC TGA TTT TGA TG 3';
- ✚ *HIF1 $\alpha$* , h*HIF1 $\alpha$* /Fw, 5' AGTCACCACAGGACAGTACAGGATGCTT 3', and h*HIF1 $\alpha$* /Rw 5' GACACATTCTGTTTGTGGAAGGGAGAAAAT 3';
- ✚ *LOX*, h*LOX*/Fw, 5' GTCCTGGCTGTTATGATACCTATGGTG 3', and h*LOX*/Rw 5' CACCATAGGTATCATAACAGCCAGGAC 3';
- ✚ *MDR1*, h*MDR1*/Fw, 5' GCAGTAGCTGAAGAGGTCTTGGCAG 3', and h*MDR1*/Rw, TAGATCAGCAGGAAAGCAGCACCTATAGAA 3';
- ✚ *CX43*, h*CX43*/Fw, 5' CATCCTCCAAGGAGTTCAATCACTTG 3' and h*CX43*/Rw, ACACCTTCCCTCCAGCAGTTGAG 3';
- ✚ *hTERT*, h*TERT*/Fw, 5' TCCAGACGGTGTGCACCAACATCTACAAG 3' and h*TERT*/Rw, ACATCCCTGCGTTCTTGGCTTTCAGGAT.

### **3.14. Immunofluorescence analysis of $\gamma$ -H2AX foci**

4x10<sup>5</sup> U251 cells/well were seeded in a 6-well plate and infected with LV\_Pgk1p-rtTA-M2-WPRE and LV\_TREt-IRES-PLAP-WPRE (Ctrl) or LV\_TREt-Emx2-WPRE (Emx2-GOF), each at moi 8. Three days before irradiation, cells were trypsinized and reseeded at 1.2x10<sup>5</sup> cells/well in a poly-lysinated 24-well coverslips in a medium containing 2 $\mu$ g/mL doxycycline. Cells were further irradiated with 5Gy X-rays dosage and fixed with 4% PFA after 1h and 16hrs.

Briefly, cells were incubated with blocking solution for 40min at RT after being permeabilized with PBS1X + TRITON 0,1% for 10min at RT; they were then incubated with Ab I 1:500 anti-*gamma H2A.X (phospho S139) (abcam 26350)* for 1h at RT, washed twice with 1X PBS + TRITON 0.1%, incubated with Ab II 1:600 for 30min at RT, washed twice and counterstained with DAPI 1:200 for 15 min.

Immunos were photographed on a Nikon Eclipse TI confocal microscope equipped with a 63X oil objective and 3.5 electronic zoom. Data analysis was performed by Volocity software (Quorum Technologies).

### **3.15. Traffic light reporter assay: homologous recombination-mediated DNA repair detection by flow cytometry and Real Time PCR**

To study the homologous recombination mediated DNA repair, we took advantage of a fluorescent reporter, called traffic light reporter (Certo et al. 2011).

1x10<sup>6</sup> GBM cells (U87MG and U251) were seeded in a 12-well plate, infected with pCVL Traffic Light Reporter 1.1 (Sce target) Ef1a Puro (#Addgene 31482, named *TLR-LV*) at moi 0.05 and subjected to puromycin selection for 5 days (1 $\mu$ g/mL for U87MG; 2 $\mu$ g/mL for U251). Only puromycin-resistant cells (named *U87-TLR* and *U251-TLR*) were kept as adherent cultures and employed to perform the experiments.

3x10<sup>5</sup> U87-TLR and U251-TLR cells/well were seeded in a 12-well plate and infected with LV\_Pgk1p-rtTA-M2-WPRE and LV\_TREt-IRES-PLAP-WPRE (Ctrl) or LV\_TREt-Emx2-WPRE (Emx2-GOF), each at moi 8. 72hrs later, cells were infected with the endonuclease pCVL SFFV-EF1s HA-NLS.Sce(opt) (#Addgene 31479, named *I-Sce I*) and the integrating-defective template pCVL SFFV d14GFP Donor (#Addgene 31475, named *ID-Donor*). The fluorescence intensity was determined after 3 days with a flow cytometer. Forward scatter (FSC) and side scatter (SSC) were used to exclude debris and cell aggregates (live gate). Cells belonging to the live



gate were evaluated for their EGFP fluorescence profile. Data analysis was performed by Flowjo™ software (Tree Star, Ashland).

\* \* \*

We also designed a set of primers specifically detecting only the fully reconstructed EGFP-cds fragment after HR-mediated repair, and we employed them to quantify such fragment by real time PCR.

For these sets of experiments, “wild type” U87MG and U251 GBM cells were employed. Specifically,  $3 \times 10^5$  U87 and U251 cells/well were seeded in a 12-well plate and infected with pCVL Traffic Light Reporter 1.1 (Sce target) Ef1a Puro (#Addgene 31482, *named TLR-LV*) at moi 10; 3 days later, cells were infected with LV\_Pgk1p-rtTA-M2-WPRE and LV\_TREt-IRES-PLAP-WPRE (Ctrl) or LV\_TREt-*Emx2*-WPRE (*Emx2*-GOF), each at moi. 8. After 72hrs, cells underwent trypsinization and infected with pCVL SFFV d14GFP EF1s HA.NLS.Sce(opt) (#Addgene 31476, *named I-sceI + donor*), encoding for both I-sceI endonuclease and the donor template, at moi 8.

The quantification was performed by RT-PCR by performing the following protocol: 98° for 4min, 98° for 10sec, 65° for 30sec, 72° for 1min, 72° for 3sec, 74° for 3sec, 76° for 3sec, 85° for 3sec, 39 times with the following primers: HR/F1: CCA CAA GTT CAG CGT GTC CGG CGA G, HR/R1s: CTC ACC GGA TCC AGT TAC TTG TAC AG.

Each biological replicate was scored at least in technical triplicate and data were normalized against mCherry sequence, which is included in the pCVL Traffic Light Reporter 1.1 (Sce target) Ef1a Puro. Results were averaged and further normalized on their controls.

### **3.16. Statistical analysis**

Data were analysed using the Student's *t*-test (one tail, unpaired) or 2-way ANOVA for independent samples. *P*-value <0.05 was considered significant.

## 4. RESULTS

### 4.1. *Emx2* overexpression increases the survival of immunocompromised GBM-xenografted hosts and enhances GBM sensitivity to temozolomide (TMZ) treatment

#### 4.1.1. *Emx2* overexpression outperforms TMZ treatment in experimental therapy of GBM-xenografted mouse hosts

To assess if *Emx2* can antagonize glioblastoma multiforme growth *in vivo*, we transplanted EGFP-labelled U87MG GBM cells into the striatum of 5 weeks old nude mice. In particular, we injected 300.000 control cells to a former group and 300.000 *Emx2*-GOF cells to the other group. We kept the gene off for one week using the Tet-OFF technology and one day before the transplantation we removed doxycycline, in order to activate the genes. Four days after transplantation, we administered temozolomide (TMZ) orally to 26 out of 54 transplanted mice; in this way we created four groups: the “control group”, the “*Emx2*-GOF group” and the equivalent ones treated also with TMZ.

We found that mice transplanted with *Emx2*-GOF GBM cells displayed a median survival of 56 days against the 35 days of the control group ( $p < 0.0001$ ,  $n=14,14$ ) (Fig. 4.1.1). Remarkably, *Emx2* overexpression outperformed temozolomide treatment, extending the median survival time by 9 days ( $p < 0.0001$ ,  $n=14,13$ ). No significative difference was appreciable between “*Emx2*-GOF” mice receiving or not TMZ ( $p=ns$ ,  $n=14,13$ ). Taken together, these results indicate that *Emx2* exerts a robust antioncogenic activity *in vivo*, even stronger than the current standard treatment.

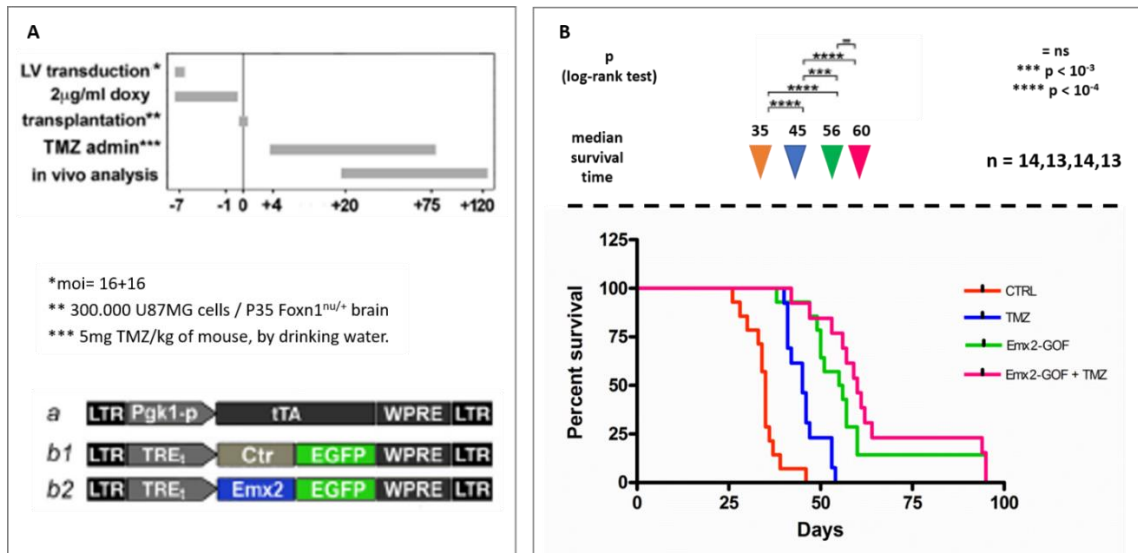


**Figure 4.1.1. *Emx2* antioncogenic activity in vivo, long-term survival tests.** Experimental strategy and lentiviral vectors employed for its implementation are shown in (A). EGFP-labelled, *Emx2*-GOF or control engineered U87MG GBM cells were transplanted into the cortical parenchyma of juvenile immunosuppressed (*Foxn1<sup>nu/+</sup>*) mice. 4 days after transplantation, 5mg TMZ/kg body weight\*day was administered by drinking water to experimental groups. Animal survival profiles were scored (B). n is the number of mice for each group. P-value was calculated by long-rank test.

#### 4.1.2. The outcome of combined *Emx2*/TMZ delivery exceeds the antitumour impact of single *Emx2* and TMZ treatments on GBM cultures

To better investigate the therapeutic relevance of these *in vivo* results, we decided to move to *in vitro* assays, testing the outcome of combined *Emx2*-TMZ treatment on 2 GBM commercial cell lines (U87MG and U251) and 2 primary cultures originating from GBM-affected patients (GbmA and GbmF). GBM cultures were engineered to overexpress *Emx2* via lentiviral vectors and Tet-ON technology and treated with 2µg/mL doxycycline. Where due, TMZ was added to culture medium together with doxycycline. U87MG, GbmA and GbmF cells, sensitive to low doses of this drug, were exposed to 200µM TMZ (Fig. 4.1.2.E-L). In case of more resistant U251 cells, [TMZ] was raised to 1800 µM, to achieve an appreciable biological effect (Fig. 4.1.2.B-D).

In all 4 GBM samples tested, combined *Emx2*-GOF/TMZ treatment accelerated tumour cell death, inducing cultures to collapse in less than one week. Remarkably, this approach performed always better than TMZ and, in 2 out of 4 cell lines (U87MG and GbmA), it also outperformed the *Emx2* treatment alone. Specifically in the case of the U87MG cell line, the

impact of the combined *Emx2*-GOF/TMZ treatment exceeded the linear combination of the two single treatments ( $p_{(Emx2-GOF/TMZ \text{ interaction})} < 0.024$ , as assessed by 2-ways ANOVA).

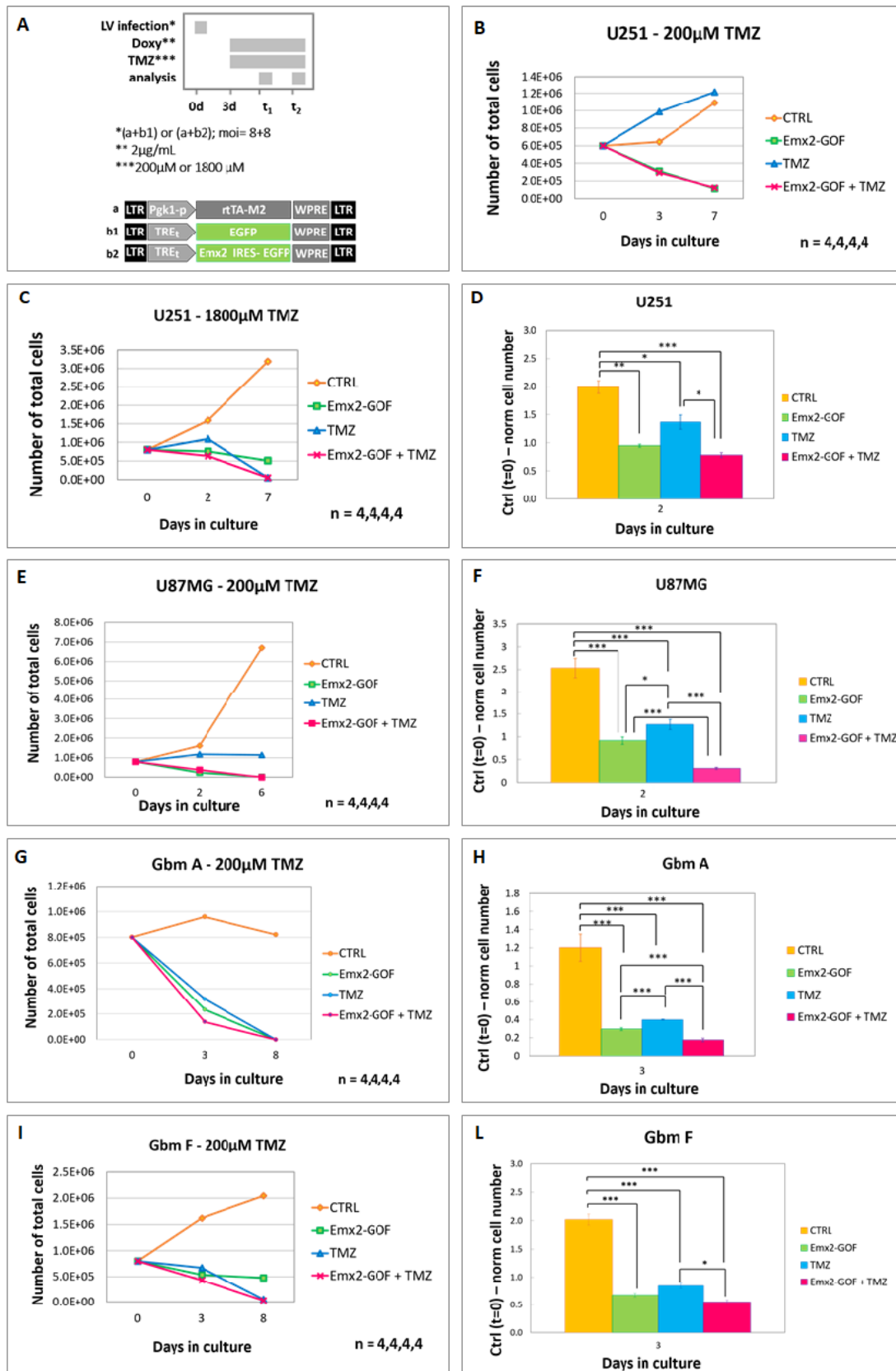


**Figure 4.1.2. Population dynamics of GBM cultures made gain-of-function for *Emx2* and treated by temozolomide.** In vitro kinetic progression of U251, U87MG, GbmA and GbmF GBM lines (B,C,E,G,I), engineered by lentiviral vectors and TetON technology and kept under temozolomide as in (A). Cells were kept as adherent (U87MG and U251) or floating cultures (GbmA and GbmF) under Fgf2 and Egf supplements. In (D,F,H,L),  $t_1$  cell numbers were normalized against  $Ctrl(t_0)$  values. n is the number of biological replicates. p-value was calculated by t-test (one-tail, unpaired): \* $p < 0.05$ , \*\* $p < 0.01$ , \*\*\* $p < 0.001$ .

#### 4.1.3. *Screening for molecular mediators of Emx2 enhancement of TMZ impact on GBM*

To cast light on molecular mechanisms underlying *Emx2* enhancement of TMZ impact on GBM kinetics, we overexpressed its coding sequence in two GBM cell lines (U87MG, U251) and two primary cell cultures (GbmA, GbmF) (Falcone et al. 2016) and scored mRNA levels of selected genes that are involved in tumour chemo-resistance. More in detail, we analyzed *CONNEXIN43* (*CX43*), encoding for the building block of gap junctions detectable at high levels in glioma-associated-astrocytes (Munoz et al. 2014) (Caltabiano et al. 2010), the multi drug resistance 1 (*MDR1*), an ATP-dependent efflux pump that prevent drug to enter the cells (Munoz et al., 2014), and the telomerase reverse transcriptase (*TERT*) (Chen et al. 2014).

In all 4 samples analyzed, *Emx2* downregulated *CX43* both in basal conditions and in the presence of TMZ. Next, it lowered *MDR1*-mRNA levels in the absence of TMZ and, specifically in U87MG and GbmA cultures, even upon TMZ treatment. Finally, limited to U251 and GbmF cultures, *Emx2* overexpression led to a reduction of *TERT*-mRNA levels, which, in GbmF cells, was also detectable in the presence of TMZ.

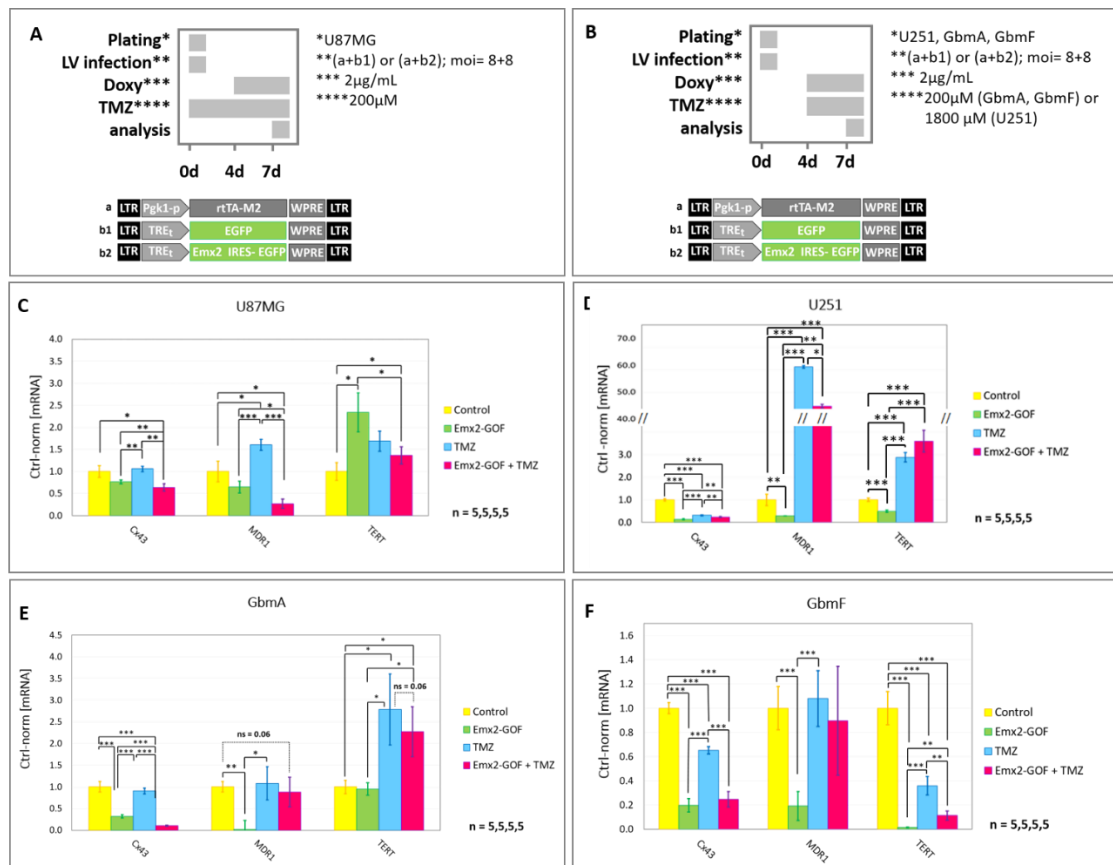


**Figure 4.1.3. mRNA levels of presumptive mediators of *Emx2* enhancement of TMZ impact on GBM.** Engineered U87MG GBM cells were treated as in A. 4 days after lentiviral infection and TMZ administration, doxycycline was added at 2 µg/ml. RNA samples were collected at day 7. U251, GbmA and GbmF were treated as in B. 4 days after lentiviral infection, both doxycycline (at 2 µg/ml) and TMZ (1800µM in U251; 200µM in GbmA and GbmF) were added to the cultures. RNA samples were collected at day 7. qRT-PCR results, normalized against *hGAPDH* and further normalized against their controls, are shown as average  $\pm$  s.e.m. ns, not significant. n is the number of biological replicates. p-value was calculated by t-test (one-tail, unpaired): \*p<0.05, \*\*p<0.01, \*\*\*p<0.001.

## 4.2. *Emx2* overexpression radiosensitizes GBM cells, by depressing HR-mediated DNA repair

### 4.2.1. *Emx2* overexpression radio-sensitizes GBM cells

In an attempt to set up an experimental protocol suitable to unveil possible synergy between *Emx2* overexpression and radiotherapy, we tested the kinetic trend of the two GBM lines (U87MG and U251) exposed to different doses of X-ray radiation. As seen in figure 4.2.1 B-C, a dose of 15Gy was needed to induce the collapse of both GBM cultures within 15 days; on the other hand, lower X-ray doses slowed down culture expansion but were not able to eradicate the tumour.

Next, we exposed pre-engineered GBM cells to different doses of doxycycline, in order to induce a light *Emx2* overexpression, preventing GBM culture expansion while avoiding fast tumour culture collapse. We found that 1ng/mL and 30ng/mL were two doxycycline concentrations suitable to reproducibly achieve this goal at three days post-transgene activation, in case of U87MG and U251 cultures, respectively (figure 4.2.1 E-F).

Based on these premises, we set up a new, combined experimental protocol, articulated as follows. We engineered U87MG and U251 cells by infecting them with *Emx2*-encoding lentivirus; as control, we employed an EGFP-encoding lentivirus. Two days before irradiation, we gently activated the transgenes by adding 1ng/mL and 30ng/mL doxycycline to culture media, in case of U87MG and U251 cells, respectively, and finally we exposed cells to 15Gy irradiation.

Under these conditions, we found that *Emx2* considerably amplified the impact of X-rays, revealing a statistically significant, positive interaction between transgene overexpression and irradiation ( $p_{(\text{interaction})}$ ), as evaluated by 2-ways ANOVA, reported in figure 4.2.1 H-I).

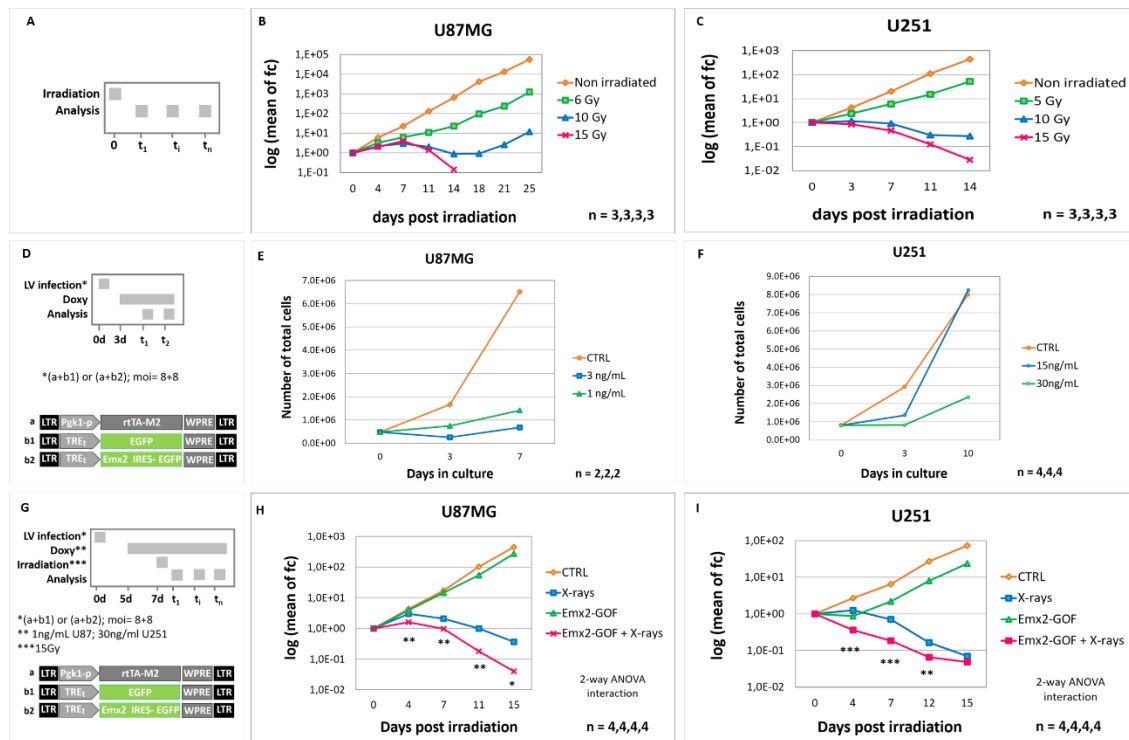


**Figure 4.2.1. Population dynamics of irradiated/*Emx2*-overexpressing GBM cultures. (A-C)** *In vitro* kinetic progression of U87MG and U251 GBM cells irradiated with different X-rays dosage: (A) protocol and (B,C) results. **(D-F)** *In vitro* kinetic progression of “Control” or “*Emx2*-GOF” U87MG and U251 GBM cells cultured under different doxycycline concentrations: (D) protocol and (E,F) results. **(G-I)** *In vitro* kinetic progression of U87MG and U251 GBM cells made “*Emx2*-GOF” and irradiated with 15Gy X-rays dosage: (G) protocol and (H,I) results. n is the number of biological replicates. In (H,I) the p-value of the *Emx2*/Xray interaction was calculated by 2-way ANOVA for independent samples: \*\*p<0.01, \*\*\*p<0.001.

#### 4.2.2. *Emx2* overexpression increases $\gamma$ -H2AX foci, in basal conditions and upon irradiation

Higher radiosensitivity of *Emx2*-GOF tumor cells suggested us a possible implication of this gene in DNA damage. To address this issue, we decided to score  $\gamma$ -H2AX foci in U251 cells, after *Emx2* overexpression and X-rays exposure. For this purpose, an *Emx2* transgene was expressed by the TetON platform, for three days under maximum doxycycline dosage, then cells were treated by X-rays (5Gy) and finally collected for the analysis, 1hr and 16hrs after irradiation.

Both *Emx2* overexpression and radiation doubled the number of DSBs foci detectable 1h after X-rays treatment. The combined treatment increased this number by four folds, suggesting that no statistically significant interaction took place between the two antitumoral effectors ( $p_{(Emx2-GOF/X-rays\ interaction)} \gg 0.05$ , as evaluated by 2-ways ANOVA).



16hrs later, the  $\gamma$ H2AX foci number in irradiated control cells returned to the basal level, meaning that 16hrs are sufficient to repair the radio-induced DNA-DSBs (t-test between X-rays treated samples, at 1hr and 16 hrs, blue bars, gave  $p < 0.001$ ). Furthermore, at this time there was no difference between irradiated and non-irradiated *Emx2*-GOF cells, confirming that 16 hrs were enough to fully repair radio-induced DNA damage.

However, *Emx2* overexpression alone was able to evoke an increase of  $\gamma$ H2AX foci at 16hrs compared to 1h, (t-test between *Emx2*-GOF samples, at 1hr and 16 hrs, green bars, gave  $p < 0.001$ ). This suggests that *Emx2* could be intrinsically mutagen or it could slow down the repair of DNA damage basally induced by environmental factors.

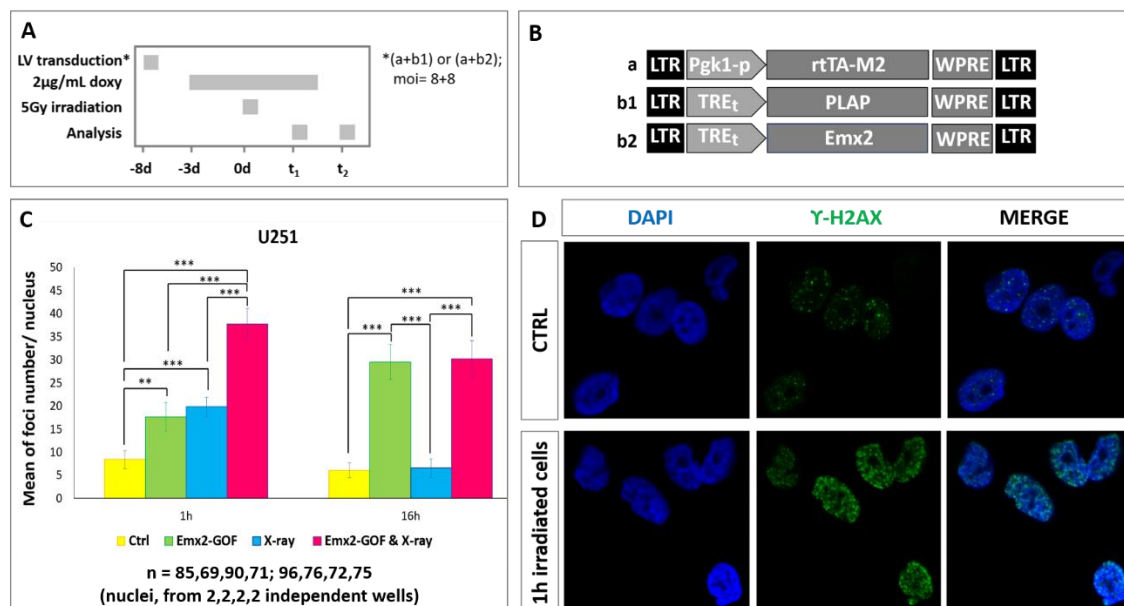


**Figure 4.2.2. *Emx2* overexpression increases  $\gamma$ -H2AX foci, in basal conditions and upon irradiation.** Immunofluorescence evaluation of  $\gamma$ -H2AX foci in U251 cells engineered by lentiviral vectors and TetON technology and irradiated with 5Gy: **(A,B)** protocols and **(C,D)** results. Average numbers of  $\gamma$ -H2AX foci/nucleus were evaluated by Volocity software (C). In (D) shown is an example of cells immunoprofiled 1 hour after irradiation. Scale bar=s.e.m. n is the number of biological replicates. p-value was calculated by t-test (one tail, unpaired): \*\* $p < 0.01$ , \*\*\* $p < 0.001$ .

#### 4.2.3. *Emx2* overexpression inhibits DNA repair via homologous recombination

It has been shown that GBMs repair radio-induced DSBs mainly by homologous recombination (HR) (King et al. 2017). As results of the previous experiment did not provide us with any firm proofs about an involvement of *Emx2* in inhibiting DNA repair machinery, we decided to address this issue by a complementary approach, based on a specific DNA recombination sensor called Traffic Light Reporter (TLR), able to reveal the occurrence of HR

events (Certo et al. 2011). In this construct, a double-strand break is produced at an I-SceI nuclease cleavage site, embedded within a functionally dead EGFP-cds, and the repair of the break, achieved via HR thanks to an EGFP-like editor DNA, rescues the EGFP-cds and leads to generation of a green fluorescent signal. Thanks to a lentiviral vector, this construct (as well as its I-SceI-expressing and editor sequence-harboring companions) may be easily delivered to tumor cells, where it provides a comfortable readout of the efficiency by which these cells repair their DNA.

To evaluate this efficiency, we firstly infected tumor cells with the TLR-encoding lentivirus (TLR-LV) and made them *Emx2*-GOF. Next, we induced a light overexpression of our transgene (TetON platform, doxycyclin at 1ng/mL in U87MG and 10ng/mL in U251, for three days). Then, we induced the DNA-DSBs (and their subsequent homologous recombination repair) by providing lentiviruses encoding for the I-SceI endonuclease and the exogenous editor DNA. Finally, we scored cells by FACS analysis, evaluating the frequency of green ones. As seen in figure 4.2.3a.C-D, *Emx2* significantly affected the HR repair mechanism, indeed the frequency of EGFP<sup>+</sup> cells (HR<sup>+</sup>) was halved when compared to controls, both in U87MG and U251 GBM cell lines (t-test, p<0.001).

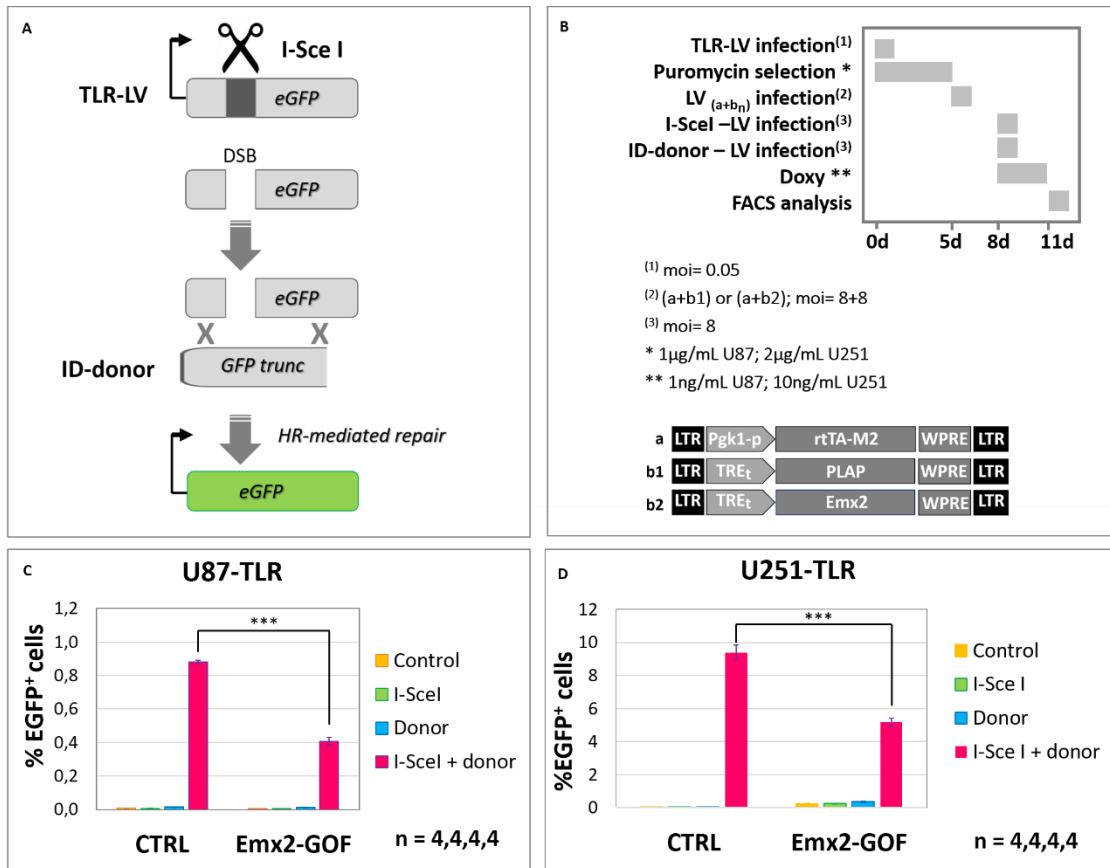


**Figure 4.2.3a. Evaluation of *Emx2* impact on homologous recombination by FACS analysis. (A)** Diagram of the experimental strategy. If the break induced by I-SceI endonuclease is resolved through the HDR pathway, the full eGFP sequence will be reconstituted, and cells will fluoresce green. **(B)** Experimental protocol. **(C,D)** Absolute frequencies of EGFP positive cells, as detected by FACS analysis. Scale bar=s.e.m. n is the number of biological replicates. p-value was calculated by t-test (one tail, unpaired): \*\*\*p<0.001.

To corroborate these results, we further designed a set of primers specifically detecting the reconstructed EGFP-cds fragment, after HR-mediated repair, and we employed them to quantify such fragment by real time PCR. Interestingly, upon a light *Emx2* overexpression, the number of EGFP<sup>HR</sup> amplicons - normalized against non recombinant lentiviral reference sequences and controls - was halved in U87MG cells (t-test, p<0.001) and reduced by one quarter in U251 cells, in substantial agreement with previous flow cytometric data (Figure 4.2.3b).

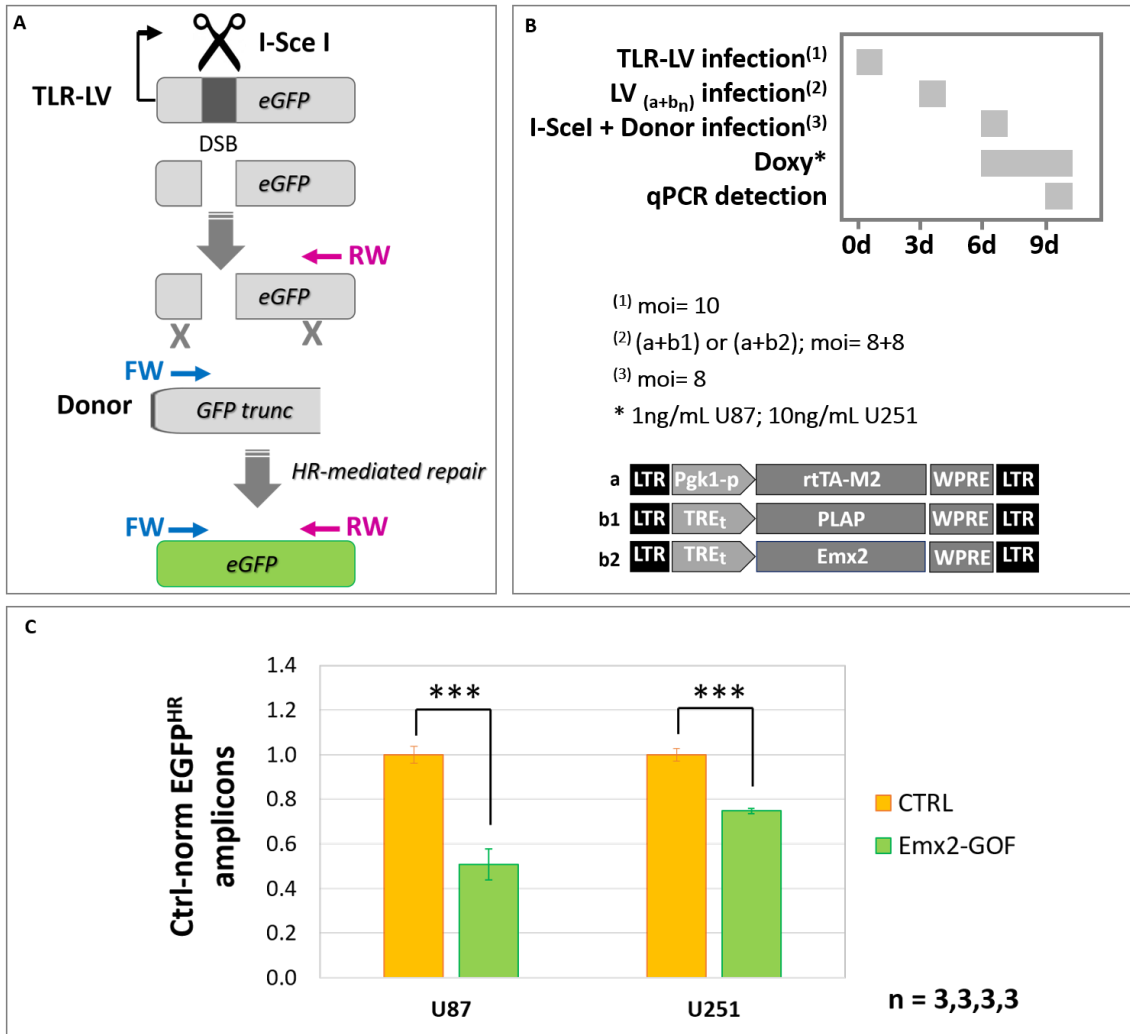


**Figure 4.2.3.b. Evaluation of *Emx2* impact on homologous recombination by qPCR analysis. (A)** Experimental strategy, as in Fig. 4.2.3.a. Here, a set of primers was designed to detect the fully reconstituted EGFP sequence by real time PCR. **(B)** Experimental protocol. **(C,D)** qPCR results, data double-normalized, against TLR-LV sequences and controls. n is the number of biological replicates. Scale bar=s.e.m. p-value was calculated by t-test (one tail, unpaired): \*\*\*p<0.001

#### 4.2.4. Screening for potential mediators of *Emx2* HR-repair suppressing activity

To get hints on molecular mechanisms mediating such *Emx2* / X-rays interaction and, in particular, *Emx2* suppression of HR-repair, we performed a comparative RNA-seq analysis of 4 GBM samples (U87MG, U251, GbmA, GbmC), wt or made gain-of-function for *Emx2*. A selection of differentially expressed genes, implicated in glioblastoma tumour radioresistance and/or HR-mediated DNA-repair was taken into account (Table 4.2.4.a and references therein).

Locus (Ensembl)	Gene symbol	Impact on HR repair	Refs	logFC	logCPM	P value	FDR
ENSG00000181449	<i>SOX2</i>	+	[1]	-3.13	7.30	8.92E-13	1.26E-10
ENSG00000146648	<i>EGFR</i>	+	[2]	-1.22	7.33	9.40E-04	6.07E-03
ENSG00000176165	<i>FOXP1</i>	+	[3]	-1.92	4.42	4.07E-06	7.30E-05
ENSG00000113083	<i>LOX</i>	+	[4]	-1.42	6.52	1.73E-04	1.57E-03
ENSG00000100644	<i>HIF1A</i>	+	[5]	-1.30	9.72	1.10E-02	4.04E-02
ENSG00000130066	<i>SAT1</i>	+	[6]	-0.71	7.34	5.59E-02	1.37E-01
ENSG00000116717	<i>GADD45A</i>	-	[7]	1.82	6.36	0.00034	0.00271
ENSG00000099860	<i>GADD45B</i>	-	[8]	3.07	5.24	1.15E-17	5.78E-15
ENSG00000182185	<i>RAD51B</i>	+	[9]	-0,80	3,11	2,49E-02	7,47E-02
ENSG00000149311	<i>ATM</i>	+	[10]	-0,73	6,90	2,10E-03	1,12E-02
ENSG00000166454	<i>ATMIN</i>	-	[11]	1,28	7,35	1,30E-05	1,92E-04
ENSG00000104517	<i>UBR5</i>	+	[12]	-0,68	7,48	4,12E-03	1,88E-02
ENSG00000141510	<i>TP53</i>	-	[13]	0.36	6.53	0.16	0.29

**Table 4.2.4.a. List of potential mediators of *Emx2* impact on HR-repair, compiled on the basis of RNASeq data and literature.** RNAseq data were generated from 2 GBM lines (U87MG,U251) and 2 primary GBM cultures (GbmA, GbmC) made gain of function for *Emx2*, as detailed in Materials and Methods. Genes listed above were generally mis-regulated upon *Emx2* overexpression in all four lines, in a statistically significant way. TP53 and SAT1 were upregulated and downregulated in 3/4 (U87MG, U251, GbmC) and 2/4 (U87MG, GbmC) GBM cell types, respectively. logFC and logCPM are log<sub>2</sub> of Fold Change and Counts Per Million, respectively.

Two of these genes, *SOX2* and *EGFR*, had been already reported to be robustly downregulated by *Emx2* (Falcone et al. 2016). Among others, *Foxg1*, *LOX*, *HIF1α*, *SAT1* and *GADD45A* were further profiled by qRT-PCR, in U87MG and U251 cells, overexpressing *Emx2* or a control, in baseline conditions as well as upon irradiation (Figure 4.2.4.b). Interestingly, in both cell lines, *Emx2* resulted to downregulate *Foxg1*, *LOX* and *HIF1α*, and upregulate *GADD45A*, both upon irradiation or in the absence of it. This dynamic was superimposed to changes evoked by X-rays, generally according to a linear pattern, sometimes resulting in a pronounced dampening of the latter (e.g., *LOX* in U87MG cells). Unexpectedly, *Emx2* upregulated SAT1, except in unirradiated U251 cells, where its impact was opposite.

Altogether, these data pointed to a possible contribution of these genes to *Emx2* anti-HR repair activity.

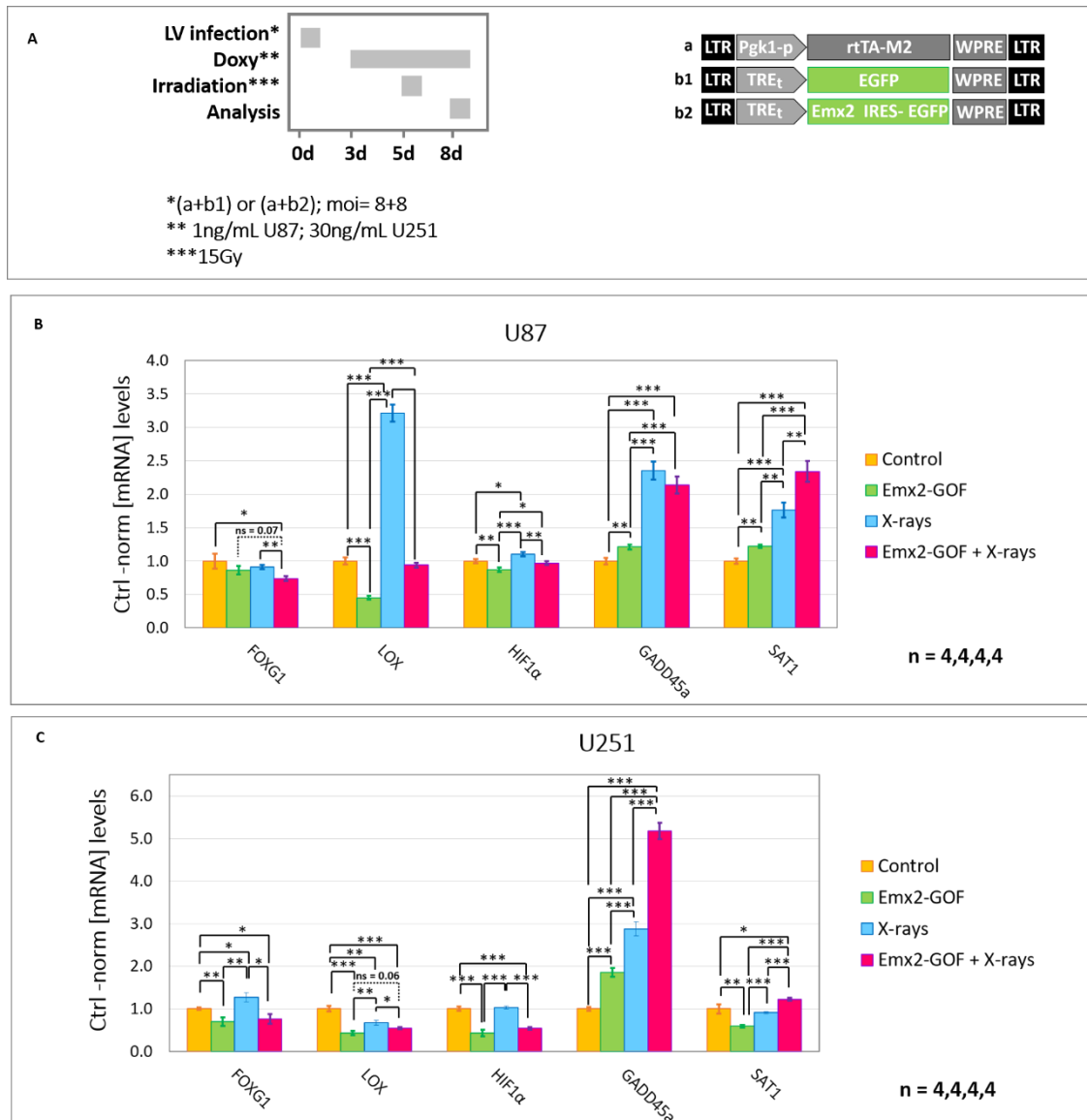


**Figure 4.2.4.b.** mRNA levels of presumptive mediators of *Emx2* enhancement of X rays impact on GBM. **(A)** Protocol. Here, 3 days after lentiviral infection, doxycycline was added to the culture at 1ng/mL in U87MG cells and 30ng/mL in U251. 48 hours later, cells were exposed to a 15Gy X rays dose. RNA samples were collected at day 8 and qRT-PCR-profiled. **(B,C)** Results, double-normalized, against *GAPDH* and controls, are shown as average  $\pm$  s.e.m. ns, not significant. n is the number of biological replicates. p-value was calculated by t-test (one-tail, unpaired).

#### 4.2.5. Validation of selected presumptive mediators of anti-HR *Emx2* activity

Moving from the results described above, we next tested the ability of some putative mediator genes to restore HR-repair activity in U87MG and U251 GBM cell lines, previously made gain of function for *Emx2*. For this purpose, we transduced these cells (and their controls) with lentiviruses driving Tet<sup>ON</sup>-dependent, *Foxg1* and *Sox2* overexpression (Figure 4.2.5a. C-F), as well as constitutive, p<sub>Pgk1</sub>-dependent *EGFR* overexpression (Figure 4.2.5a.G-H), and then we evaluated HR-mediated DNA repair, by real time PCR. Remarkably, *Foxg1* restored HR repair in both cell lines, *Sox2* only in U87MG cells, *EGFR* was ineffective.

As *Foxg1* overexpression doubled HR-activity in "wt" U251 cells, it is possible that the apparent rescue of HR levels elicited by this gene manipulation in *Emx2*-GOF U251 cells was not due to an actual involvement of *Foxg1* in *Emx2*-dependent HR deficit, but reflected a trivial "functional compensation" of such deficit exerted by high *Foxg1* levels.

To address this issue, we mimicked *Emx2*-induced *Foxg1* downregulation by RNAi, and scored the impact of this manipulation on HR repair, in both U251 and U87MG naive cells (Figure 4.2.5.b). Remarkably, despite the small decrease of *Foxg1*-mRNA elicited by  $\alpha$ -*Foxg1*-shRNA (around -30%), in both cases such decrease evoked a drop in HR-frequency comparable to that induced by *Emx2* overexpression, implying that *Foxg1* is a key mediator of *Emx2* impact on HR-repair.

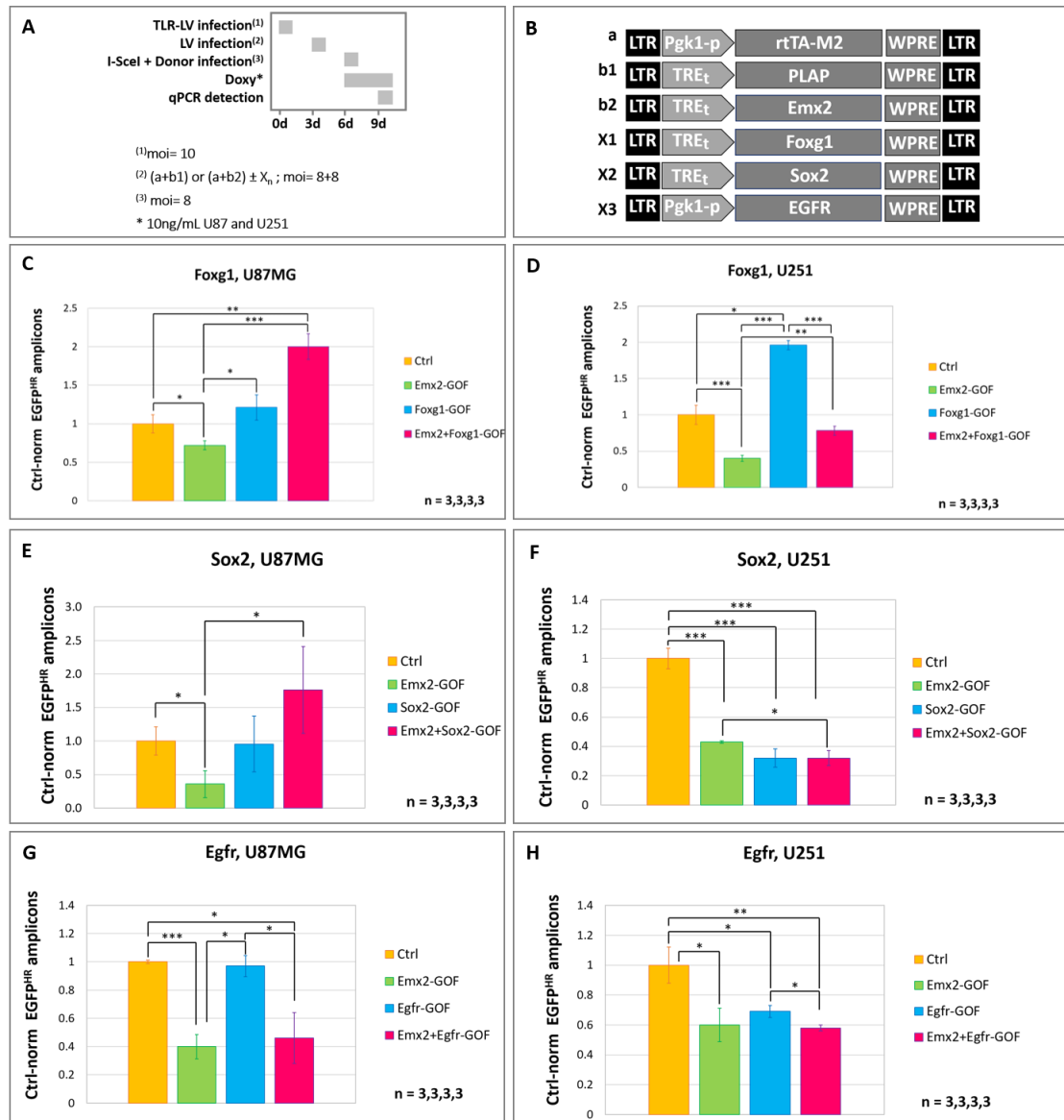


**Figure 4.2.5.a. Rescue of anti-HR Emx2 activity via modulation of its presumptive mediators.** U87MG and U251 cells were engineered as in (A,B). Cells were scored for the capability of selected “X” agents (restoring presumptive mediators of anti-HR Emx2 activity) to rescue the HR-mediated DNA repair (C-H) More in detail, U87MG infected cells were activated with 5ng/mL and 1ng/mL doxycycline in Foxg1/SOX2 and EGFR experiments, respectively. Data were normalized against control. Scale bar=s.e.m. n is the number of biological replicates. p-value was calculated by t-test (one-tail, unpaired): \*p<0.05, \*\*p<0.01, \*\*\*p<0.001.



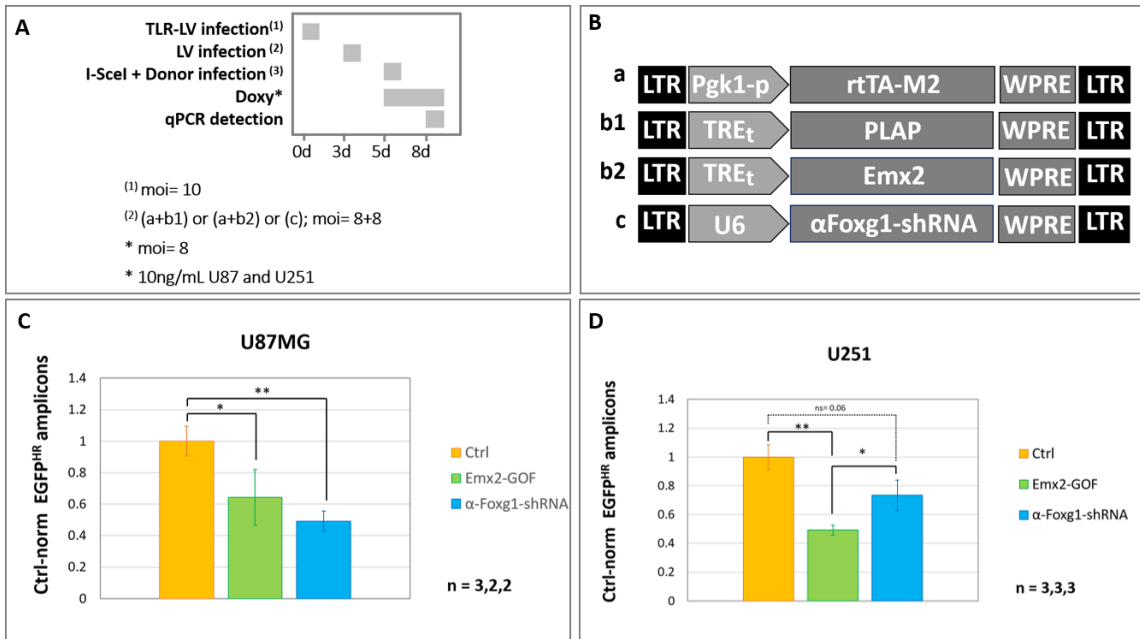


**Figure 4.2.5.b. Mimicking anti-HR Emx2 activity via down-regulation of its presumptive Foxg1 mediator.** U87MG and U251 cells were engineered as in (A,B). Cells were scored for the capability of  $\alpha$ -Foxg1-shRNA to replicate the *Emx2*-evoked, HR defect (C,D). Data were normalized against control. Scale bar=s.e.m. n is the number of biological replicates. p-value was calculated by t-test (one-tail, unpaired): \*p<0.05, \*\*p<0.01.

### 4.3. Herpetic viral vectors as suitable tools for *Emx2* delivery in vivo

#### 4.3.1. *The oncolytic Myb34.5 HSV-1 displays a pronounced anti-GBM activity*

Although allowing cheap and fast dissection of key issues associated to *Emx2* gene therapy, lentiviral vectors have two main limits: (a) they are genotoxic and therefore harmful to healthy neural cells; (b) they can hardly transduce all GBM cells *in vivo*. As such, they are not the best choice for actual gene therapy of GBM in patients. In this respect, we reasoned that, among available tools, herpetoviral amplicon vectors (i.e. gutless, replication defective HSV1 derivatives, accomodating large and/or multimerized transgenes) (de Silva and Bowers 2009), supplemented by herpetoviral oncolytic vectors (undergoing replication only in intermitotic cells) (Gayral et al. 2014), might offer two substantial advantages. First, both effectors are not mutagenic. Second, beyond a likely antiblastic synergy among them, simultaneous administration of tiny amounts of oncolytic herpesviruses and *Emx2*-encoding amplicon vectors might ignite a diffuse chain-reaction, including tumor-hosted, oncolytic virus-aided amplicon vector neogeneration (possibly leading *in vivo* to *Emx2*/oncolytic virus-mediated eradication of all GBM cells). We preliminarily tested some of these predictions *in vitro*. Results were as it follows.

To test the anti-tumour activity of the oncolytic Myb34.5 HSV-1 in glioblastoma multiforme, we infected 2 GBM cell lines (U87MG and U251) and 2 primary GBM cultures (GbmA and GbmF) with different m.o.i. In all 4 samples tested, extremely low Myb34.5 moi's were sufficient to elicit a powerful anti-tumour effect. In particular, Myb34.5 preparations administered at moi 0.1 induced collapse of all four GBM cultures in about 1 week (Figure 4.3.1.A), moi=0.025 was sufficient to suppress U87MG and U251 cultures in 10 days (Figure 4.3.1B), whereas moi=0.005 eradicated U87MG cultures in 15 days (Figure 4.3.1C).

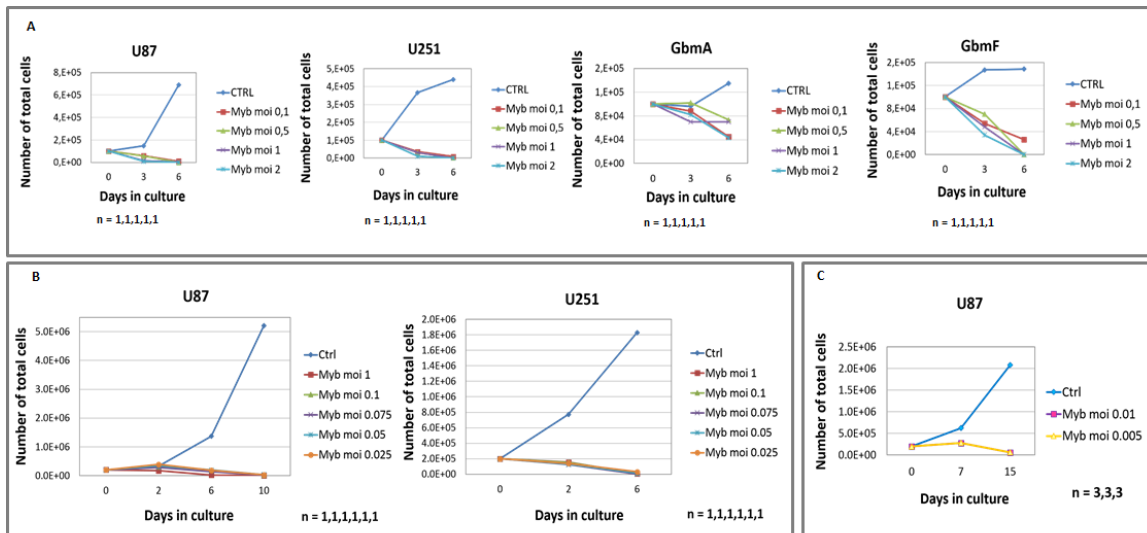


**Figure 4.3.1. Population dynamics of GBM cultures infected with Myb 34.5 HSV-1.** In vitro kinetic progression of U87MG, U251, GbmA and GbmF lines (A-C), infected with different moi's. n is the number of biological replicates.

*4.3.2. Low Myb34.5 titres are able to eradicate U87MG cultures, while not affecting "healthy" murine, perinatal neocortical tissue, in vitro*

In order to assess if low Myb34.5 doses are harmful to the healthy neural tissue, we administered it to neural co-cultures including healthy, late-gestational neocortical precursors and U87MG cells at very low moi's.

Upon delivery at moi 0.01, Myb34.5 displayed a pronounced anti-GBM activity, as detectable at post infection-in vitro day 4 (PI-IVD4); this outcome was even more pronounced at PI-IVD8 (Figure 4.4.3.B). As for mixed neuronal-astroglial primary cultures, they were not affected by HSV-1 activity initially, but unfortunately, over time, Myb34.5 at moi=0.01 made them to die. The scenario was different when cells were infected with Myb34.5 at moi=0.005. While that resulted into a robust therapeutic impact on GBM cells (t-test, p=0.001), no major damages apparently occurred to healthy cells, both at short and long term, as assessed by cell counting.

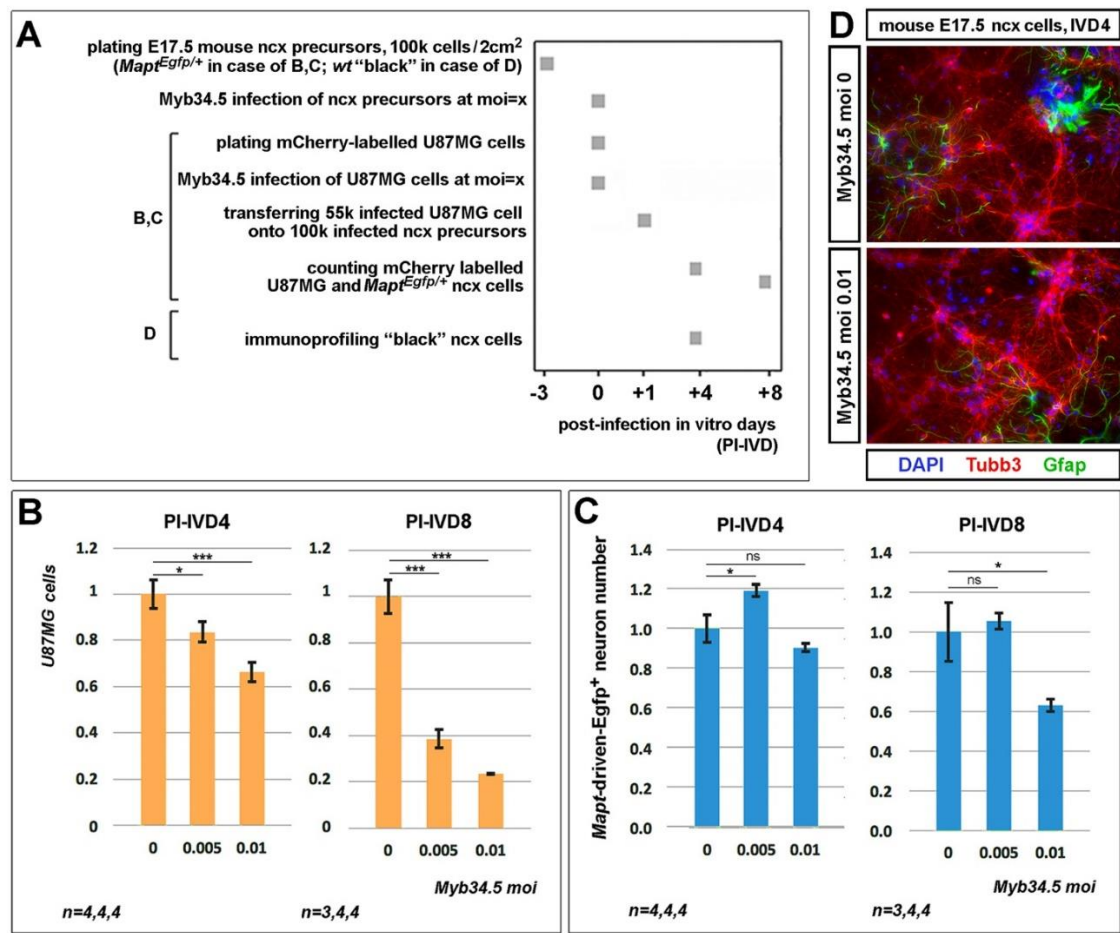


**Figure 4.3.2. Selective impact of oncolytic Myb34.5 on U87MG cells co-cultured with healthy precursors of murine neocortex.** (A) Protocol. 100.000 *Mapt*-driven *Egfp* positive E17.5 mouse ncx precursors were seeded in a 24-well plate and infected 3 days later with Myb 34.5 at moi 0.01 or 0.005. After 24 hours,  $0.5 \times 10^5$  mCherry-labelled U87MG cells, pre-infected with Myb 34.5 at moi 0.01 or 0.005 the day before, were transferred onto infected neocortex precursors. FACS analysis was performed 3 and 7 days later. Concomitantly, an immunofluorescence against TUBB3 and GFAP was performed on mouse neocortex cells at days PI-IVD 3, to evaluate the neuronal and glial morphology. (B-C) Absolute frequencies of mCherry positive U87MG cells and *Mapt*-driven *Egfp* positive neurons at PI-IVD4 and PI-IVD8, as detected by FACS analysis. Scale bar=s.e.m. n is the number of biological replicates. p-value was calculated by t-test (one-tail, unpaired). In (D) shown is an example of healthy murine neocortex after Myb 34.5 infection at moi=0.01. p-value was calculated by t-test (one-tail, unpaired): \*p<0.05, \*\*p<0.01, \*\*\*p<0.001.

#### 4.3.3. *Myb34.5* and lentiviral *Emx2* expressors exert a synergic anti-blastic effect on U87MG GBM cultures

To assess if any functional cooperation may take place between oncolytic vectors and *Emx2*, U87MG cells were co-treated by the *Emx2* transgene (delivered via lentiviral vectors and activated at low level, by TetON technology, under the control of a constitutive promoter and in the presence of 1 ng/ml doxycycline) and the oncolytic Myb34.5 HSV-1 (administered at moi=0.005). This resulted in a synergistic integration of *Emx2* and Myb34.5 therapeutic

effects. Specifically, such treatment halved the size of the GBM population in only 5 days, whereas the control population increased by a factor around 4 and none of the two single therapeutic agents could prevent culture expansion.

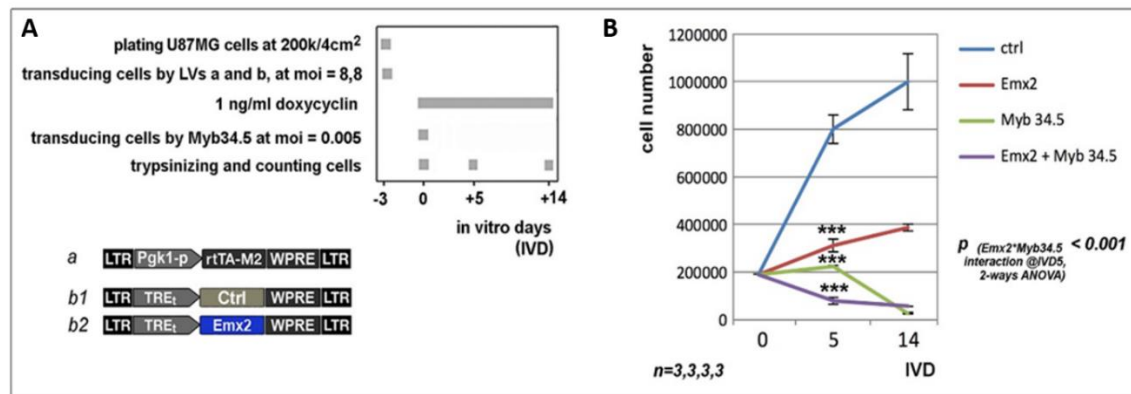


**Figure 4.3.3. Population dynamics of U87MG cells, co-infected by Emx2-LV and Myb 34.5 HSV-1.** (A) Protocol. In vitro kinetic progression of U87MG cells, made “Emx2-GOF” and co-transduced by low Myb 34.5 moi. (B) Results. n is the number of biological replicates. The p-value of the Emx2/Myb 34.5 interaction was calculated by 2-way ANOVA for independent samples: \*\*\*p<0.001.

#### 4.3.4. Both U87MG-GBM cells and “healthy” human neocortex precursors are able to host Myb34.5-helped amplification of EGFP-encoding herpes viral amplicon vectors

As a substrate potentially permissive to Myb34.5-helped vAM-GFP amplification, U87MG “Reactor” R-cells were coinfecting by Myb34.5, at moi = 0.01, and vAM-GFP, at moi = 5, in all four possible Myb34.5(±)vAM-GFP(±) combinations. To secure herpes viral infection and remove the excess of primarily infecting viral particles, 8 hours later, cell medium was discarded and fully replaced by fresh medium. Next, 3 days later, *one half* of such new medium (plus an equal volume of fresh medium) was transferred to U251 “Sensor” S-cells, which, 3 more days later, were scored for the presence of EGFP-expressing elements, as an index of U87MG-hosted vAM-GFP neosynthesis.

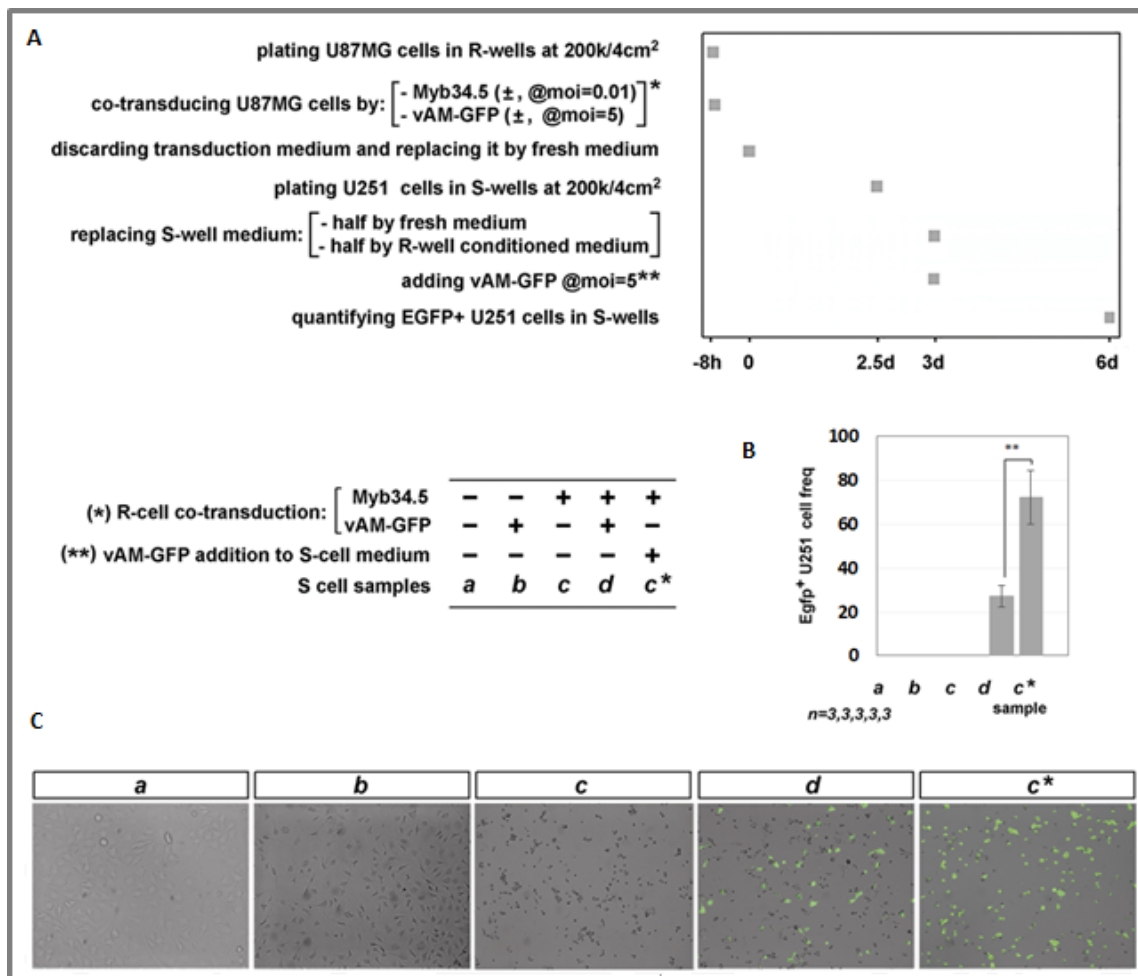


**Figure 4.3.4.a Detection of freshly neogenerated vAM-GFP amplicon vectors, released by U87MG cells upon vAM-GFP/Myb34.5 co-transduction. (A) Protocol.** 200.000 U87MG “Reactor” cells were infected with Myb 34.5 at moi 0.01 and vAM-GFP at moi=5. 8hrs later, cells were washed twice to remove all viral particles and cultured with new fresh medium for three days. In parallel, 200.000 U251 “Sensor” cells were seeded separately, and 12hrs later, their medium was discarded and replaced by a new one, half made from fresh medium and half by R-well conditioned medium. 3 days later, U251 “Sensor” cells were scored for the presence of EGFP-expressing elements, as an index of U87MG-hosted vAM-GFP neosynthesis. **(B) Results.** Scale bar=s.e.m. n is the number of biological replicates. p-value was calculated by t-test (one-tail, unpaired): \*p<0.05, \*\*p<0.01, \*\*\*p<0.001. In **(C)** shown is an example of U251 “Sensor” cells cultured with different conditioned medium..

Remarkably, only medium from Myb34.5(+)/vAM-GFP(+)-infected U87MG cultures gave a substantial fraction of fluorescent U251MG sensor cells (d sample). Media from U87MG cultures infected according to the other three combinations did not elicit any "staining" of sensor cells. All that implies that: (1) no unwanted carryover of viral particles primarily delivered to U87MG cells to U251MG cells took place; (2) a substantial number of vAM-GFP particles were neo-generated by Myb34.5/vAM-GFP-coinfected U87MG cells.

Interestingly, when - in a parallel assay - one half of medium conditioned by Myb34.5(+)/vAM-GFP(-) U87MG cells was acutely supplemented with vAM-GFP at moi 5 and then transferred

to U251MG sensor cells, sensor cells (c\* sample) became fluorescent at frequencies about 3 times higher compared to those achieved with medium conditioned by Myb34.5(+)/vAM-GFP(+)-infected U87MG cultures. This suggests that, by 3 days after Myb34.5(+)/vAM-GFP(+)-coinfection, double-infected U87MG cells could have generated as many new vAM-GFP amplicons as about 2/3 of those administered them at the beginning of the experiment.

\* \* \*

A similar assay was run to assess the ability of "healthy human neocortical tissue" to host Myb34.5-helped amplification of EGFP-encoding herpetoviral amplicon vectors, where a mixed neuronal-astroglial primary culture originating from differentiation of human neocortical precursors replaced U87MG cells as a potentially permissive substrate hosting vAM-GFP neosynthesis (Figure 4.3.4.b).

Interestingly, such culture supported neosynthesis of recombinant vAM-GFP amplicon vectors, like U87MG cells. The yield of the process was quite high. Again, within only 3 days, it re-generated about 2/3 of the amplicon vector input originally co-delivered to it with the Myb34.5 helper.

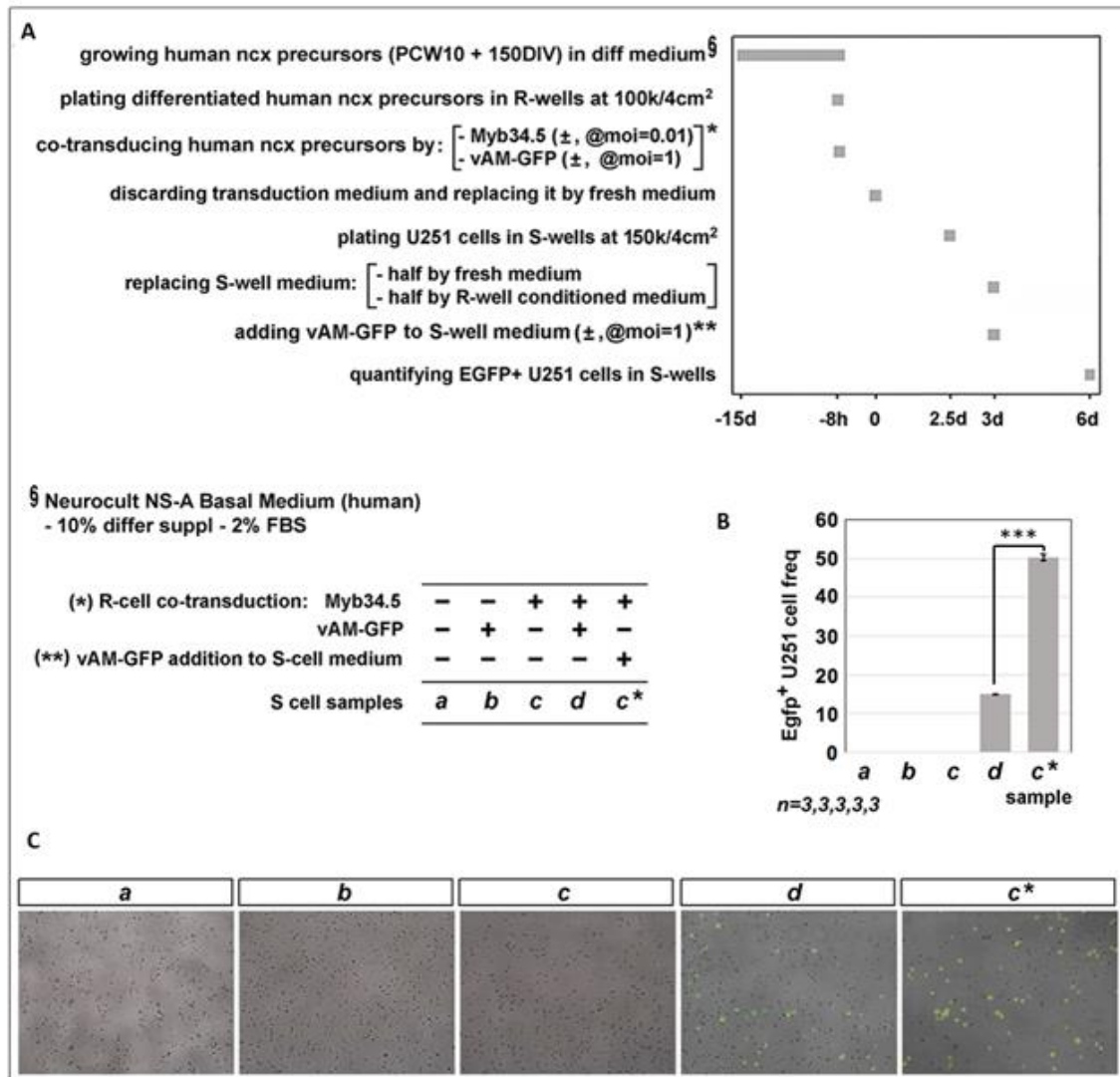


**Figure 4.3.4b. Detection of freshly neogenerated vAM-GFP amplicon vectors, released by differentiated human neocortical precursors upon vAM-GFP/Myb34.5 co-transduction. (A)** Protocol. 100.000 human ncx "Reactor" precursors were infected with Myb 34.5 at moi 0.01 and vAM-GFP at moi=1. 8hrs later, cells were washed twice to remove all viral particles and cultured with new fresh medium for three days. In parallel, 150.000 U251 "Sensor" cells were seeded separately, and 12hrs later, their medium was discarded and replaced by a new one, half made from fresh medium and half by R-well conditioned medium. 3 days later, U251 "Sensor" cells were scored for the presence of EGFP-expressing elements, as an index of human ncx precursors-hosted vAM-GFP neosynthesis. **(B)** Results. Scale bar=s.e.m. n is the number of biological replicates. p-value was calculated by t-test (one-tail, unpaired): \*p<0.05, \*\*p<0.01, \*\*\*p<0.001. In **(C)** shown is an example of U251 "Sensor" cells cultured with different conditioned medium.



## 5. DISCUSSION

Previous experiments done in my laboratory demonstrated the *Emx2* role in limiting cortico-cerebral astrogenesis. In particular, it was shown that *Emx2* overexpression in pallial stem cells inhibits the proliferation of astrocytes-committed precursors, leading to a reduction of their ultimate glial output. This control takes place via a functional cascade, which includes stimulation of Bmp signaling and *Sox2* repression, through the downregulation of *Egfr* and *Fgf9* (Falcone et al., 2015).

Next, inspired by these findings, Carmen Falcone demonstrated that *Emx2* overexpression kills glioblastoma cells in vitro within 7-10 days, by inducing cell death and inhibiting cell proliferation. All glioblastomas tested in this study (and later) were sensitive to this treatment. The *Emx2* antitumoral activity was replicated *in vivo*, in dedicated short-term assays. Molecular mechanisms underlying this phenomenon resulted to be very complex and included perturbation of cell-cycle control genes, RTK cascades, and other malignancy-related effectors. Such pleiotropic impact of *Emx2* on cell metabolism was proposed to account for the wide spectrum of tumors sensitive to this gene and to be of potential advantage in prevention of relapses (Falcone et al., 2016).

Starting from these premises and from limits of conventional therapies, here I first evaluated the actual advantage of experimental *Emx2* gene therapy, in immunocompromised mice transplanted by engineered human GBM cells. It turned out *Emx2* overexpression almost doubled the survival time of these animals.

Next, a step forward towards its possible future adoption in oncotherapy, I investigated the interaction of *Emx2* overexpression with current standard therapies, including chemo and radiotherapy. Combined *Emx2*/TMZ treatment resulted more effective than TMZ alone. Moreover, *Emx2* improved the therapeutic effects of radiotherapy, making GBM cells more sensitive to radiation, due to inhibition of DNA-repair mechanisms.

Last, interested in developing new effective and biosafety strategies for *in vivo* delivery, based on HSV-1 derived viruses, I achieved key proofs-of-principle prefiguring that oncolytic HSV-1 and amplicon vectors could be combinatorially exploited as powerful tools for *in vivo* *Emx2* delivery.

\* \* \*

In the first part of my work, I showed that *Emx2* can antagonize GBM growth *in vivo*, prolonging the survival of immunotolerant mice orthotopically transplanted with *Emx2*-GOF tumor cells. In particular, the median survival time moved from 35 days of controls to 56 days of *Emx2*-treated mice. Even more strikingly, 3/14 mice transplanted with *Emx2*-GOF cells survived about 3 months, whereas only 1/14 animals transplanted with control cells remained alive at one month and half. However, we were not able to eradicate the tumor, possibly because of late *in vivo* silencing of the therapeutic transgene and/or *in vivo* selection of rare GBM cells not transduced at all by this transgene or expressing it at very low levels *ab initio*. Moreover, both *Emx2* overexpression and combined *Emx2*/TMZ protocol outperformed the TMZ treatment alone.

\* \* \*

This remarkable result was also confirmed by *in vitro* kinetic assays, where we discovered at least an additive effect between the standard treatment and our gene therapy and, specifically in U87MG GBM cells, an *Emx2*-dependent cell sensitization to the chemotherapeutic agent. Chemo-resistance of GBM cells can occur by intercellular communication through gap junctions (Gielen et al. 2013), and it is also well known that CX43 is expressed at high levels in astrocytes and astrocytomas (Caltabiano et al., 2010). Munoz and colleagues (Jessian L. Munoz et al. 2014) showed that TMZ resistance in GBM occurs partly via EGFR, that mediates the induction of CX43 through the activation of JNK-ERK-AP1 pathway. The same pathway seems to regulate also MDR1 expression, an ATP-dependent efflux pump responsible for tumour chemo-resistance. Even if molecular mechanisms underlying *Emx2*/TMZ interaction can be very complex, CX43 and MDR1 seem to have a central role in mediating this effect.

We discovered that *Emx2* downregulates both CX43 and MDR1, still in the presence of TMZ (in all 4 cell lines tested for CX43 and in 2 out of 4 samples for MDR1); furthermore, we previously demonstrated that, in our cells lines, *Emx2* downregulates EGFR (Falcone et al. 2016).

Apparently, *Emx2* could sensitize cells to chemotherapy by manipulating at different levels the mediators of the EGFR-JNK-ERK-AP1-CX43/MDR1 pathway and preventing TMZ resistance.

Although the molecular mechanisms are still very complex and many aspects need to be clarified, we can conclude that *Emx2* gene therapy represents an efficient option to treat GBM, and together with the pre-existent therapies, could be successful in those tumours that display chemo-resistance.

\* \* \*

In the third part of this work we were interested in evaluating if *Emx2* overexpression sensitize GBM cells to radiotherapy, leading to an enhanced anti-oncogenic effect, compared to the therapeutic agent alone.

According to our experience, to be successful, this assay requires a careful pre-calibration of X-ray doses and *Emx2* overexpression levels, to be done line by line. Too much radiation or too much *Emx2*-activating doxycycline would - even alone - acutely kill the cells, making their interaction effect hidden by the experimental noise.

The growth curves, reconstructed for U87MG and U251 GBM cell lines, showed that *Emx2* considerably amplified the impact of X-rays, revealing a statistically significant, positive interaction between transgene overexpression and irradiation.

To dissect the biological mechanisms through which *Emx2* increases radio-sensitivity of GBM cells, we envisaged two possible, not mutually exclusive classes of explanations: *Emx2* could increase DNA damage or it could inhibit DNA repair mechanisms.

To test the first hypothesis, we evaluated the dynamic progression of radio-induced DNA damage, by quantifying the levels of  $\gamma$ -H2AX in U251 cells.  $\gamma$ -H2AX histone is a variant of H2A, one of the five main histone proteins involved in the structure of chromatin in eukaryotic cells.; upon DNA damage, SSBs or DSBs, it can be phosphorylated on serine 139 (Sharma et al., 2012). Genotoxic stress, such as that evoked by radio- and chemotherapy, is considered to be the main inducer of phosphorylated H2AX ( $\gamma$ H2AX), which forms distinct foci at sites of DNA damage where DNA repair factors accumulate.

In our system, *Emx2* alone increases the number of nuclear  $\gamma$ H2AX foci over time, while, on the other hand, those acutely evoked by radiation alone return to basal levels by 16 hours;

notably, 16hrs after X-ray treatment, there are no differences between *Emx2*-GOF cells, having undergone or not irradiation. This suggests that *Emx2* could be intrinsically a mutagen or it could slow down DNA damage repair induced by environmental factors.

In order to clarify a possible involvement of *Emx2* in the inhibition of DNA-repair mechanisms, we decided to monitor the ability of GBM cells to repair a DNA-DSB, evoked by a well-controlled system called Traffic light reporter (TLR) (Certo et al. 2011). In this way, we fix a certain amount of damage and subsequently we monitor cell ability to repair it, depending on the cell genotype (Control or *Emx2*-GOF). The TLR generates a flow-cytometric readout of homology-directed repair (HDR)-mediated gene targeting; indeed, it is well known that glioblastoma tumour cells, in particular the stem cell counterpart, have enhanced DNA repair pathways, predominantly via homologous recombination (Lim et al. 2012), (Lim et al. 2014), which confer greater survival and contribute to radio-resistance.

Our experiments allowed us to demonstrate unequivocally that *Emx2*-GOF cells repair DNA-DSBs with reduced efficiency, negatively impacting on the homologous recombination machinery.

In order to deeply investigate the potential mediators of *Emx2* HR-repair suppressing activity, we performed a RNA-seq on 4 GBM samples and validated some candidates by qPCR.

Among them, *Foxg1* and *SOX2* seem to be involved in the *Emx2* HR-repair suppressing activity, indeed their overexpression restore totally the DNA damage repair.

*Foxg1*, which encodes a DNA-binding transcriptional repressor factor belonging to the forkhead protein family, not only plays an important role in brain development, but it's also a key determinant of GBM malignity (Verginelli et al. 2013). Furthermore, the FOXG1 protein physically interacts with POLE (Li et al. 2015), the catalytic epsilon subunit of DNA polymerase, involved in both DNA replication and repair (Henninger and Pursell 2014). This interaction might be mechanistically bridge *Emx2*-dependent *Foxg1* downregulation to defective GBM DNA repair.

On the other hand, *SOX2*, a member of the SRY-related HMG-box (SOX) family of transcription factors, is a stemness factor expressed at high levels in glioma initiating cells (GICs), a group of aberrant stem cells suggested to be the main responsible for radio-resistance. Remarkably, these cells also express high levels of Rad51 protein (King et al. 2017) and display an efficient DNA repair ability, mainly through the activation of the

homologous recombination pathway (Bao et al., 2006). All these data may suggest that SOX2 impairment, mediated by *Emx2*, could lead to a dramatic reduction of the HR-mediated DNA repair, eventually resulting in increased sensitivity to ionising radiation (Lim et al. 2014).

In conclusion, although much still needs to be clarified, we demonstrated that *Emx2* negatively regulates DNA repair mechanisms, one of the most important process in the life cycle of tumour cells. By blocking this machinery, it permits to sensitise GBM cells to irradiation, and forced them undergo apoptosis. This happens trough the downregulation of two master genes involved in gliomagenesis, SOX2 and FOXG1.

All these data not only reinforce the anti-oncogenic role of *Emx2* but also highlight the importance of an in vivo combined approach.

\* \* \*

As for the last part of this work, we decided to investigate the antitumour activity of the oncolytic virus Myb34.5; it is a second-generation replication-conditional HSV-1 mutant in which ICP6 gene expression is defective and expression of the HSV-1  $\gamma_1$ 34.5 gene is regulated by the cellular B-myb promoter. ICP6 encodes the large subunit of viral ribonucleotide reductase (RR), an enzyme involved in de novo synthesis of deoxynucleotides. In the absence of viral RR, virus replication depends on host cell RR activity, which has been reported to be higher in cancer cells (Gayral et al. 2014). Consequently, HSV-1 mutants with deletions in the ICP6 gene preferentially replicate in actively dividing cells such as malignant cells. Infection of tumour cells by Myb 34.5 leads to cell destruction and simultaneous release of progeny virion that can infect adjacent tumour cells.

It was employed for the first time in pancreatic tumours, where it displayed an important antitumor effect, inducing a reduction in tumour growth.

In our experiments performed on 2 GBM cell lines and 2 primary cultures, we found that very low doses of Myb34.5 are able to induce a powerful anti-tumour activity, by inducing the collapse of all 4 GBM cultures in about one week. Furthermore, the oncolytic Myb34.5 herpesvirus, administered at moi=0.005, is still able to induce a rapid collapse of GBM tumours in vitro, while not affecting the surrounded "healthy neural tissue". These results suggest Myb34.5 as a new powerful tool for the treatment of glioblastoma multiforme.

Considering these results, we asked whether *Emx2* gene therapy could improve the anti-GBM effects elicited by oncolytic herpesvirus, as it occurs when associated to chemo and radiotherapy. In a preliminary test, performed on U87MG GBM cells, *Emx2*, delivered by a lentiviral vector and weakly activated by low doxycycline, synergizes with Myb34.5, allowing to employ the latter at the minimal moi, enough to elicit a satisfactory therapeutic effect.

Taken together, all these results point *Emx2* and HSV-1 as a novel, promising combined tool for GBM gene therapy. However, it is well known that lentiviral vectors are not suitable for in vivo treatment, due to their low infection capability and insertional mutagenesis generated from their random integration into the genome. On the other hand, oncolytic HSV-1 do not integrate into the genome of infected cells, there are several available anti-HSV-1-specific drugs, such as acyclovir to control unwanted infection and relatively low moi's are needed to kill tumour cells (Xu et al., 2013); furthermore, they are currently investigated in preclinical and phase I to III clinical trials, where they have been shown to be safe.

For all these reasons, we thought to employ HSV-derived amplicon vectors as a Trojan horse for in vivo *Emx2* administration to tumour cells. The starting point is a plasmid, called amplicon, to which minimal HSV-1 sequences are added, in order to allow it to be packaged into virus particles and neogenerated with the aid of a helper virus.

To test this hypothesis, we evaluated the neo-generation of a neutral amplicon vector harbouring an EGFP coding sequence both in tumour cells and in "healthy" murine, perinatal neocortical tissue, employing the oncolytic Myb34.5 as helper virus. Surprisingly, when co-delivered with Myb34.5, the amplicon vector vAM-GFP is robustly neo-generated by both glioblastoma cells and "healthy neural cells" (the latter ones possibly corresponding to still intermitotic astrocytes permissive to HSV1 replication).

All these data suggest that administering the therapeutic *Emx2* transgene by a vAM-GFP-like amplicon vector and a Myb34.5 helper could achieve fine, self-sustaining spreading of the "Myb34.5 - vAM-*Emx2*" therapeutic cocktail in vivo, up to full tumour eradication. This prediction is currently being tested in our lab.

## 6. BIBLIOGRAPHY

- Agnihotri, S., KE Burrell, A. Wolf, S. Jalali, C. Hawkins, JT Rutka, and G. Zadeh. 2013. "Glioblastoma, a Brief Review of History, Molecular Genetics, Animal Models and Novel Therapeutic Strategies." *Arch Immunol Ther Exp (Warsz)* 61(1):25–41.
- Alifieris, C. and DT Trafalis. 2015. "Glioblastoma Multiforme: Pathogenesis and Treatment." *Pharmacol Ther* 152:63–82.
- Andtbacka, Robert H. I., Howard L. Kaufman, Frances Collichio, Thomas Amatruda, Neil Senzer, Jason Chesney, Keith A. Delman, Lynn E. Spitler, Igor Puzanov, Sanjiv S. Agarwala, Mohammed Milhem, Lee Cranmer, Brendan Curti, Karl Lewis, Merrick Ross, Troy Guthrie, Gerald P. Linette, Gregory A. Daniels, Kevin Harrington, Mark R. Middleton, Wilson H. Miller, Jonathan S. Zager, Yining Ye, Bin Yao, Ai Li, Susan Doleman, Ari Van Der Walde, Jennifer Gansert, and Robert S. Coffin. 2015. "Talimogene Laherparepvec Improves Durable Response Rate in Patients with Advanced Melanoma." *Journal of Clinical Oncology* 33(25):2780–88.
- Assudani, Deepak P., Murrium Ahmad, Geng Li, Robert C. Rees, and Selman A. Ali. 2006. "Immunotherapeutic Potential of DISC-HSV and OX40L in Cancer." *Cancer Immunology, Immunotherapy* 55(1):104–11.
- Aykut, Berk, Markus Ochs, Praveen Radhakrishnan, Adrian Brill, Hermine Höcker, Sandra Schwarz, Daniel Weissinger, Roland Kehm, Yakup Kulu, Alexis Ulrich, and Martin Schneider. 2017. "EMX2 Gene Expression Predicts Liver Metastasis and Survival in Colorectal Cancer." *BMC Cancer* 17(1):1–8.
- Berezovsky, Artem D., Laila M. Poisson, David Cherba, Craig P. Webb, Andrea D. Transou, Nancy W. Lemke, Xin Hong, Laura A. Hasselbach, Susan M. Irtenkauf, Tom Mikkelsen, and Ana C. de Carvalho. 2014. "Sox2 Promotes Malignancy in Glioblastoma by Regulating Plasticity and Astrocytic Differentiation." *Neoplasia (United States)* 16(3):193-206.e25.
- Blake, Sophia M., Stefan H. Stricker, Hanna Halavach, Anna R. Poetsch, George Cresswell, Gavin Kelly, Nnennaya Kanu, Silvia Marino, Nicholas M. Luscombe, Steven M. Pollard, and Axel Behrens. 2016. "Inactivation of the ATMIN/ATM Pathway Protects against Glioblastoma Formation." *ELife* 5(MARCH2016):1–24.
- Bommareddy, Praveen K., Megha Shettigar, and Howard L. Kaufman. 2018. "Integrating Oncolytic Viruses in Combination Cancer Immunotherapy." *Nature Reviews Immunology* 1–16.
- Brett-Morris, A., BM Wright, Y. Seo, V. Pasupuleti, J. Zhang, J. Lu, R. Spina, EE Bar, M. Gujrati, R. Schur, ZR Lu, and SM Welford. 2014. "The Polyamine Catabolic Enzyme SAT1 Modulates Tumorigenesis and Radiation Response in GBM." *Cancer Res.* 74(23):6925–34.
- Caltabiano, Rosario, Antonietta Torrisi, Daniele Condorelli, Vincenzo Albanese, and Salvatore Lanzafame. 2010. "High Levels of Connexin 43 mRNA in High Grade Astrocytomas. Study of 32 Cases with in Situ Hybridization." *Acta Histochemica* 112(6):529–35.

- Certo, Michael T., Byoung Y. Ryu, James E. Annis, Mikhail Garibov, Jordan Jarjour, David J. Rawlings, and Andrew M. Scharenberg. 2011. "Tracking Genome Engineering Outcome at Individual DNA Breakpoints." *Nature Methods* 8(8):671–76.
- Chakravarti, A., A. Dicker, and M. Mehta. 2004. "The Contribution of Epidermal Growth Factor Receptor (EGFR) Signaling Pathway to Radioresistance in Human Gliomas: A Review of Preclinical and Correlative Clinical Data." *Int J Radiat Oncol Biol Phys.* 58(3):927–31.
- Chen, Chen, Sheng Han, Lingxuan Meng, Zhonghua Li, Xue Zhang, and Anhua Wu. 2014. "TERT Promoter Mutations Lead to High Transcriptional Activity under Hypoxia and Temozolomide Treatment and Predict Poor Prognosis in Gliomas." *PLoS ONE* 9(6):3–10.
- Chung, Richard Y., Yoshinaga Saeki, and E. Antonio Chiocca. 1999. "B-Myb Promoter Retargeting of Herpes Simplex Virus  $\Gamma$ 34.5 Gene-Mediated Virulence toward Tumor and Cycling Cells." *Journal of Virology* 73(9):7556–64.
- Cliffe, A. R., D. A. Garber, and D. M. Knipe. 2009. "Transcription of the Herpes Simplex Virus Latency-Associated Transcript Promotes the Formation of Facultative Heterochromatin on Lytic Promoters." *Journal of Virology* 83(16):8182–90.
- Colman, Howard, Li Zhang, Erik P. Sulman, J. Matthew McDonald, Nasrin Latif Shooshtari, Andreana Rivera, Sonya Popoff, Catherine L. Nutt, David N. Louis, J. Gregory Cairncross, Mark R. Gilbert, Heidi S. Phillips, Minesh P. Mehta, Arnab Chakravarti, Christopher E. Pelloso, Krishna Bhat, Burt G. Feuerstein, Robert B. Jenkins, and Ken Aldape. 2010. "A Multigene Predictor of Outcome in Glioblastoma." *Neuro-Oncology* 12(1):49–57.
- Duffy, C., E. F. Mbong, and J. D. Baines. 2009. "VP22 of Herpes Simplex Virus 1 Promotes Protein Synthesis at Late Times in Infection and Accumulation of a Subset of Viral MRNAs at Early Times in Infection." *Journal of Virology* 83(2):1009–17.
- Epstein, Alberto L. 2005. "HSV-1-Based Amplicon Vectors: Design and Applications." *Gene Therapy* 12:S154–58.
- Estiar, Mehrdad Asghari and Parvin Mehdipour. 2018. "ATM in Breast and Brain Tumors: A Comprehensive Review." *Cancer Biology and Medicine* 15(3):210–27.
- Falcone, Carmen, Antonio Daga, Giampiero Leanza, and Antonello Mallamaci. 2016. "Emx2 as a Novel Tool to Suppress Glioblastoma." *Oncotarget* 7(27).
- Falcone, Carmen, Carol Filippis, Marilena Granzotto, and Antonello Mallamaci. 2015. "Emx2 Expression Levels in NSCs Modulate Astrogenesis Rates by Regulating Egfr and Fgf9." *Glia* 63(3):412–22.
- Falcone, Carmen and Antonello Mallamaci. 2015. "Tuning of Neocortical Astrogenesis Rates by Emx2 in Neural Stem Cells." *Neural Regeneration Research* 10(4):550–51.
- Fedrico, Carlos A., Ivana Grivicich, Daniel P. Schunemann, Ivan M. Chemale, Daiane D. Santos, Thais Jacobas, Patryck S. Boschetti, Geraldo P. Jotz, Aroldo B. Filho, and Adriana B. da Rocha. 2011. "Radioresistance of Human Glioma Spheroids and Expression of HSP70, P53 and EGFr." *Radiation Oncology* 6(1):156.
- Fisher, JL, JA Schwartzbaum, M. Wrensch, and JL. Wiemels. 2007. "Epidemiology of Brain Tumors." *Neurol Clin* 25(4):867–90.
- Frampton, A. R., W. F. Goins, K. Nakano, E. A. Burton, and J. C. Glorioso. 2005. "HSV



- Trafficking and Development of Gene Therapy Vectors with Applications in the Nervous System." *Gene Therapy* 12(11):891–901.
- Friedman, Henry S., Michael D. Prados, Patrick Y. Wen, Tom Mikkelsen, David Schiff, Lauren E. Abrey, W. K. Alfre. Yung, Nina Paleologos, Martin K. Nicholas, Randy Jensen, James Vredenburgh, Jane Huang, Maoxia Zheng, and Timothy Cloughesy. 2009. "Bevacizumab Alone and in Combination with Irinotecan in Recurrent Glioblastoma." *Journal of Clinical Oncology* 27(28):4733–40.
- Furnari, Frank B., Tim Fenton, Robert M. Bachoo, Akitake Mukasa, Jayne M. Stommel, Alexander Stegh, William C. Hahn, Keith L. Ligon, David N. Louis, Cameron Brennan, Lynda Chin, Ronald A. DePinho, and Webster K. Cavenee. 2007. "Malignant Astrocytic Glioma: Genetics, Biology, and Paths to Treatment." *Genes and Development* 21(21):2683–2710.
- Furuta, Y., DW Piston, and BL Hogan. 1997. "Bone Morphogenetic Proteins (BMPs) as Regulators of Dorsal Forebrain Development." *Development* 124:2203–2212.
- Gangemi, Rosaria M. R., Antonio Daga, Daniela Marubbi, Nadia Rosatto, Maria C. Capra, and Giorgio Corte. 2001. "Emx2 in Adult Neural Precursor Cells." 109:323–29.
- Gangemi, Rosaria M. R., Antonio Daga, Luca Muzio, Daniela Marubbi, Serena Coccozza, Marzia Perera, Sara Verardo, Domenico Bordo, Fabrizio Griffero, Maria C. Capra, Antonello Mallamaci, and Giorgio Corte. 2006. "Effects of Emx2 Inactivation on the Gene Expression Profile of Neural Precursors." *European Journal of Neuroscience* 23(2):325–34.
- Gayral, Marion, Hubert Lulka, Naima Hanoun, Coline Biollay, Janick Sèlves, Alix Vignolle-Vidoni, Hervé Berthommé, Pascal Trempat, Alberto L. Epstein, Louis Buscail, Jean-Luc Béjot, and Pierre Cordelier. 2014. "Targeted Oncolytic Herpes Simplex Virus Type 1 Eradicates Experimental Pancreatic Tumors." *Human Gene Therapy* 26(2):104–13.
- Gielen, Paul R., Qurratulain Aftab, Noreen Ma, Vincent C. Chen, Xiaoting Hong, Shannon Lozinsky, Christian C. Naus, and Wun Chey Sin. 2013. "Connexin43 Confers Temozolomide Resistance in Human Glioma Cells by Modulating the Mitochondrial Apoptosis Pathway." *Neuropharmacology* 75:539–48.
- Glorioso, J. C. Grandi P. 2009. "Design and Application of Oncolytic HSV Vectors for Glioblastoma Therapy." *Expert Rev Neurother* 9(4):505–17.
- Gong, Chongwen, Runxia Gu, Honglin Jin, Yao Sun, Zhenyu Li, Jing Chen, and Gang Wu. 2016. "Lysyl Oxidase Mediates Hypoxia-Induced Radioresistance in Non-Small Cell Lung Cancer A549 Cells." *Experimental Biology and Medicine* 241(4):387–95.
- Granata, T., L. Farina, A. Faiella, R. Cardini, L. D'Incerti, E. Boncinelli, and G. Battaglia. 1997. "Familial Schizencephaly Associated with EMX2 Mutation." *Neurology* 48(5):1403-6.
- Gulisano, M., V. Broccoli, C. Pardini, and E. Boncinelli. 1996. "Emx1 and Emx2 Show Different Patterns of Expression during Proliferation and Differentiation of the Developing Cerebral Cortex in the Mouse." *Eur J Neurosci.* 8(5):1037-50.
- Hanahan, Douglas and Robert A. Weinberg. 2011. "Hallmarks of Cancer: The next Generation." *Cell* 144(5):646–74.
- Hanif, Farina, Saima M. Malhi, Kahkashan Perveen, Shabana U. Simjee, and Kanza Muzaffar. 2017. "Glioblastoma Multiforme: A Review of Its Epidemiology and Pathogenesis

- through Clinical Presentation and Treatment.” *Asian Pacific Journal of Cancer Prevention* 18(1):3–9.
- Henninger, Erin E. and Zachary F. Pursell. 2014. “DNA Polymerase  $\epsilon$  and Its Roles in Genome Stability.” *IUBMB Life* 66(5):339–51.
- Hervey-Jumper, Shawn L. and Mitchel S. Berger. 2014. “Role of Surgical Resection in Low- and High-Grade Gliomas.” *Current Treatment Options in Neurology* 16(4).
- J Okamoto, T Hirata, Z Chen, H-M Zhou, I Mikami, H Li, A Beltran, M., D. Johansson, LM Coussens, G Clement, Y Shi, F Zhang, K Koizumi, K Shimizu, and and B. He Jablons. 2010. “EMX2 Is Epigenetically Silenced and Suppresses Growth in Human Lung Cancer.” *Oncogene*. 29(44):5969–5975.
- Kaufman, Howard L., Frederick J. Kohlhapp, and Andrew Zloza. 2015. “Oncolytic Viruses: A New Class of Immunotherapy Drugs.” *Nature Reviews Drug Discovery* 14(9):642–62.
- Kim, Sanghyeon, Kwong Ho Choi, Ali Fuat Baykiz, and Howard K. Gershenfeld. 2007. “Suicide Candidate Genes Associated with Bipolar Disorder and Schizophrenia: An Exploratory Gene Expression Profiling Analysis of Post-Mortem Prefrontal Cortex.” *BMC Genomics* 8:1–10.
- King, Harry O., Tim Brend, Helen L. Payne, Alexander Wright, Thomas A. Ward, Karan Patel, Teklu Egnuni, Lucy F. Stead, Anjana Patel, Heiko Wurdak, and Susan C. Short. 2017. “RAD51 Is a Selective DNA Repair Target to Radiosensitize Glioma Stem Cells.” *Stem Cell Reports* 8(1):125–39.
- Krisky, D. M., D. Wolfe, W. F. Coins, P. C. Marconi, R. Ramakrishnan, M. Mata, Rjd Rouse, D. J. Fink, and J. C. Glorioso. 1998. “Deletion of Multiple Immediate-Early Genes from Herpes Simplex Virus Reduces Cytotoxicity and Permits Long-Term Gene Expression in Neurons.” *Gene Therapy* 5(12):1593–1603.
- Kwiatkowski, D. L., H. W. Thompson, and D. C. Bloom. 2009. “The Polycomb Group Protein Bmi1 Binds to the Herpes Simplex Virus 1 Latent Genome and Maintains Repressive Histone Marks during Latency.” *Journal of Virology* 83(16):8173–81.
- Laquerre, S., R. Argnani, D. B. Anderson, S. Zucchini, R. Manservigi, and J. C. Glorioso. 1998. “Heparan Sulfate Proteoglycan Binding by Herpes Simplex Virus Type 1 Glycoproteins B and C, Which Differ in Their Contributions to Virus Attachment, Penetration, and Cell-to-Cell Spread.” *Journal of Virology* 72(7):6119–30.
- Lee, Joo Ho, Jeong Eun Lee, Jee Ye Kahng, Se Hoon Kim, Jun Sung Park, Seon Jin Yoon, Ji Yong Um, Woo Kyeong Kim, June Koo Lee, Junseong Park, Eui Hyun Kim, Ji Hyun Lee, Joon Hyuk Lee, Won Suk Chung, Young Seok Ju, Sung Hong Park, Jong Hee Chang, Seok Gu Kang, and Jeong Ho Lee. 2018. “Human Glioblastoma Arises from Subventricular Zone Cells with Low-Level Driver Mutations.” *Nature* 560(7717):243–47.
- Li, Dong, Kou Peng, Yi Li, Ying Peng, F-fdg Pet, Murtaza Mustaf, A. F. Sali, E. M. Illzam, A. M. Sharifa, M. K. Nang, Chin Hwee Goh, Yeow Yen Lu, Bik Liang Lau, Jacqueline Oy, Leng Wong, Mpath Ukm, Hock Keong Lee, M. S. Usm, Donald Ngian, San Liew, Albert Sii, Hieng Wong, East Coast, M. Mckay, Luis F. Parada, Jian Chen, Open Access, Elena I. Fomchenko, Eric C. Holland, Huamin Qin, Mirosław Janowski, Monica S. Pearl, Izabela Malysz-cymborska, Shen Li, Charles G. Eberhart, Piotr Walczak, Justin V Joseph, Ingrid A. M. Van Roosmalen, Ellen Busschers, Tushar Tomar, Miloš Vittori, Helena Motaln, and

- Tamara Lah Turnšek. 2017. *Cover Image: Primary Diagnosis of a Right Frontal Glioblastoma Following Acquisition of Axial Slices of T1-Weighted Gadolinium-Enhanced MRI (Left) and 18F-FDG PET (Right)*. See Page 158, Chapter 9 for Details. Vol. 63.
- Li, Jie, Minli Mo, Zhao Chen, Zhe Chen, Qing Sheng, Hang Mu, Fang Zhang, Yi Zhang, Xiu Yi Zhi, Hui Li, Biao He, and Hai Meng Zhou. 2012. "Adenoviral Delivery of the EMX2 Gene Suppresses Growth in Human Gastric Cancer." *PLoS ONE* 7(9):1–9.
- Li, Xu, Wenqi Wang, Jiadong Wang, Anna Malovannaya, Yuanxin Xi, Wei Li, Rudy Guerra, David H. Hawke, Jun Qin, and Junjie Chen. 2015. "Proteomic Analyses Reveal Distinct Chromatin-associated and Soluble Transcription Factor Complexes." *Molecular Systems Biology* 11(1):775.
- Lim, Yi Chieh, Tara L. Roberts, Bryan W. Day, Angus Harding, Sergei Kozlov, Amanda W. Kijas, Kathleen S. Ensbey, David G. Walker, and Martin F. Lavin. 2012. "A Role for Homologous Recombination and Abnormal Cell-Cycle Progression in Radioresistance of Glioma-Initiating Cells." *Molecular Cancer Therapeutics* 11(9):1863–72.
- Lim, Yi Chieh, Tara L. Roberts, Bryan W. Day, Brett W. Stringer, Sergei Kozlov, Shazrul Fazry, Zara C. Bruce, Kathleen S. Ensbey, David G. Walker, Andrew W. Boyd, and Martin F. Lavin. 2014. "Increased Sensitivity to Ionizing Radiation by Targeting the Homologous Recombination Pathway in Glioma Initiating Cells." *Molecular Oncology* 8(8):1603–15.
- Lin, J., Chia Ching, Kwanha Yu, Asante Hatcher, Teng Wei Huang, Hyun Kyoung Lee, Jeffrey Carlson, Matthew C. Weston, Fengju Chen, Yiqun Zhang, Wenyi Zhu, Carrie A. Mohila, Nabil Ahmed, Akash J. Patel, Benjamin R. Arenkiel, Jeffrey L. Noebels, Chad J. Creighton, and Benjamin Deneen. 2017. "Identification of Diverse Astrocyte Populations and Their Malignant Analogs." *Nature Neuroscience* 20(3):396–405.
- Louis, David N., Arie Perry, Guido Reifenberger, Andreas von Deimling, Dominique Figarella-Branger, Webster K. Cavenee, Hiroko Ohgaki, Otmar D. Wiestler, Paul Kleihues, and David W. Ellison. 2016. "The 2016 World Health Organization Classification of Tumors of the Central Nervous System: A Summary." *Acta Neuropathologica* 131(6):803–20.
- Mallamaci, Antonello, Raffaella Iannone, Paola Briata, Luisa Pintonello, Sara Mercurio, Edoardo Boncinelli, and Giorgio Corte. 1998. "EMX2 Protein in the Developing Mouse Brain and Olfactory Area." *Mechanisms of Development* 77(2):165–72.
- Mallamaci, Antonello, Sara Mercurio, Luca Muzio, Chiara Cecchi, Celia Leonor Pardini, Peter Gruss, and Edoardo Boncinelli. 2000. "The Lack of Emx2 Causes Impairment of Reelin Signaling and Defects of Neuronal Migration in the Developing Cerebral Cortex." *Journal of Neuroscience* 20(3):1109–18.
- Marampon, Francesco, Giovanni Luca Gravina, Bianca Maria Zani, Vladimir M. Popov, Amato Fratticci, Manuela Cerasani, Daniela Di Genova, Marta Mancini, Carmela Ciccarelli, Corrado Ficorella, Ernesto Di Cesare, and Claudio Festuccia. 2014. "Hypoxia Sustains Glioblastoma Radioresistance through ERKs/DNA-PKcs/HIF-1 $\alpha$  Functional Interplay." *International Journal of Oncology* 45(6):2121–31.
- Markert, James M., Peter G. Liechty, Wenquan Wang, Shanna Gaston, Eunice Braz, Matthias Karrasch, Louis B. Nabors, Michael Markiewicz, Alfred D. Lakeman, Cheryl A. Palmer, Jacqueline N. Parker, Richard J. Whitley, and George Y. Gillespie. 2009. "Phase Ib Trial of Mutant Herpes Simplex Virus G207 Inoculated Pre-and Post-Tumor Resection for

- Recurrent GBM." *Molecular Therapy* 17(1):199–207.
- Martuza, RL, A. Malick, JM Markert, KL Ruffner, and DM. Coen. 1991. "Experimental Therapy of Human Glioma by Means of a Genetically Engineered Virus Mutant." *Science* 252(5007):854-6.
- Mazzoleni, Stefania, Letterio S. Politi, Mauro Pala, Manuela Cominelli, Alberto Franzin, Lucia Sergi Sergi, Andrea Falini, Michele De Palma, Alessandro Bulfone, Pietro L. Poliani, and Rossella Galli. 2010. "Epidermal Growth Factor Receptor Expression Identifies Functionally and Molecularly Distinct Tumor-Initiating Cells in Human Glioblastoma Multiforme and Is Required for Gliomagenesis." *Cancer Research* 70(19):7500–7513.
- Monnier, Annabelle, Rachel Boniface, Régis Bouvet, Amandine Etcheverry, Marc Aubry, Tony Avril, Véronique Quillien, Eric Chevet, and Jean Mosser. 2018. "The Expression of EMX2 Lead to Cell Cycle Arrest in Glioblastoma Cell Line." *BMC Cancer* 18(1):1–11.
- Munoz, J. L., V. Rodriguez-Cruz, S. J. Greco, S. H. Ramkissoon, K. L. Ligon, and P. Rameshwar. 2014. "Temozolomide Resistance in Glioblastoma Cells Occurs Partly through Epidermal Growth Factor Receptormediated Induction of Connexin 43." *Cell Death and Disease* 5(3):e1145-10.
- Munoz, Jessian L., Vivian Rodriguez-Cruz, Steven J. Greco, Vipul Nagula, Kathleen W. Scotto, and Pranela Rameshwar. 2014. "Temozolomide Induces the Production of Epidermal Growth Factor to Regulate MDR1 Expression in Glioblastoma Cells." *Molecular Cancer Therapeutics* 13(10):2399–2411.
- Muzio, Luca, Barbara Dibenedetto, Anastassia Stoykova, Edoardo Boncinelli, Peter Gruss, and Antonello Mallamaci. 2002. "Emx2 and Pax6 Control Regionalization of the Pre-Neuronogenic Cortical Primordium." *Cerebral Cortex* 12(2):129–39.
- Muzio, Luca, Barbara DiBenedetto, Anastassia Stoykova, Edoardo Boncinelli, Peter Gruss, and Antonello Mallamaci. 2002. "Conversion of Cerebral Cortex into Basal Ganglia in Emx2-/- Pax6Sey/Sey Double-Mutant Mice." *Nature Neuroscience* 5(8):737–45.
- Nakada, Mitsutoshi, Daisuke Kita, Takuya Watanabe, Yutaka Hayashi, Lei Teng, Ilya V. Pyko, and Jun Ichiro Hamada. 2011. "Aberrant Signaling Pathways in Glioma." *Cancers* 3(3):3242–78.
- Nakamura, Hideo, Hideki Kasuya, John T. Mullen, Sam S. Yoon, Timothy M. Pawlik, Soundararajalu Chandrasekhar, James M. Donahue, E. Antonio Chiocca, Richard Y. Chung, and Kenneth K. Tanabe. 2002. "Regulation of Herpes Simplex Virus  $\Gamma$ 134.5 Expression and Oncolysis of Diffuse Liver Metastases by Myb34.5." *Journal of Clinical Investigation* 109(7):871–82.
- Noonan, FC, PJ Goodfellow, LJ Staloch, DG Mutch, and TC. Simon. 2003. "Antisense Transcripts at the EMX2 Locus in Human and Mouse." *Genomics* 81(1):58–66.
- Noonan, FC, DG Mutch, M. Ann Mallon, and PJ. Goodfellow. n.d. "Characterization of the Homeodomain Gene EMX2: Sequence Conservation, Expression Analysis, and a Search for Mutations in Endometrial Cancers."
- Ohgaki, H. 2009. "Epidemiology of Brain Tumors." *Methods Mol Biol.* 472:323–42.
- Ohgaki, Hiroko and Paul Kleihues. 2013. "The Definition of Primary and Secondary Glioblastoma." *Clinical Cancer Research* 19(4):764–72.

- Okamoto, J., T. Hirata, Z. Chen, H. M. Zhou, I. Mikami, H. Li, A. Beltran, M. Johansson, L. M. Coussens, G. Clement, Y. Shi, F. Zhang, K. Koizumi, K. Shimizu, D. Jablons, and B. He. 2010. "EMX2 Is Epigenetically Silenced and Suppresses Growth in Human Lung Cancer." *Oncogene* 29(44):5969–75.
- Okamoto, Junichi, Johannes Kratz, Tomomi Hirata, Iwao Mikami, Dan Raz, Mark Segal, Zhao Chen, Hai Meng Zhou, Patrick Pham, Hui Li, Adam Beltran, M. Roshni Ray, Kiyoshi Koizumi, Kazuo Shimizu, David Jablons, and Biao He. 2011. "Downregulation of EMX2 Is Associated with Clinical Outcomes in Lung Adenocarcinoma Patients." *Clinical Lung Cancer* 12(4):237–44.
- Ostrom, Quinn T., Luc Bauchet, Faith G. Davis, Isabelle Deltour, James L. Fisher, Chelsea Eastman Langer, Melike Pekmezci, Judith A. Schwartzbaum, Michelle C. Turner, Kyle M. Walsh, Margaret R. Wrensch, and Jill S. Barnholtz-Sloan. 2014. "The Epidemiology of Glioma in Adults: A State of the Science Review." *Neuro-Oncology* 16(7):896–913.
- Parsons, DW, S. Jones, X. Zhang, JC Lin, RJ Leary, P. Angenendt, P. Mankoo, H. Carter, IM Siu, GL Gallia, A. Olivieri, R. McLendon, BA Rasheed, S. Keir, T. Nikolskaya, Y. Nikolsky, DA Busam, H. Tekleab, LA Jr Diaz, J. Hartigan, DR Smith, RL Strausberg, SK Marie, SM Shinjo, H. Yan, GJ Riggins, DD Bigner, R. Karchin, N. Papadopoulos, G. Parmigiani, B. Vogelstein, VE Velculescu, and KW Kinzler. 2008. "An Integrated Genomic Analysis of Human Glioblastoma Multiforme." *Science* 26(321):1807–12.
- Pellegrini, M., A. Mansouri, A. Simeone, E. Boncinelli, and P. Gruss. 1996. "Dentate Gyrus Formation Requires Emx2." *Development* 122(12):3893–98.
- Perry, JR, N. Laperriere, CJ O'Callaghan, AA Brandes, C. Menten, K. Ding, and WP Mason. 2017. "Short-Course Radiation plus Temozolomide in Elderly Patients with Glioblastoma." *N Engl J Med.* 16(376):1027–37.
- Pertel, Peter E., Alina Fridberg, Mary L. Parish, and Patricia G. Spear. 2001. "Cell Fusion Induced by Herpes Simplex Virus Glycoproteins GB, GD, and GH-GL Requires a GD Receptor but Not Necessarily Heparan Sulfate." *Virology* 279(1):313–24.
- Phillips, Heidi S., Samir Kharbanda, Ruihuan Chen, William F. Forrest, Robert H. Soriano, Thomas D. Wu, Anjan Misra, Janice M. Nigro, Howard Colman, Liliana Soroceanu, P. Mickey Williams, Zora Modrusan, Burt G. Feuerstein, and Ken Aldape. 2006. "Molecular Subclasses of High-Grade Glioma Predict Prognosis, Delineate a Pattern of Disease Progression, and Resemble Stages in Neurogenesis." *Cancer Cell* 9(3):157–73.
- Raciti, Marilena, Marilena Granzotto, Minh Do Duc, Cristina Fimiani, Giada Cellot, Enrico Cherubini, and Antonello Mallamaci. 2013. "Reprogramming Fibroblasts to Neural-Precursor-like Cells by Structured Overexpression of Pallial Patterning Genes." *Molecular and Cellular Neuroscience* 57:42–53.
- Salvati, Maurizio, Alessandro Frati, Natale Russo, Emanuela Caroli, Filippo Maria Polli, Giuseppe Minniti, and Roberto Delfini. 2003. "Radiation-Induced Gliomas: Report of 10 Cases and Review of the Literature." *Surgical Neurology* 60(1):60–67.
- Saydam, Okay, Daniel L. Glauser, Irma Heid, Gulen Turkeri, Monika Hilbe, Andreas H. Jacobs, Mathias Ackermann, and Cornel Fraefel. 2005. "Herpes Simplex Virus 1 Amplicon Vector-Mediated siRNA Targeting Epidermal Growth Factor Receptor Inhibits Growth of Human Glioma Cells in Vivo." *Molecular Therapy* 12(5):803–12.

- Shah, Khalid, Yi Tang, Xandra Breakefield, and Ralph Weissleder. 2003. "Real-Time Imaging of TRAIL-Induced Apoptosis of Glioma Tumors in Vivo." *Oncogene* 22(44):6865–72.
- Sharma A, Almasan A. 2012. "Histone H2AX Phosphorylation: A Marker for DNA Damage." *Methods Mol Biol.* 920:613–2.
- Shinozaki, Koji, Toshihiko Miyagi, Michio Yoshida, Takaki Miyata, Masaharu Ogawa, Shinichi Aizawa, and Yoko Suda. 2002. "Absence of Cajal-Retzius Cells and Subplate Neurons Associated with Defects of Tangential Cell Migration from Ganglionic Eminence in Emx1/2 Double Mutant Cerebral Cortex." *Development* 129(14):3479–92.
- de Silva, Suresh and William J. Bowers. 2009. "Herpes Virus Amplicon Vectors." *Viruses* 1(3):594–629.
- Simeone, A., D. Acampora, M. Gulisano, A. Stornaiuolo, and E. Boncinelli. n.d. "Nested Expression Domains of Four Homeobox Genes in Developing Rostral Brain."
- Simeone, A., M. Gulisano, D. Acampora, A. Stornaiuolo, M. Rambaldi, and E. Boncinelli. 1992. "Two Vertebrate Homeobox Genes Related to the Drosophila Empty Spiracles Gene Are Expressed in the Embryonic Cerebral Cortex." *The EMBO Journal* 11(7):2541–50.
- Spaete, RR and N. Frenkel. 1982. "The Herpes Simplex Virus Amplicon: A New Eucaryotic Defective-Virus Cloning-Amplifying Vector." *Cell* 30(1):295-304.
- Spigoni, Giulia, Chiara Gedressi, and Antonello Mallamaci. 2010. "Regulation of Emx2 Expression by Antisense Transcripts in Murine Cortico-Cerebral Precursors." *PLoS ONE* 5(1).
- Stupp, R., WP Mason, MJ Van den Bent, M. Weller, and RO Mirimanoff. 2005. "Radiotherapy plus Concomitant and Adjuvant Temozolomide for Glioblastoma." *N Engl J Med.* 352(10):987-96.
- Tamura, RE, JF de Vasconcellos, D. Sarkar, TA Libermann, PB Fisher, and LF. Zerbini. 2012. "GADD45 Proteins: Central Players in Tumorigenesis." *Curr Mol Med* 12(5):634-51.
- TCGA. 2008. "Comprehensive Genomic Characterization Defines Human Glioblastoma Genes and Core Pathways." *Nature* 23(455):1061–1068.
- Tucker, Kerry Lee, Michael Meyer, and Yves Alain Barde. 2001. "Neurotrophins Are Required for Nerve Growth during Development." *Nature Neuroscience* 4(1):29–32.
- Verginelli, Federica, Alessandro Perin, Rola Dali, Karen H. Fung, Rita Lo, Pierluigi Longatti, Marie Christine Guiot, Rolando F. Del Maestro, Sabrina Rossi, Umberto Di Porzio, Owen Stechishin, Samuel Weiss, and Stefano Stifani. 2013. "Transcription Factors FOXG1 and Groucho/TLE Promote Glioblastoma Growth." *Nature Communications* 4.
- Verhaak, Roel G. W., Katherine A. Hoadley, Elizabeth Purdom, Victoria Wang, Yuan Qi, Matthew D. Wilkerson, C. Ryan Miller, Li Ding, Todd Golub, Jill P. Mesirov, Gabriele Alexe, Michael Lawrence, Michael O'Kelly, Pablo Tamayo, Barbara A. Weir, Stacey Gabriel, Wendy Winckler, Supriya Gupta, Lakshmi Jakkula, Heidi S. Feiler, J. Graeme Hodgson, C. David James, Jann N. Sarkaria, Cameron Brennan, Ari Kahn, Paul T. Spellman, Richard K. Wilson, Terence P. Speed, Joe W. Gray, Matthew Meyerson, Gad Getz, Charles M. Perou, and D. Neil Hayes. 2010. "Integrated Genomic Analysis Identifies Clinically Relevant Subtypes of Glioblastoma Characterized by Abnormalities in PDGFRA, IDH1, EGFR, and NF1." *Cancer Cell* 17(1):98–110.

- Vlazny, D. A. and N. Frenkel. 1981. "Replication of Herpes Simplex Virus DNA: Localization of Replication Recognition Signals within Defective Virus Genomes." *Proceedings of the National Academy of Sciences of the United States of America* 78(2 II):742–46.
- Wang, Suming, Jianguo Qi, Michael Smith, and Charles J. Link. 2002. "Antitumor Effects on Human Melanoma Xenografts of an Amplicon Vector Transducing the Herpes Thymidine Kinase Gene Followed by Ganciclovir." *Cancer Gene Therapy* 9(1):1–8.
- Watanabe, K., O. Tachibana, K. Sata, Y. Yonekawa, P. Kleihues, and H. Ohgaki. 1996. "Overexpression of the EGF Receptor and P53 Mutations Are Mutually Exclusive in the Evolution of Primary and Secondary Glioblastomas." *Brain Pathol.* 6(3217–223).
- Wesseling, Pieter, Johan M. Kros, and Judith W. M. Jeuken. 2011. "The Pathological Diagnosis of Diffuse Gliomas: Towards a Smart Synthesis of Microscopic and Molecular Information in a Multidisciplinary Context." *Diagnostic Histopathology* 17(11):486–94.
- Yoshida, M., Y. Suda, I. Matsuo, N. Miyamoto, N. Takeda, S. Kuratani, and S. Aizawa. 1997. "Emx1 and Emx2 Functions in Development of Dorsal Telencephalon." *Development (Cambridge, England)* 124(1):101–11.
- Yue, Dongsheng, Hui Li, Juanjuan Che, Yi Zhang, Bhairavi Tolani, Minli Mo, Hua Zhang, Qingfeng Zheng, Yue Yang, Runfen Cheng, Joy Q. Jin, Thomas W. Luh, Cathryn Yang, Hsin Hui K. Tseng, Etienne Giroux-Leprieur, Gavitt A. Woodard, Xishan Hao, Changli Wang, David M. Jablons, and Biao He. 2015. "EMX2 Is a Predictive Marker for Adjuvant Chemotherapy in Lung Squamous Cell Carcinomas." *PLoS ONE* 10(7):1–17.
- Zhang, Tianyi, Janet Cronshaw, Nnennaya Kanu, Ambrosius P. Snijders, and Axel Behrens. 2014. "UBR5-Mediated Ubiquitination of ATMIN Is Required for Ionizing Radiation-Induced ATM Signaling and Function." *Proceedings of the National Academy of Sciences of the United States of America* 111(33):12091–96.

\* \* \*

**References referring to Table 4.2.4.a:**

- [1] (King et al. 2017)
- [2] (Chakravarti, Dicker, and Mehta 2004)
- [3] (Li et al. 2015)
- [4] (Gong et al. 2016)
- [5] (Marampon et al. 2014)
- [6] (Brett-Morris et al. 2014)
- [7], [8] (Tamura et al. 2012)
- [9] (King et al. 2017)
- [10] (Estiar and Mehdipour 2018)

[11] (Blake et al. 2016)

[12] (Zhang et al. 2014)

[13] (Fedrigo et al. 2011)



# ACKNOWLEDGMENTS

Lots of people helped me during these four years and contribute with joy and passion to this work.

Thanks to my supervisor Antonello for the support he gave me during these years.

Thanks to Dott. Antonio Daga from the Department of Medical Oncology, Ospedale Policlinico San Martino in Genova for providing us patients' derived GBM cells; Prof. Giampiero Leanza for helping us during the *in vivo* xenograft transplantation experiments; Dott. Aulo Beorchia and Dott.ssa Rossella Vidimari, SOC Radioterapia AOUST, for the precious collaboration during the *in vitro* irradiation experiments; Dott. Alberto Tommasini and Dott.ssa Erika Valencic from IRCSS Burlo Garofalo for hosting and helping us in the settings and analysis of flow cytometric experiments.

Finally, but not least, I will thank all my labmates, in particular Carmen Falcone and Viviana Opinato who worked closely to me, for helping me and supporting me in all difficult moments, but above all for having lightened the long working days and having filled them with laughter and cheerfulness.